

# 1 Title Page

## Bimodal inference in humans and mice

### Authors:

Veith Weilnhammer<sup>1,2</sup>, Heiner Stuke<sup>1,2</sup>, Kai Standvoss<sup>1,3,5</sup>, Philipp Sterzer<sup>1,3,4,5</sup>

### Affiliations:

<sup>1</sup> Department of Psychiatry, Charité-Universitätsmedizin Berlin, corporate member of Freie Universität Berlin and Humboldt-Universität zu Berlin, 10117 Berlin, Germany

<sup>2</sup> Berlin Institute of Health, Charité-Universitätsmedizin Berlin and Max Delbrück Center, 10178 Berlin, Germany

<sup>3</sup> Bernstein Center for Computational Neuroscience, Charité-Universitätsmedizin Berlin, 10117 Berlin, Germany

<sup>4</sup> Berlin School of Mind and Brain, Humboldt-Universität zu Berlin, 10099 Berlin, Germany

<sup>5</sup> Einstein Center for Neurosciences Berlin, 10117 Berlin, Germany

### Corresponding Author:

Veith Weilnhammer, Department of Psychiatry, Charité Campus Mitte, Charitéplatz 1, 10117 Berlin, phone: 0049 (0)30 450 517 317, email: veith.weilnhammer@gmail.com

## <sup>1</sup> 2 Abstract

<sup>2</sup> Perception is known to cycle through periods of enhanced and reduced sensitivity to exter-  
<sup>3</sup> nal information. Here, we asked whether such infra-slow fluctuations arise as a noise-related  
<sup>4</sup> epiphenomenon of limited processing capacity or, alternatively, represent a structured mecha-  
<sup>5</sup> nism of perceptual inference. Using two large-scale datasets, we found that humans and mice  
<sup>6</sup> waver between alternating intervals of externally- and internally-oriented modes of sensory  
<sup>7</sup> analysis. During external mode, perception aligned more closely with the external sensory  
<sup>8</sup> information, whereas internal mode was characterized by enhanced biases toward perceptual  
<sup>9</sup> history. Computational modeling indicated that dynamic changes in mode are enabled by  
<sup>10</sup> two interlinked factors: (i), the integration of subsequent inputs over time and, (ii), infra-  
<sup>11</sup> slow anti-phase oscillations in the perceptual impact of external sensory information versus  
<sup>12</sup> internal predictions that are provided by perceptual history. Simulated data suggested that  
<sup>13</sup> between-mode fluctuations may benefit perception by generating unambiguous error signals  
<sup>14</sup> that enable robust learning and metacognition in volatile environments.

## <sup>15</sup> 3 One sentence summary

<sup>16</sup> Humans and mice fluctuate between external and internal modes of sensory processing.

<sup>17</sup>

<sup>18</sup>

<sup>19</sup> **4 Introduction**

<sup>20</sup> The capacity to respond to changes in the environment is a defining feature of life<sup>1–3</sup>. In-  
<sup>21</sup> triguingly, the ability of living things to process their surroundings fluctuates considerably  
<sup>22</sup> over time<sup>4,5</sup>. In humans and mice, perception<sup>6–12</sup>, cognition<sup>13</sup> and memory<sup>14</sup> cycle through  
<sup>23</sup> prolonged periods of enhanced and reduced sensitivity to external information, suggesting  
<sup>24</sup> that the brain detaches from the world in recurring intervals that last from milliseconds  
<sup>25</sup> to seconds and even minutes<sup>4,5</sup>. Yet breaking from external information is risky, as swift  
<sup>26</sup> responses to the environment are often crucial to survival.

<sup>27</sup> What could be the reason for these fluctuations in perceptual performance<sup>11</sup>? First, periodic  
<sup>28</sup> fluctuations in the ability to parse external information<sup>11,15,16</sup> may arise simply due to band-  
<sup>29</sup> width limitations and noise. Second, it may be advantageous to actively reduce the costs  
<sup>30</sup> of neural processing by seeking sensory information only in recurring intervals<sup>5,17</sup>, otherwise  
<sup>31</sup> relying on random or stereotypical responses to the external world. Third, spending time  
<sup>32</sup> away from the ongoing stream of sensory inputs may also reflect a functional strategy that  
<sup>33</sup> facilitates flexible behavior and learning<sup>18</sup>: Intermittently relying more strongly on informa-  
<sup>34</sup> tion acquired from past experiences may enable agents to build up stable internal predictions  
<sup>35</sup> about the environment despite an ongoing stream of external sensory signals<sup>19</sup>. By the same  
<sup>36</sup> token, recurring intervals of enhanced sensitivity to external information may help to detect  
<sup>37</sup> changes in both the state of the environment and the amount of noise that is inherent in  
<sup>38</sup> sensory encoding<sup>19</sup>.

<sup>39</sup> In this work, we sought to elucidate whether periodicities in the sensitivity to external infor-  
<sup>40</sup> mation represent an epiphenomenon of limited processing capacity or, alternatively, result  
<sup>41</sup> from a structured and adaptive mechanism of perceptual inference. To this end, we ana-  
<sup>42</sup> lyzed two large-scale datasets on perceptual decision-making in humans<sup>20</sup> and mice<sup>21</sup>. When  
<sup>43</sup> less sensitive to external stimulus information, humans and mice showed stronger serial  
<sup>44</sup> dependencies<sup>22–33</sup>, which have been conceptualized as internal predictions that reflect the

45 auto-correlation of natural environments<sup>34</sup> and bias perceptual decisions toward preceding  
46 choices<sup>30,31,35</sup>. Computational modeling indicated that ongoing changes in perceptual perfor-  
47 mance may be driven by systematic fluctuations between externally- and internally-oriented  
48 modes of sensory analysis. Model simulations suggested that such bimodal inference may  
49 improve, (i), the ability to robustly determine the statistical properties of volatile environ-  
50 ments and, (ii), the ability to calibrate internal beliefs about the degree of noise inherent in  
51 the encoding of sensory information.

## 52 **5 Results**

### 53 **5.1 Human perception fluctuates between epochs of enhanced and** 54 **reduced sensitivity to external information**

55 We began by selecting 66 studies from the Confidence Database<sup>20</sup> that investigated how  
56 human participants ( $N = 4317$ ) perform binary perceptual decisions (Figure 1A; see Methods  
57 section for details on inclusion criteria). As a metric for perceptual performance (i.e., the  
58 sensitivity to external sensory information), we asked whether the participant's response  
59 and the presented stimulus matched (*stimulus-congruent* choices) or differed from each other  
60 (*stimulus-incongruent* choices; Figure 1B and C) in a total of 21.05 million trials.

61 In a first step, we asked whether the ability to accurately perceive sensory stimuli is con-  
62 stant over time or, alternatively, fluctuates in periods of enhanced and reduced sensitivity to  
63 external information. We found perception to be stimulus-congruent in  $73.46\% \pm 0.15\%$  of  
64 trials (mean  $\pm$  standard error of the mean; Figure 2A), which was highly consistent across  
65 the selected studies (Supplemental Figure S1A). In line with previous work<sup>8</sup>, we found that  
66 the probability of stimulus-congruence was not independent across successive trials: At the  
67 group level, stimulus-congruent perceptual choices were significantly autocorrelated for up to  
68 15 trials. Autocorrelation coefficients decayed exponentially over time (rate  $\gamma = -1.92 \times 10^{-3}$

69  $\pm 4.5 \times 10^{-4}$ ,  $T(6.88 \times 10^4) = -4.27$ ,  $p = 1.98 \times 10^{-5}$ ; Figure 2B). Importantly, the autocor-  
70 relation of stimulus-congruent perception was not a trivial consequence of the experimental  
71 design, but remained significant when controlling for the trial-wise autocorrelation of task  
72 difficulty (Supplemental Figure S2A) or the sequence of presented stimuli (Supplemental  
73 Figure S2B).

74 In addition, stimulus-congruence was significantly autocorrelated not only at the group-  
75 level, but also in individual participants, where the autocorrelation of stimulus-congruent  
76 perception exceeded the respective autocorrelation of randomly permuted data within an  
77 interval of  $3.24 \pm 2.39 \times 10^{-3}$  trials (Figure 2C). In other words, if a participant's experience  
78 was congruent (or incongruent) with the external stimulus information at a given trial, her  
79 perception was more likely to be stimulus-congruent (or incongruent) for approximately 3  
80 trials into the future.

81 To further corroborate the autocorrelation of stimulus-congruence, we used logistic regression  
82 models that predicted the stimulus-congruence of perception at the index trial  $t = 0$  from the  
83 stimulus-congruence at the preceding trials within a lag of 25 trials. We found that regression  
84 weights were significantly greater than zero for up to 16 trials (Supplemental Figure S3).

85 These results confirm that the ability to process sensory signals is not constant over time, but  
86 unfolds in multi-trial epochs of enhanced and reduced sensitivity to external information<sup>8</sup>.

87 As a consequence of this autocorrelation, the dynamic probability of stimulus-congruent  
88 perception (i.e., computed in sliding windows of  $\pm 5$  trials; Figure 1C) fluctuated considerably  
89 within participants (average minimum:  $35.46\% \pm 0.22\%$ , maximum:  $98.27\% \pm 0.07\%$ ). In  
90 line with previous findings<sup>9</sup>, such fluctuations in the sensitivity to external information had a  
91 power density that was inversely proportional to the frequency in the infra-slow spectrum<sup>11</sup>  
92 ( $\text{power} \sim 1/f^\beta$ ,  $\beta = -1.32 \pm 3.14 \times 10^{-3}$ ,  $T(1.84 \times 10^5) = -419.48$ ,  $p = 0$ ; Figure 2D).

93 This feature, which is also known as *1/f noise*<sup>36,37</sup>, represents a characteristic of ongoing  
94 fluctuations in complex dynamic systems such as the brain<sup>38</sup> and the cognitive processes it

95 entertains<sup>9,10,13,39,40</sup>.

96 **5.2 Human perception fluctuates between external and internal  
97 modes of sensory processing**

98 In a second step, we sought to explain why perception cycles through periods of enhanced and  
99 reduced sensitivity to external information<sup>4,5</sup>. We reasoned that observers may intermittently  
100 rely more strongly on internal information, i.e., on predictions about the environment that  
101 are constructed from previous experiences<sup>19,31</sup>.

102 In perception, *serial dependencies* represent one of the most basic internal predictions that  
103 cause perceptual decisions to be systematically biased toward preceding choices<sup>22–33</sup>. Such  
104 effects of perceptual history mirror the continuity of the external world, in which the recent  
105 past often predicts the near future<sup>30,31,34,35,41</sup>. Therefore, as a metric for the perceptual  
106 impact of internal information, we computed whether the participant’s response at a given  
107 trial matched or differed from her response at the preceding trial (*history-congruent* and  
108 *history-incongruent perception*, respectively; Figure 1B and C).

109 First, we ensured that perceptual history played a significant role in perception despite the  
110 ongoing stream of external information. With a global average of  $52.7\% \pm 0.12\%$  history-  
111 congruent trials, we found a small but highly significant perceptual bias towards preceding  
112 experiences ( $\beta = 16.18 \pm 1.07$ ,  $T(1.09 \times 10^3) = 15.07$ ,  $p = 10^{-46}$ ; Figure 2A) that was  
113 largely consistent across studies (Supplemental Figure 1B) and more pronounced in partic-  
114 ipants who were less sensitive to external sensory information (Supplemental Figure 1C).

115 Logistic regression confirmed the internal information provided by perceptual history made  
116 a significant contribution to perception ( $\beta = 0.11 \pm 5.79 \times 10^{-3}$ ,  $z = 18.53$ ,  $p = 1.1 \times 10^{-76}$ )  
117 over and above the ongoing stream of external sensory information ( $\beta = 2.2 \pm 5.87 \times 10^{-3}$ ,  
118  $z = 375.11$ ,  $p = 0$ ) and general response biases toward one of the two potential outcomes  
119 ( $\beta = 15.19 \pm 0.08$ ,  $z = 184.98$ ,  $p = 0$ ; see Supplemental Figure S4A for model comparisons

120 within individual participants).

121 In addition, we confirmed that history-congruence was not a corollary of the sequence of  
122 presented stimuli: History-congruent perceptual choices were more frequent at trials when  
123 perception was stimulus-incongruent ( $56.03\% \pm 0.2\%$ ) as opposed to stimulus-congruent  
124 ( $51.77\% \pm 0.11\%$ ,  $\beta = -4.26 \pm 0.21$ ,  $T(8.57 \times 10^3) = -20.36$ ,  $p = 5.28 \times 10^{-90}$ ; Figure 2A,  
125 lower panel). Despite being adaptive in auto-correlated real-world environments<sup>19,34,35,42</sup>,  
126 perceptual history thus represented a source of error in the randomized experimental designs  
127 studied here<sup>24,28,30,31,43</sup>.

128 Second, we asked whether perception cycles through multi-trial epochs during which per-  
129 ception is characterized by stronger or weaker biases toward preceding experiences. Indeed,  
130 in close analogy to stimulus-congruence, history-congruence was significantly autocorrelated  
131 for up to 21 trials (Figure 2B). Following a peak at the first trial, the respective autocorre-  
132 lation coefficients decreased exponentially over time (rate  $\gamma = -6.11 \times 10^{-3} \pm 5.69 \times 10^{-4}$ ,  
133  $T(6.75 \times 10^4) = -10.74$ ,  $p = 7.18 \times 10^{-27}$ ). History-congruence remained significantly auto-  
134 correlated when controlling for task difficulty (Supplemental Figure S2A) and the sequence  
135 of presented stimuli (Supplemental Figure S2B). In individual participants, the autocorre-  
136 lation of history-congruence was elevated above randomly permuted data for a lag of  $4.87$   
137  $\pm 3.36 \times 10^{-3}$  trials (Figure 2C), confirming that the autocorrelation of history-congruence  
138 was not only a group-level phenomenon. The autocorrelation of history-congruence was con-  
139 firmed by logistic regression models that successfully predicted the history-congruence of  
140 perception at an index trial  $t = 0$  from the history-congruence at the preceding trials within  
141 a lag of 17 trials (Supplemental Figure S3).

142 Third, we asked whether the impact of internal information fluctuates as 1/f noise (i.e.,  
143 a noise characteristic classically associated with fluctuations in the sensitivity to external  
144 information<sup>9,10,13,39,40</sup>). The dynamic probability of history-congruent perception (i.e., com-  
145 puted in sliding windows of  $\pm 5$  trials; Figure 1C) varied considerably over time, ranging

<sup>146</sup> between a minimum of  $12.77\% \pm 0.14\%$  and a maximum  $92.23\% \pm 0.14\%$ . In analogy to  
<sup>147</sup> stimulus-congruence, we found that history-congruence fluctuated as  $1/f$  noise, with power  
<sup>148</sup> densities that were inversely proportional to the frequency in the infra-slow spectrum<sup>11</sup>  
<sup>149</sup> ( $\text{power} \sim 1/f^\beta$ ,  $\beta = -1.34 \pm 3.16 \times 10^{-3}$ ,  $T(1.84 \times 10^5) = -423.91$ ,  $p = 0$ ; Figure 2D).

<sup>150</sup> Finally, we ensured that fluctuations in stimulus- and history-congruence are linked to each  
<sup>151</sup> other. When perceptual choices were less biased toward external information, participants  
<sup>152</sup> relied more strongly on internal information acquired from perceptual history (and vice  
<sup>153</sup> versa,  $\beta = -0.1 \pm 8.59 \times 10^{-4}$ ,  $T(2.1 \times 10^6) = -110.96$ ,  $p = 0$ ). Thus, while sharing  
<sup>154</sup> the characteristic of  $1/f$  noise, fluctuations in stimulus- and history-congruence were shifted  
<sup>155</sup> against each other by approximately half a cycle and showed a squared coherence of  $6.49 \pm$   
<sup>156</sup>  $2.07 \times 10^{-3}\%$  (Figure 2E and F; we report the average phase and coherence for frequencies  
<sup>157</sup> below  $0.1 / N_{trials}$ ; see Methods for details).

<sup>158</sup> In sum, our analyses indicate that perceptual decisions may result from a competition be-  
<sup>159</sup> tween external sensory signals with internal predictions provided by perceptual history. Cru-  
<sup>160</sup> cially, we show that the impact of these external and internal sources of information is not  
<sup>161</sup> stable over time, but fluctuates systematically, emitting overlapping autocorrelation curves  
<sup>162</sup> and antiphase  $1/f$  noise profiles.

<sup>163</sup> These links between stimulus- and history-congruence suggest that the fluctuations in the  
<sup>164</sup> impact of external and internal information may be generated by a unifying mechanism that  
<sup>165</sup> causes perception to alternate between two opposing *modes*<sup>18</sup> (Figure 1D): During *external*  
<sup>166</sup> *mode*, perception is more strongly driven by the available external stimulus information.  
<sup>167</sup> Conversely, during *internal mode*, participants rely more heavily on internal predictions that  
<sup>168</sup> are implicitly provided by preceding perceptual experiences. Fluctuations in mode (i.e.,  
<sup>169</sup> the degree of bias toward external versus internal information) may thus provide a novel  
<sup>170</sup> explanation for ongoing fluctuations in the sensitivity to external information<sup>4,5,18</sup>.

171 **5.3 Internal and external modes of processing facilitate re-**  
172 **response behavior and enhance confidence in human perceptual**  
173 **decision-making**

174 Alternatively, however, fluctuating biases toward externally- and internally-oriented modes  
175 may not represent a perceptual phenomenon, but result from cognitive processes that are  
176 situated up- or downstream of perception. For instance, it may be argued that participants  
177 may be prone to stereotypically repeat the preceding choice when not attending to the  
178 experimental task. Thus, fluctuations in mode may arise due to systematic changes in the  
179 level of tonic arousal<sup>44</sup> or on-task attention<sup>45,46</sup>. Since arousal and attention typically link  
180 closely with response times<sup>45,47</sup> (RTs), this alternative explanation entails that RTs increase  
181 monotonically as one moves away from externally-biased and toward internally-biases modes  
182 of sensory processing.

183 As expected, stimulus-congruent (as opposed to stimulus-incongruent) choices were associ-  
184 ated with faster responses ( $\beta = -0.14 \pm 1.61 \times 10^{-3}$ ,  $T(1.99 \times 10^6) = -85.91$ ,  $p = 0$ ;  
185 Figure 2G). Intriguingly, whilst controlling for the effect of stimulus-congruence, we found  
186 that history-congruent (as opposed to history-incongruent) choices were also characterized  
187 by shorter RTs ( $\beta = -9.73 \times 10^{-3} \pm 1.38 \times 10^{-3}$ ,  $T(1.99 \times 10^6) = -7.06$ ,  $p = 1.66 \times 10^{-12}$ ;  
188 Figure 2G).

189 When analyzing the speed of response against the mode of sensory processing (Figure 2H),  
190 we found that RTs were shorter during externally-oriented perception ( $\beta_1 = -11.07 \pm 0.55$ ,  
191  $T(1.98 \times 10^6) = -20.14$ ,  $p = 3.17 \times 10^{-90}$ ). Crucially, as indicated by a quadratic relationship  
192 between the mode of sensory processing and RTs ( $\beta_2 = -19.86 \pm 0.52$ ,  $T(1.98 \times 10^6) =$   
193  $-38.43$ ,  $p = 5 \times 10^{-323}$ ), participants became faster at indicating their perceptual decision  
194 when biases toward both internal and external mode grew stronger. This argued against  
195 the view that the dynamics of pre-perceptual variables such as arousal or attention provide  
196 a plausible alternative explanation for the fluctuating perceptual impact of internal and

<sup>197</sup> external information.

<sup>198</sup> Second, it may be assumed that participants tend to repeat preceding choices when they are  
<sup>199</sup> not yet familiar with the experimental task, leading to history-congruent choices that are  
<sup>200</sup> caused by insufficient training. In the Confidence database<sup>20</sup>, training effects were visible  
<sup>201</sup> from RTs that were shortened by increasing exposure to the task ( $\beta = -7.53 \times 10^{-5} \pm 6.32 \times$   
<sup>202</sup>  $10^{-7}$ ,  $T(1.81 \times 10^6) = -119.15$ ,  $p = 0$ ). Intriguingly, however, history-congruent choices  
<sup>203</sup> became more frequent with increased exposure to the task ( $\beta = 3.6 \times 10^{-5} \pm 2.54 \times 10^{-6}$ ,  
<sup>204</sup>  $z = 14.19$ ,  $p = 10^{-45}$ ), speaking against the proposition that insufficient training induces  
<sup>205</sup> seriality in response behavior.

<sup>206</sup> As a third caveat, it could be argued that biases toward internal information reflect a post-  
<sup>207</sup> perceptual strategy that repeats preceding choices when the subjective confidence in the  
<sup>208</sup> perceptual decision is low. According to this view, subjective confidence should increase  
<sup>209</sup> monotonically as biases toward external mode become stronger.

<sup>210</sup> Stimulus-congruent (as opposed to stimulus-incongruent) choices were associated with en-  
<sup>211</sup> hanced confidence ( $\beta = 0.04 \pm 1.18 \times 10^{-3}$ ,  $T(2.06 \times 10^6) = 36.86$ ,  $p = 2.93 \times 10^{-297}$ ;  
<sup>212</sup> Figure 2I). Yet whilst controlling for the effect of stimulus-congruence, we found that history-  
<sup>213</sup> congruence also increased confidence ( $\beta = 0.48 \pm 1.38 \times 10^{-3}$ ,  $T(2.06 \times 10^6) = 351.89$ ,  $p =$   
<sup>214</sup> 0; Figure 2I).

<sup>215</sup> When depicted against the mode of sensory processing (Figure 2J), subjective confidence was  
<sup>216</sup> indeed enhanced when perception was more externally-oriented ( $\beta_1 = 92.63 \pm 1$ ,  $T(2.06 \times 10^6)$   
<sup>217</sup> = 92.89,  $p = 0$ ). Importantly, however, participants were more confident in their perceptual  
<sup>218</sup> decision for stronger biases toward both internal and external mode ( $\beta_2 = 39.3 \pm 0.94$ ,  
<sup>219</sup>  $T(2.06 \times 10^6) = 41.95$ ,  $p = 0$ ). In analogy to RTs, subjective confidence thus showed  
<sup>220</sup> a quadratic relationship to the mode of sensory processing (Figure 2J), contradicting the  
<sup>221</sup> notion that biases toward internal mode may reflect a post-perceptual strategy employed in  
<sup>222</sup> situations of low subjective confidence.

223 The above results indicate that reporting behavior and metacognition do not map linearly  
224 onto the mode of sensory processing, suggesting that slow fluctuations in the respective  
225 impact of external and internal information are most likely to affect perception at an early  
226 level of sensory analysis<sup>48,49</sup>. Such low-level processing may integrate perceptual history with  
227 external inputs into a decision variable<sup>50</sup> that influences not only perceptual choices, but also  
228 downstream functions such as speed of response and subjective confidence. Consequently,  
229 our findings predict that human participants lack full metacognitive insight into how strongly  
230 external signals and internal predictions contribute to perceptual decision-making. Stronger  
231 biases toward perceptual history thus lead to two seemingly contradictory effects: more  
232 frequent errors (Supplemental Figure 1C) and increasing subjective confidence (Figure 2I-J).  
  
233 This observation generates an intriguing prediction regarding the association of between-  
234 mode fluctuations and perceptual metacognition: Metacognitive efficiency should be lower  
235 in individuals who spend more time in internal mode, since their confidence reports are less  
236 predictive of whether the corresponding perceptual decision is correct. We computed each  
237 participant's M-ratio<sup>51</sup> ( $\text{meta-}d'/d' = 0.85 \pm 0.02$ ) to probe this hypothesis independently of  
238 inter-individual differences in perceptual performance. Indeed, we found that biases toward  
239 internal information (i.e., as defined by the average probability of history-congruence) were  
240 stronger in participants with lower metacognitive efficiency ( $\beta = -2.98 \times 10^{-3} \pm 9.82 \times 10^{-4}$ ,  
241  $T(4.14 \times 10^3) = -3.03$ ,  $p = 2.43 \times 10^{-3}$ ).

## 242 **5.4 Fluctuations between internal and external mode modulate 243 perceptual performance beyond the effect of general response 244 biases**

245 The above sections provide correlative evidence that recurring intervals of stronger perceptual  
246 history temporally reduce the participants' sensitivity to external information. Importantly,  
247 the history-dependent biases that characterize internal mode processing must be differenti-

248 ated from general response biases. In binary perceptual decision-making, general response  
249 biases are defined by a propensity to choose one of the two outcomes more often than the  
250 alternative. Indeed, in the experiments considered here, participants selected the more fre-  
251 quent of the two possible outcomes in  $58.71\% \pm 0.22\%$  of trials.

252 Two caveats have to be considered to make sure that the effect of history-congruence is  
253 distinct from the effect of general response biases. First, history-congruent states become  
254 more likely for larger response biases that cause a increasing imbalance in the likelihood of  
255 the two outcomes ( $\beta = 0.24 \pm 6.93 \times 10^{-4}$ ,  $T(2.09 \times 10^6) = 342.43$ ,  $p = 0$ ). One may thus  
256 ask whether the autocorrelation of history-congruence could be entirely driven by general  
257 response biases. Yet the above analyses account for general response biases by computing  
258 group-level autocorrelations (see Figure 2C) relative to randomly permuted data (i.e., by  
259 subtracting the autocorrelation of randomly permuted data from the raw autocorrelation  
260 curve). This precludes that general response biases contribute to the observed autocorrela-  
261 tion of history-congruence (see Supplemental Figure S5 for a visualization of the correction  
262 procedure for simulated data with general response biases ranging from 60 to 90%).

263 Second, it may be argued that fluctuations in perceptual performance may be solely driven  
264 by ongoing changes in the strength of general response biases. To assess the links between  
265 dynamic fluctuations in stimulus-congruence on the one hand and history-congruence as  
266 well as general response bias on the other hand, we computed all variables as dynamic  
267 probabilities in sliding windows of  $\pm 5$  trials (see Figure 1C). Linear mixed effects modeling  
268 indicated that fluctuations in history-congruent biases were larger in amplitude than the  
269 corresponding fluctuations in general response biases ( $\beta_0 = 0.03 \pm 7.34 \times 10^{-3}$ ,  $T(64.94) =$   
270  $4.46$ ,  $p = 3.28 \times 10^{-5}$ ). Crucially, ongoing fluctuations in history-congruence had a significant  
271 effect on stimulus-congruence ( $\beta_1 = -0.05 \pm 5.63 \times 10^{-4}$ ,  $T(2.1 \times 10^6) = -84.21$ ,  $p = 0$ )  
272 beyond the effect of ongoing changes in general response biases ( $\beta_2 = -0.06 \pm 5.82 \times 10^{-4}$ ,  
273  $T(2.1 \times 10^6) = -103.51$ ,  $p = 0$ ). In sum, the above control analyses confirm that the observed

274 influence of preceding choices on perceptual decision-making cannot not be reduced to general  
275 response biases.

276 **5.5 Internal mode is characterized by lower thresholds as well as**  
277 **by history-dependent changes in biases and lapses**

278 In a final control analysis, we asked whether history-independent changes in biases and  
279 lapses may provide an alternative explanation of internal mode processing. To this end, we  
280 estimated full and history-conditioned psychometric curves to investigate how internal and  
281 external mode relate to biases (i.e., the horizontal position of the psychometric curve), lapses  
282 (i.e., the asymptotes of the psychometric curve) and thresholds (i.e., 1/sensitivity, estimated  
283 from the slope of the psychometric curve). We used a maximum likelihood procedure to  
284 predict trial-wise choices  $y$  ( $y = 0$  and  $y = 1$  for outcomes A and B respectively) from the  
285 choice probabilities  $y_p$ .  $y_p$  was computed from difficulty-weighted inputs  $s_w$  via a parametric  
286 error function defined by the parameters  $\gamma$  (lower lapse),  $\delta$  (upper lapse),  $\mu$  (bias) and  $t$   
287 (threshold; see Methods for details):

$$y_p = \gamma + (1 - \gamma - \delta) * (\text{erf}(\frac{s_w + \mu}{t}) + 1)/2 \quad (1)$$

288 Across the full dataset (i.e., irrespective of the preceding perceptual choice  $y_{t-1}$ ), biases  $\mu$   
289 were distributed around zero ( $-0.05 \pm 0.03$ ;  $\beta_0 = 7.37 \times 10^{-3} \pm 0.09$ ,  $T(36.8) = 0.08$ ,  $p =$   
290 0.94; see Figure 3A and B, upper panel). When conditioned on perceptual history, biases  
291  $\mu$  varied according to the preceding perceptual choice, with negative biases for  $y_{t-1} = 0$   
292 ( $-0.22 \pm 0.04$ ;  $\beta_0 = 0.56 \pm 0.12$ ,  $T(43.39) = 4.6$ ,  $p = 3.64 \times 10^{-5}$ ) and positive biases for  
293  $y_{t-1} = 1$  ( $0.29 \pm 0.03$ ;  $\beta_0 = 0.56 \pm 0.12$ ,  $T(43.39) = 4.6$ ,  $p = 3.64 \times 10^{-5}$ ). Absolute biases  
294  $|\mu|$  were larger in internal mode ( $1.84 \pm 0.03$ ) as compared to external mode ( $0.86 \pm 0.02$ ;  
295  $\beta_0 = -0.62 \pm 0.07$ ,  $T(45.62) = -8.38$ ,  $p = 8.59 \times 10^{-11}$ ; controlling for differences in lapses  
296 and thresholds).

297 Lower and upper lapses amounted to  $\gamma = 0.13 \pm 2.83 \times 10^{-3}$  and  $\delta = 0.1 \pm 2.45 \times 10^{-3}$  (see  
298 Figure 3A, C and D). Lapses were larger in internal mode ( $\gamma = 0.17 \pm 3.52 \times 10^{-3}$ ,  $\delta = 0.14$   
299  $\pm 3.18 \times 10^{-3}$ ) as compared to external mode ( $\gamma = 0.1 \pm 2.2 \times 10^{-3}$ ,  $\delta = 0.08 \pm 2 \times 10^{-3}$ ;  
300  $\beta_0 = -0.05 \pm 5.73 \times 10^{-3}$ ,  $T(47.03) = -9.11$ ,  $p = 5.94 \times 10^{-12}$ ; controlling for differences  
301 in biases and thresholds).

302 Conditioning on the previous perceptual choice revealed that the between-mode difference  
303 in lapse was not general, but depended on perceptual history: For  $y_{t-1} = 0$ , only higher  
304 lapses  $\delta$  differed between internal and external mode ( $\beta_0 = -0.1 \pm 9.58 \times 10^{-3}$ ,  $T(36.87) =$   
305  $-10.16$ ,  $p = 3.06 \times 10^{-12}$ ), whereas lower lapses  $\gamma$  did not ( $\beta_0 = 0.01 \pm 7.77 \times 10^{-3}$ ,  $T(33.1)$   
306  $= 1.61$ ,  $p = 0.12$ ). Vice versa, for  $y_{t-1} = 1$ , lower lapses  $\gamma$  differed between internal and  
307 external mode ( $\beta_0 = -0.11 \pm 0.01$ ,  $T(40.11) = -9.59$ ,  $p = 6.14 \times 10^{-12}$ ), whereas higher  
308 lapses  $\delta$  did not ( $\beta_0 = 0.01 \pm 7.74 \times 10^{-3}$ ,  $T(33.66) = 1.58$ ,  $p = 0.12$ ).

309 Thresholds  $t$  were estimated at  $3 \pm 0.06$  (see Figure 3A and E). Thresholds  $t$  were larger  
310 in internal mode ( $3.66 \pm 0.09$ ) as compared to external mode ( $2.02 \pm 0.03$ ;  $\beta_0 = -1.77 \pm$   
311  $0.25$ ,  $T(50.45) = -7.14$ ,  $p = 3.48 \times 10^{-9}$ ; controlling for differences in biases and lapses).

312 In contrast to the bias  $\mu$  and the lapse rates  $\gamma$  and  $\delta$ , thresholds  $t$  were not modulated by  
313 perceptual history ( $\beta_0 = 0.04 \pm 0.06$ ,  $T(2.97 \times 10^3) = 0.73$ ,  $p = 0.47$ ).

314 In sum, the above analyses showed that internal and external mode differ with respect  
315 to biases, lapses and thresholds. Internally-biased processing was characterized by higher  
316 thresholds, indicating a reduced sensitivity to sensory information, as well as by larger biases  
317 and lapses. Importantly, between-mode differences in biases and lapses strongly depended  
318 on perceptual history. This confirmed that internal mode processing cannot be explained  
319 solely on the ground of a general (i.e., history-independent) increase in lapses or bias.

320 **5.6 Mice waver between external and internal modes of perceptual**  
321 **decision-making**

322 In a prominent functional explanation for serial dependencies<sup>22–28,32,33,48</sup>, perceptual his-  
323 tory is cast as an internal prediction that leverages the temporal autocorrelation of natural  
324 environments for efficient decision-making<sup>30,31,34,35,41</sup>. We reasoned that, since this autocor-  
325 relation is one of the most basic features of our sensory world, fluctuating biases toward  
326 preceding perceptual choices should not be a uniquely human phenomenon.

327 To test whether externally and internally oriented modes of processing exist beyond the  
328 human mind, we analyzed data on perceptual decision-making in mice that were extracted  
329 from the International Brain Laboratory (IBL) dataset<sup>21</sup>. Here, we restricted our analyses  
330 to the *basic* task<sup>21</sup>, in which mice responded to gratings of varying contrast that appeared  
331 either in the left or right hemifield of with equal probability. We excluded sessions in which  
332 mice did not respond correctly to stimuli presented at a contrast above 50% in more than  
333 80% of trials (see Methods), which yielded a final sample of  $N = 165$  adequately trained  
334 mice that went through 1.46 million trials.

335 In line with humans, mice were biased toward perceptual history in  $54.03\% \pm 0.17\%$  of trials  
336 ( $T(164) = 23.65$ ,  $p = 9.98 \times 10^{-55}$ ; Figure 4A and Supplemental Figure S1D). Perceptual  
337 history effects remained significant ( $\beta = 0.51 \pm 4.49 \times 10^{-3}$ ,  $z = 112.84$ ,  $p = 0$ ) when  
338 controlling for external sensory information ( $\beta = 2.96 \pm 4.58 \times 10^{-3}$ ,  $z = 646.1$ ,  $p = 0$ )  
339 and general response biases toward one of the two potential outcomes ( $\beta = -1.78 \pm 0.02$ ,  
340  $z = -80.64$ ,  $p = 0$ ; see Supplemental Figure S4C-D for model comparisons and  $\beta$  values  
341 computed within individual mice).

342 In the *basic* task of the IBL dataset<sup>21</sup>, stimuli were presented at random in either the left  
343 or right hemifield. Stronger biases toward perceptual history should therefore decrease per-  
344 ceptual performance. Indeed, history-congruent choices were more frequent when perception  
345 was stimulus-incongruent ( $61.59\% \pm 0.07\%$ ) as opposed to stimulus-congruent ( $51.81\% \pm$

<sup>346</sup> 0.02%,  $T(164) = 31.37$ ,  $p = 3.36 \times 10^{-71}$ ;  $T(164) = 31.37$ ,  $p = 3.36 \times 10^{-71}$ ; Figure 4A,  
<sup>347</sup> lower panel), confirming that perceptual history was a source of error<sup>24,28,30,31,43</sup> as opposed  
<sup>348</sup> to a feature of the experimental paradigm. Overall, perception was stimulus-congruent in  
<sup>349</sup>  $81.37\% \pm 0.3\%$  of trials (Figure 4A).

<sup>350</sup> At the group level, we found significant autocorrelations in both stimulus-congruence (86  
<sup>351</sup> consecutive trials) and history-congruence (8 consecutive trials), which remained significant  
<sup>352</sup> when taking into account the respective autocorrelation of task difficulty and external stim-  
<sup>353</sup> ulation (Supplemental Figure 2C-D). In contrast to humans, mice showed a negative auto-  
<sup>354</sup> correlation coefficient of stimulus-congruence at trial 2. This was due to a feature of the  
<sup>355</sup> experimental design: Errors at a contrast above 50% were followed by a high-contrast stimu-  
<sup>356</sup> lus at the same location. Thus, stimulus-incongruent choices on easy trials were more likely  
<sup>357</sup> to be followed by stimulus-congruent perceptual choices that were facilitated by high-contrast  
<sup>358</sup> visual stimuli<sup>21</sup>.

<sup>359</sup> The autocorrelation of history-congruence closely overlapped with the human data and de-  
<sup>360</sup> cayed exponentially after a peak at the first trial (rate  $\gamma = -6.7 \times 10^{-3} \pm 5.94 \times 10^{-4}$ ,  
<sup>361</sup>  $T(3.69 \times 10^4) = -11.27$ ,  $p = 2.07 \times 10^{-29}$ ; Figure 4B). On the level of individual mice, au-  
<sup>362</sup> tocorrelation coefficients were elevated above randomly permuted data within a lag of  $4.59$   
<sup>363</sup>  $\pm 0.06$  trials for stimulus-congruence and  $2.58 \pm 0.01$  trials for history-congruence (Figure  
<sup>364</sup> 4C).

<sup>365</sup> To further corroborate a significant autocorrelation of stimulus- and history-congruence in  
<sup>366</sup> mice, we used logistic regression models that predicted the stimulus-/history-congruence of  
<sup>367</sup> perception at the index trial  $t = 0$  from the stimulus/history-congruence at the preceding  
<sup>368</sup> trials within a lag of 25 trials. We found that regression weights were significantly greater  
<sup>369</sup> than zero for more than 25 trials for stimulus-congruence. For history-congruence, regression  
<sup>370</sup> weights significantly greater than zero for 8 trials prior to the index trial (Supplemental  
<sup>371</sup> Figure S3). In analogy to humans, mice showed anti-phase 1/f fluctuations in the sensitivity

<sup>372</sup> to internal and external information (Figure 4D-F).

<sup>373</sup> Next, we asked how external and internal modes relate to the trial duration (TD, a coarse  
<sup>374</sup> measure of RT in mice that spans the interval from stimulus onset to feedback<sup>21</sup>). Stimulus-  
<sup>375</sup> congruent (as opposed to stimulus-incongruent) choices were associated with shorter TDs ( $\delta$   
<sup>376</sup>  $= -262.48 \pm 17.1$ ,  $T(164) = -15.35$ ,  $p = 1.55 \times 10^{-33}$ ), while history-congruent choices were  
<sup>377</sup> characterized by longer TDs ( $\delta = 30.47 \pm 5.57$ ,  $T(164) = 5.47$ ,  $p = 1.66 \times 10^{-7}$ ; Figure 4G).

<sup>378</sup> Across the full spectrum of the available data, TDs showed a linear relationship with the  
<sup>379</sup> mode of sensory processing, with shorter TDs during external mode ( $\beta_1 = -4.16 \times 10^4 \pm$   
<sup>380</sup>  $1.29 \times 10^3$ ,  $T(1.35 \times 10^6) = -32.31$ ,  $p = 6.03 \times 10^{-229}$ , Figure 4H). However, an explorative  
<sup>381</sup> post-hoc analysis limited to TDs that differed from the median TD by no more than  $1.5 \times$   
<sup>382</sup> MAD (median absolute distance<sup>52</sup>) indicated that, when mice engaged with the task more  
<sup>383</sup> swiftly, TDs did indeed show a quadratic relationship with the mode of sensory processing  
<sup>384</sup> ( $\beta_2 = -1.97 \times 10^3 \pm 843.74$ ,  $T(1.19 \times 10^6) = -2.34$ ,  $p = 0.02$ , Figure 4I).

<sup>385</sup> As in humans, it is an important caveat to consider whether the observed serial dependencies  
<sup>386</sup> in murine perception reflect a phenomenon of perceptual inference, or, alternatively, an  
<sup>387</sup> unspecific strategy that occurs at the level of reporting behavior. We reasoned that, if mice  
<sup>388</sup> indeed tended to repeat previous choices as a general response pattern, history effects should  
<sup>389</sup> decrease during training of the perceptual task. We therefore analyzed how stimulus- and  
<sup>390</sup> history-congruent perceptual choices evolved across sessions in mice that, by the end of  
<sup>391</sup> training, achieved proficiency (i.e., stimulus-congruence  $\geq 80\%$ ) in the *basic* task of the IBL  
<sup>392</sup> dataset<sup>21</sup>.

<sup>393</sup> As expected, we found that stimulus-congruent perceptual choices became more frequent ( $\beta$   
<sup>394</sup>  $= 0.34 \pm 7.13 \times 10^{-3}$ ,  $T(8.51 \times 10^3) = 47.66$ ,  $p = 0$ ; Supplemental Figure S6) and TDs were  
<sup>395</sup> progressively shortened ( $\beta = -22.14 \pm 17.06$ ,  $T(1.14 \times 10^3) = -1.3$ ,  $p = 0$ ) across sessions.  
<sup>396</sup> Crucially, the frequency of history-congruent perceptual choices also increased during train-  
<sup>397</sup> ing ( $\beta = 0.13 \pm 4.67 \times 10^{-3}$ ,  $T(8.4 \times 10^3) = 27.04$ ,  $p = 1.96 \times 10^{-154}$ ; Supplemental Figure

<sup>398</sup> S6).

<sup>399</sup> As in humans, longer within-session task exposure was associated with an increase in history-  
<sup>400</sup> congruence ( $\beta = 3.6 \times 10^{-5} \pm 2.54 \times 10^{-6}$ ,  $z = 14.19$ ,  $p = 10^{-45}$ ) and a decrease in TDs ( $\beta$   
<sup>401</sup>  $= -0.1 \pm 3.96 \times 10^{-3}$ ,  $T(1.34 \times 10^6) = -24.99$ ,  $p = 9.45 \times 10^{-138}$ ). In sum, these findings  
<sup>402</sup> strongly argue against the proposition that mice show biases toward perceptual history due  
<sup>403</sup> to an unspecific response strategy.

<sup>404</sup> As in humans, fluctuations in the strength of history-congruent biases were, (i), larger in  
<sup>405</sup> amplitude than the corresponding fluctuations in general response biases ( $\beta_0 = -5.26 \times 10^{-3}$   
<sup>406</sup>  $\pm 4.67 \times 10^{-4}$ ,  $T(2.12 \times 10^3) = -11.28$ ,  $p = 1.02 \times 10^{-28}$ ) and, (ii), had a significant effect on  
<sup>407</sup> stimulus-congruence ( $\beta_1 = -0.12 \pm 7.17 \times 10^{-4}$ ,  $T(1.34 \times 10^6) = -168.39$ ,  $p = 0$ ) beyond the  
<sup>408</sup> effect of ongoing changes in general response biases ( $\beta_2 = -0.03 \pm 6.94 \times 10^{-4}$ ,  $T(1.34 \times 10^6)$   
<sup>409</sup>  $= -48.14$ ,  $p = 0$ ). This confirmed that, in both humans and mice, perceptual performance  
<sup>410</sup> is modulated by systematic fluctuations between externally- and internally-oriented modes  
<sup>411</sup> of sensory processing.

<sup>412</sup> Finally, we fitted full and history-conditioned psychometric curves to the data from the  
<sup>413</sup> IBL database. When estimated based on the full dataset (i.e., irrespective of the preceding  
<sup>414</sup> perceptual choice  $y_{t-1}$ ), biases  $\mu$  were distributed around zero ( $3.87 \times 10^{-3} \pm 9.81 \times 10^{-3}$ ;  
<sup>415</sup>  $T(164) = 0.39$ ,  $p = 0.69$ ; Figure 5A and B, upper panel). When conditioned on the preceding  
<sup>416</sup> perceptual choice, biases were negative for  $y_{t-1} = 0$  ( $-0.02 \pm 8.7 \times 10^{-3}$ ;  $T(164) = -1.99$ ,  $p =$   
<sup>417</sup> 0.05; Figure 5A and B, middle panel) and positive for  $y_{t-1} = 1$  ( $0.02 \pm 9.63 \times 10^{-3}$ ;  $T(164)$   
<sup>418</sup>  $= 1.91$ ,  $p = 0.06$ ; Figure 5A and B, lower panel). As in humans, mice showed larger biases  
<sup>419</sup> during internal mode ( $0.14 \pm 7.96 \times 10^{-3}$ ) as compared to external mode ( $0.07 \pm 8.7 \times 10^{-3}$ ;  
<sup>420</sup>  $\beta_0 = -0.18 \pm 0.03$ ,  $T = -6.38$ ,  $p = 1.77 \times 10^{-9}$ ; controlling for differences in lapses and  
<sup>421</sup> thresholds).

<sup>422</sup> Lower and upper lapses amounted to  $\gamma = 0.1 \pm 4.35 \times 10^{-3}$  and  $\delta = 0.11 \pm 4.65 \times 10^{-3}$   
<sup>423</sup> (see Figure 5A, C and D). Lapse rates were higher in internal mode ( $\gamma = 0.15 \pm 5.14 \times 10^{-3}$ ,

<sup>424</sup>  $\delta = 0.16 \pm 5.79 \times 10^{-3}$ ) as compared to external mode ( $\gamma = 0.06 \pm 3.11 \times 10^{-3}$ ,  $\delta = 0.07$   
<sup>425</sup>  $\pm 3.34 \times 10^{-3}$ ;  $\beta_0 = -0.11 \pm 4.39 \times 10^{-3}$ ,  $T = -24.8$ ,  $p = 4.91 \times 10^{-57}$ ; controlling for  
<sup>426</sup> differences in biases and thresholds).

<sup>427</sup> For  $y_{t-1} = 0$ , the difference between internal and external mode was more pronounced for  
<sup>428</sup> higher lapses  $\delta$  ( $T(164) = 21.44$ ,  $p = 1.93 \times 10^{-49}$ ). Conversely, for  $y_{t-1} = 1$ , the difference  
<sup>429</sup> between internal and external mode was more pronounced for lower lapses  $\gamma$  ( $T(164) = -$   
<sup>430</sup>  $18.24$ ,  $p = 2.68 \times 10^{-41}$ ). In contrast to the human data, higher lapses  $\delta$  and lower lapses  
<sup>431</sup>  $\gamma$  were significantly elevated during internal mode irrespective of the preceding perceptual  
<sup>432</sup> choice (higher lapses  $\delta$  for  $y_{t-1} = 1$ :  $T(164) = -2.65$ ,  $p = 8.91 \times 10^{-3}$ ; higher lapses  $\delta$  for  
<sup>433</sup>  $y_{t-1} = 0$ :  $T(164) = -28.29$ ,  $p = 5.62 \times 10^{-65}$ ; lower lapses  $\gamma$  for  $y_{t-1} = 1$ :  $T(164) = -32.44$ ,  
<sup>434</sup>  $p = 2.92 \times 10^{-73}$ ; lower lapses  $\gamma$  for  $y_{t-1} = 0$ :  $T(164) = -2.5$ ,  $p = 0.01$ ).

<sup>435</sup> In mice, thresholds  $t$  amounted to  $0.15 \pm 6.52 \times 10^{-3}$  (see Figure 5A and E) and were higher  
<sup>436</sup> in internal mode ( $0.27 \pm 0.01$ ) as compared to external mode ( $0.09 \pm 4.44 \times 10^{-3}$ ;  $\beta_0 =$   
<sup>437</sup>  $-0.28 \pm 0.04$ ,  $T = -7.26$ ,  $p = 1.53 \times 10^{-11}$ ; controlling for differences in biases and lapses).  
<sup>438</sup> Thresholds  $t$  were not modulated by perceptual history ( $T(164) = 0.94$ ,  $p = 0.35$ ).

<sup>439</sup> In sum, the above analyses of the psychometric function in mice corroborated our findings in  
<sup>440</sup> humans. Higher thresholds indicated a reduced sensitivity to external information during in-  
<sup>441</sup> ternal mode. Additionally, internally-biased processing was characterized history-dependent  
<sup>442</sup> modulation of biases and lapses.

## <sup>443</sup> **5.7 Fluctuations in mode result from coordinated changes in the 444 impact of external and internal information on perception**

<sup>445</sup> The empirical data presented above indicate that, for both humans and mice, perception  
<sup>446</sup> fluctuates between internal and external modes, i.e., multi-trial epochs that are characterized  
<sup>447</sup> by enhanced sensitivity toward either internal or external information. Since natural envi-  
<sup>448</sup> ronments typically show high temporal redundancy<sup>34</sup>, previous experiences are often good

<sup>449</sup> predictors of new stimuli<sup>30,31,35,41</sup>. Serial dependencies may therefore induce autocorrelations in perception by serving as an internal prediction (or *memory* processes<sup>9,13</sup>) about the environment that actively integrates noisy sensory information over time<sup>53</sup>.

<sup>452</sup> Previous work has shown that such internal predictions are built by dynamically updating the estimated probability of being in a particular perceptual state from the sequence of preceding experiences<sup>35,48,54</sup>. The integration of sequential inputs may lead to accumulating effects of perceptual history that progressively override incoming sensory information, enabling internal mode processing<sup>19</sup>. However, since such a process would lead to internal biases that may eventually become impossible to overcome<sup>55</sup>, we assumed that changes in mode may additionally be driven by ongoing wave-like fluctuations<sup>9,13</sup> in the perceptual impact of external and internal information that occur *irrespective* of the sequence of previous experiences and temporarily de-couple the decision variable from implicit internal representations of the environment<sup>19</sup>.

<sup>462</sup> Following Bayes' theorem, we reasoned that binary perceptual decisions depend on the posterior log ratio  $L$  of the two alternative states of the environment that participants learn about via noisy sensory information<sup>54</sup>. We computed the posterior by combining the sensory evidence available at time-point  $t$  (i.e., the log likelihood ratio  $LLR$ ) with the prior probability  $\psi$ :

$$L_t = LLR_t * \omega_{LLR} + \psi_t(L_{t-1}, H) * \omega_\psi \quad (2)$$

<sup>467</sup> We derived the prior probability  $\psi$  at timepoint  $t$  from the posterior probability of perceptual outcomes at timepoint  $L_{t-1}$ . Since a switch between the two states can occur at any time, the effect of perceptual history varies according to both the sequence of preceding experiences and the estimated stability of the external environment (i.e., the *hazard rate*  $H$ <sup>54</sup>):

$$\psi_t(L_{t-1}, H) = L_{t-1} + \log\left(\frac{1-H}{H}\right) + \exp(-L_{t-1}) - \log\left(\frac{1-H}{H}\right) - \exp(L_{t-1}) \quad (3)$$

<sup>471</sup> The *LLR* was computed from inputs  $s_t$  by applying a sigmoid function defined by parameter  
<sup>472</sup>  $\alpha$  that controls the sensitivity of perception to the available sensory information (see Methods  
<sup>473</sup> for detailed equations on humans and mice):

$$u_t = \frac{1}{1 + \exp(-\alpha * s_t)} \quad (4)$$

$$LLR_t = \log\left(\frac{u_t}{1 - u_t}\right) \quad (5)$$

<sup>474</sup> To allow for *bimodal inference*, i.e., alternating periods of internally- and externally-biased  
<sup>475</sup> modes of perceptual processing that occur irrespective of the sequence of preceding experi-  
<sup>476</sup> ences, we assumed that the relative influences of likelihood and prior show coherent anti-  
<sup>477</sup> phase fluctuations governed by  $\omega_{LLR}$  and  $\omega_\psi$  that are determined by amplitude  $a$ , frequency  
<sup>478</sup>  $f$  and phase  $p$ :

$$\omega_{LLR} = a_{LLR} * \sin(f * t + p) + 1 \quad (6)$$

$$\omega_\psi = a_\psi * \sin(f * t + p + \pi) + 1 \quad (7)$$

<sup>479</sup> Finally, a sigmoid transform of the posterior  $L_t$  yields the probability of observing the  
<sup>480</sup> perceptual decision  $y_t$  at a temperature determined by  $\zeta^{-1}$ :

$$P(y_t = 1) = 1 - P(y_t = 0) = \frac{1}{1 + \exp(-\zeta * L_t)} \quad (8)$$

481 Fitting the bimodal inference model outlined above to behavioral data (see Methods for  
482 details) characterizes each subject by a sensitivity parameter  $\alpha$  that captures how strongly  
483 perception is driven by the available sensory information, and a hazard rate parameter  $H$   
484 that controls how heavily perception is biased by perceptual history. As a sanity check for  
485 model fit, we tested whether the frequency of stimulus- and history-congruent trials in the  
486 Confidence database<sup>20</sup> and IBL database<sup>21</sup> correlate with the estimated parameters  $\alpha$  and  
487  $H$ , respectively. As expected, the estimated sensitivity toward stimulus information  $\alpha$  was  
488 positively correlated with the frequency of stimulus-congruent perceptual choices (humans:  
489  $\beta = 8.4 \pm 0.26$ ,  $T(4.31 \times 10^3) = 32.87$ ,  $p = 1.3 \times 10^{-211}$ ; mice:  $\beta = 1.93 \pm 0.12$ ,  
490  $T(2.07 \times 10^3) = 16.21$ ,  $p = 9.37 \times 10^{-56}$ ). Likewise,  $H$  was negatively correlated with the frequency of  
491 history-congruent perceptual choices (humans:  $\beta = -11.84 \pm 0.5$ ,  $T(4.29 \times 10^3) = -23.5$ ,  
492  $p = 5.16 \times 10^{-115}$ ; mice:  $\beta = -6.18 \pm 0.66$ ,  $T(2.08 \times 10^3) = -9.37$ ,  $p = 1.85 \times 10^{-20}$ ).

493 Our behavioral analyses have shown that humans and mice showed significant ef-  
494 fects of perceptual history that impaired performance in randomized psychophysical  
495 experiments<sup>24,28,30,31,43</sup> (Figure 2A and 3A). We therefore expected that humans and mice  
496 underestimated the true hazard rate  $\hat{H}$  of the experimental environments (Confidence  
497 database<sup>20</sup>:  $\hat{H}_{Humans} = 0.5 \pm 1.58 \times 10^{-5}$ ); IBL database<sup>21</sup>:  $\hat{H}_{Mice} = 0.49 \pm 6.47 \times 10^{-5}$ ).  
498 Indeed, when fitting the bimodal inference model outlined above to the trial-wise perceptual  
499 choices (see Methods), we found that the estimated (i.e., subjective) hazard rate  $H$  was  
500 lower than  $\hat{H}$  for both humans ( $H = 0.45 \pm 4.8 \times 10^{-5}$ ,  $\beta = -6.87 \pm 0.94$ ,  $T(61.87) =$   
501  $-7.33$ ,  $p = 5.76 \times 10^{-10}$ ) and mice ( $H = 0.46 \pm 2.97 \times 10^{-4}$ ,  $\beta = -2.91 \pm 0.34$ ,  $T(112.57)$   
502  $= -8.51$ ,  $p = 8.65 \times 10^{-14}$ ).

503 Simulations from the bimodal inference model (based on the posterior model parameters  
504 obtained in humans; see Methods for details) closely matched the empirical results outlined  
505 above: Simulated perceptual decisions resulted from a competition of perceptual history with  
506 incoming sensory signals (Figure 6A). Stimulus- and history-congruence were significantly

507 auto-correlated (Figure 6B-C), fluctuating in anti-phase as 1/f noise (Figure 6D-F). Simu-  
508 lated posterior certainty<sup>28,30,50</sup> (i.e., the absolute of the posterior log ratio  $|L_t|$ ) showed a  
509 quadratic relationship to the mode of sensory processing (Figure 6H), mirroring the relation  
510 of RTs and confidence reports to external and internal biases in perception (Figure 2G-H  
511 and Figure 4G-H). Crucially, the overlap between empirical and simulated data broke down  
512 when we removed the anti-phase oscillations ( $\omega_{LLR}$  and/or  $\omega_\psi$ ) or the accumulation of evi-  
513 dence over time (i.e., setting  $H$  to 0.5) from the bimodal inference model (see Supplemental  
514 Figure S7-10).

515 To further probe the validity of the bimodal inference model, we tested whether posterior  
516 model quantities could explain aspects of the behavioral data that the model was not fitted  
517 to. First, we predicted that the posterior decision variable  $L_t$  not only encodes perceptual  
518 choices (i.e., the variable used for model estimation), but should also predict the speed of  
519 response and subjective confidence<sup>30,50</sup>. Indeed, the estimated trial-wise posterior decision  
520 certainty  $|L_t|$  correlated negatively with RTs in humans ( $\beta = -4.36 \times 10^{-3} \pm 4.64 \times 10^{-4}$ ,  
521  $T(1.98 \times 10^6) = -9.41$ ,  $p = 5.19 \times 10^{-21}$ ) and TDs mice ( $\beta = -35.45 \pm 0.86$ ,  $T(1.28 \times 10^6) =$   
522  $-41.13$ ,  $p = 0$ ). Likewise, subjective confidence was positively correlated with the estimated  
523 posterior decision certainty in humans ( $\beta = 7.63 \times 10^{-3} \pm 8.32 \times 10^{-4}$ ,  $T(2.06 \times 10^6) =$   
524  $9.18$ ,  $p = 4.48 \times 10^{-20}$ ).

525 Second, the dynamic accumulation of information inherent to our model entails that biases  
526 toward perceptual history are stronger when the posterior decision certainty at the preceding  
527 trial is high<sup>30,31,54</sup>. Due to the link between posterior decision certainty and confidence, we  
528 reasoned that confident perceptual choices should be more likely to induce history-congruent  
529 perception at the subsequent trial<sup>30,31</sup>. Indeed, logistic regression indicated that history-  
530 congruence was predicted by the posterior decision certainty  $|L_{t-1}|$  (humans:  $\beta = 8.22 \times 10^{-3}$   
531  $\pm 1.94 \times 10^{-3}$ ,  $z = 4.25$ ,  $p = 2.17 \times 10^{-5}$ ; mice:  $\beta = -3.72 \times 10^{-3} \pm 1.83 \times 10^{-3}$ ,  $z =$   
532  $-2.03$ ,  $p = 0.04$ ) and subjective confidence (humans:  $\beta = 0.04 \pm 1.62 \times 10^{-3}$ ,  $z = 27.21$ ,  $p$

<sub>533</sub>  $= 4.56 \times 10^{-163}$ ) at the preceding trial.

<sub>534</sub> In sum, computational modeling thus suggested that between-mode fluctuations are best  
<sub>535</sub> explained by two interlinked processes (Figure 1E): (i), the dynamic accumulation of infor-  
<sub>536</sub> mation across successive trials (i.e., following the estimated hazard rate  $H$ ) and, (ii), ongoing  
<sub>537</sub> anti-phase oscillations in the impact of external and internal information (i.e., as determined  
<sub>538</sub> by  $\omega_\psi$  and  $\omega_{LLR}$ ).

## <sub>539</sub> **5.8 Bimodal inference improves learning and perceptual metacog- 540 nition in the absence of feedback**

<sub>541</sub> Is there a computational benefit to be gained from temporarily down-regulating biases to-  
<sub>542</sub> ward preceding choices (Figure 2-3 B and C), instead of combining them with external  
<sub>543</sub> sensory information at a constant weight (Supplemental Figure S7)? In their adaptive func-  
<sub>544</sub> tion for perceptual decision-making, internal predictions critically depend on error-driven  
<sub>545</sub> learning to remain aligned with the current state of the world<sup>56</sup>. Yet when the same network  
<sub>546</sub> processes external and internal information in parallel, inferences may become circular and  
<sub>547</sub> maladaptive<sup>57</sup>: Ongoing decision-related activity may be distorted by noise in external sen-  
<sub>548</sub> sory signals that are fed forward from the periphery or, alternatively, by aberrant internal  
<sub>549</sub> predictions about the environment that are fed back from higher cortical levels<sup>18,57</sup>.

<sub>550</sub> Purely parallel processing therefore creates at least two challenges for perception: First,  
<sub>551</sub> due to the sequential integration of inputs over time, internal predictions may progressively  
<sub>552</sub> override sensory information<sup>55</sup>, leading to false inferences about the presented stimuli<sup>19</sup>. As a  
<sub>553</sub> consequence, purely parallel processing may also lead to false inferences about the statistical  
<sub>554</sub> regularities of volatile environments, where the underlying hazard rate  $\hat{H} = P(s_t \neq s_{t-1})$   
<sub>555</sub> (i.e., the probability of a change in the state of the environment between two trials) may  
<sub>556</sub> change over time. In the absence of feedback, agents have to update the estimate about  $\hat{H}$   
<sub>557</sub> solely on the grounds of their experience, which is determined by the posterior log ratio  $L_t$ .

558 Yet  $L_t$  depends not only on external information from the environment (the log likelihood  
559 ratio  $LLR_t$ ), but also on internal predictions, i.e., the log prior ratio  $L_{t-1}$  and the assumed  
560 hazard rate  $H_t$ . This circularity may impair the ability to learn about changes in  $H$  that  
561 occur in volatile environments (Figure 7A).

562 Second, purely parallel processing may also reduce the capacity to calibrate metacognitive  
563 beliefs about ongoing changes in the precision at which sensory signals are encoded. In the  
564 absence of feedback, agents depend on internal confidence signals<sup>58</sup> (i.e., the absolute of  
565 the posterior log ratio  $|L_t|$ ) to update beliefs  $M_t$  about the precision of sensory encoding  
566  $\hat{M} = 1 - |s_t - u_t|$ . While  $\hat{M}$  depends only on the likelihood  $LLR_t$ , the estimate  $M_t$  is  
567 informed by the posterior  $L_t$ , which, in turn, is additionally modulated by the prior  $L_{t-1}$   
568 and  $H_t$ . Relying on internal predictions may thus distort metacognitive beliefs about the  
569 precision of sensory encoding (Figure 7B). This problem becomes particularly relevant when  
570 agents do not have full insight into the strength at which external and internal sources of  
571 information contribute to perceptual inference (i.e., when confidence is high during both  
572 internally- and externally-biased processing; Figure 2I-J; Figure 6G-H).

573 Here, we propose that bimodal inference may provide potential solutions to these problems  
574 of circular inference. By intermittently decoupling the decision variable  $L_t$  from internal  
575 predictions, between-mode fluctuations may create unambiguous error signals that adaptively  
576 update estimates about the hazard rate  $\hat{H}$  and the precision of sensory encoding  $\hat{M}$ .

577 To illustrate this hypothesis, we simulated data for a total of 1000 participants who performed  
578 binary perceptual decisions for a total of 20 blocks of 100 trials each. Each block differed  
579 with respect to the true hazard rate  $\hat{H}$  (either 0.1, 0.3, 0.5, 0.7 or 0.9) and the sensitivity  
580 parameter  $\alpha$  (either 2, 3, 4, 5 or 6, determining  $\hat{M}$  via the absolute of the log likelihood ratio  
581  $|LLR_t|$ , Figure 7A-B, upper panel). Importantly, the synthetic participants did not receive  
582 feedback on whether their perceptual decisions were correct.

583 We initialized each participant at a random value of  $H'_t$  (ranging from  $-0.25$  to  $0$ ) and  $M'_t$

584 (ranging from 0.25 to 2), which were transformed into the unit interval to yield trial-wise  
585 estimates for  $H_t$  and  $M_t$ :

$$H_t = \frac{1}{1 + \exp(-(H'_t))} \quad (9)$$

$$M_t = \frac{1}{1 + \exp(-(M'_t))} \quad (10)$$

586 For each block, we generated stimuli  $s_t$  using the true hazard rate  $\hat{H}$ . Detected inputs  $u_t$   
587 were computed according to the block-wise sensitivity parameter  $\alpha$ . Perceptual decisions  
588  $y_t$  were generated using the bimodal inference model with ( $a_\psi = a_{LLR} = 1$ ,  $\zeta = 1$  and  $f$   
589 between 0.05 and 0.15) and a unimodal control model ( $a_\psi = a_{LLR} = 0$ ,  $\zeta = 1$ ).

590 Leaning about  $H$  was driven by the error-term  $\epsilon_H$  (Figure 7A, lower panel), reflecting the  
591 difference between  $H_t$  and presence of a perceived change in the environment  $|y_t - y_{t-1}|$ :

$$\epsilon_H = |y_t - y_{t-1}| - H_t \quad (11)$$

592 Trial-wise updates to  $H$  were provided by a Resorla-Wagner-rule with learning rate  $\beta_H$   
593 (ranging from 0.05 to 0.25). Since  $y_t$  is more likely to accurately reflect the state of the  
594 environment during external mode, updates to  $H$  were additionally modulated by  $\omega_{LLR}$ :

$$H'_t = H'_{t-1} + \beta_H * \omega_{LLR} * \epsilon_H \quad (12)$$

595 Learning about  $\hat{M}$  was driven by error-term  $\epsilon_M$  (Figure 7B, lower panel), reflecting the  
596 difference between  $M_t$  and the posterior decision-certainty ( $1 - |y_t - P(y_t = 1)|$ ):

$$\epsilon_M = (1 - |y_t - P(y_t = 1)|) - M_t \quad (13)$$

597 In analogy to  $H$ , we modeled trial-wise updates to  $M$  using a Rescorla-Wagner-rule with  
 598 learning rate  $\beta_M$  (ranging from 0.05 to 0.25). Since  $y_t$  reflects the log likelihood ratio  $LLR_t$   
 599 (and therefore the precision of sensory encoding) more closely during external mode, updates  
 600 to  $P$  were additionally modulated by  $\omega_{LLR}$ :

$$M'_t = M'_{t-1} + \beta_M * \omega_{LLR} * \epsilon_M \quad (14)$$

601 For each participant, we simulated data using both the bimodal inference model described  
 602 above and a unimodal control model, in which the between-mode fluctuations were removed  
 603 by setting the amplitude parameter  $a$  to zero ( $a_\psi = a_{LLR} = 0$ ). We compared the bimodal  
 604 model of perceptual inference to the unimodal control model in terms of three dependent  
 605 variables: the probability of stimulus-congruent perceptual choices, the error in the estimate  
 606 about  $H$  (i.e.,  $|H - \hat{H}|$ ) and the error in the estimate about  $M$  (i.e.,  $|M - \hat{M}|$ , with  $\hat{M} =$   
 607  $1 - (|s_t - u_t|)$ ).

608 We found that the bimodal inference model achieved lower stimulus-congruence in compar-  
 609 ison to the unimodal control model ( $\beta_1 = -6.71 \pm 0.03$ ,  $T(8.42 \times 10^3) = -234.31$ ,  $p =$   
 610 0, Figure 7C). At the same time, the bimodal inference model yielded lower errors in the  
 611 estimated hazard rate  $H$  ( $\beta_1 = -2.94 \times 10^{-3} \pm 2.89 \times 10^{-4}$ ,  $T(4.96 \times 10^3) = -10.18$ ,  $p =$   
 612  $4.11 \times 10^{-24}$ ) and probability of stimulus-congruent choices  $P$  ( $\beta_1 = -0.03 \pm 1.86 \times 10^{-4}$ ,  
 613  $T(6.07 \times 10^3) = -137.75$ ,  $p = 0$ , Figure 7E). This suggests that between-mode fluctuations  
 614 may play an adaptive role for learning and perceptual metacognition by supporting robust  
 615 inferences about the statistical regularities of volatile environments and ongoing changes in  
 616 the precision of sensory encoding.

617 Finally, we asked whether differences between the bimodal inference model the unimodal  
 618 control model depend on the presence of external feedback. We predicted that the benefits  
 619 of the bimodal inference model over the unimodal control model should be lost when feedback  
 620 is provided: With feedback, the error terms that induce updates in  $H$  and  $P$  can be informed

621 by the true state of the environment  $s_t$  instead of posterior stimulus probabilities that are  
622 distorted by circular inferences:

$$\epsilon_H = |s_t - s_{t-1}| - H_t \quad (15)$$

$$\epsilon_M = (1 - (|y_t - s_t|)) - M_t \quad (16)$$

623 We repeated the above simulation for each participant while providing feedback on a subset  
624 of trials (10%, 20%, 30%, 40%, 50%, 60%, 70%, 80%, 90% and 100%). With increasing  
625 availability of external feedback, the bimodal inference model lost its advantage over the  
626 unimodal control model in terms of, (i), the estimated hazard rate  $H$  ( $\beta_2 = 1.43 \times 10^{-3} \pm$   
627  $3.71 \times 10^{-5}$ ,  $T(10 \times 10^3) = 38.58$ ,  $p = 9.44 \times 10^{-304}$ ) and, (ii), the estimated probability of  
628 stimulus-congruent choices  $M$  ( $\beta_2 = 3.91 \times 10^{-3} \pm 2.51 \times 10^{-5}$ ,  $T(10 \times 10^3) = 156.18$ ,  $p =$   
629 0, Figure 7F). This indicates that the benefits of bimodal inference are limited to situations  
630 in which external feedback is sparse.

631 **6 Discussion**

632 This work investigates the behavioral and computational characteristics of ongoing fluctuations  
633 in perceptual decision-making using two large-scale datasets in humans<sup>20</sup> and mice<sup>21</sup>.  
634 We found that humans and mice cycle through recurring intervals of reduced sensitivity to  
635 external sensory information, during which they relied more strongly on perceptual history,  
636 i.e., an internal prediction that is provided by the sequence of preceding choices. Computational  
637 modeling indicated that these infra-slow periodicities are governed by two interlinked  
638 factors: (i), the dynamic integration of sensory inputs over time and, (ii), anti-phase os-  
639 cillations in the strength at which perception is driven by internal versus external sources  
640 of information. These cross-species results suggest that ongoing fluctuations in perceptual  
641 decision-making arise not merely as a noise-related epiphenomenon of limited processing  
642 capacity, but result from a structured and adaptive mechanism that fluctuates between  
643 internally- and externally-oriented modes of sensory analysis.

644 **6.1 Serial dependencies represent a pervasive and adaptive aspect  
645 of perceptual decision-making in humans and mice**

646 A growing body of literature has highlighted that perception is modulated by preceding  
647 choices<sup>22–28,30,32,33</sup>. Our work provides converging cross-species evidence supporting the no-  
648 tion that such serial dependencies are a pervasive and general phenomenon of perceptual  
649 decision-making (Figures 2 and 4, Supplemental Figures 1 and 3). While introducing errors  
650 in randomized psychophysical designs<sup>24,28,30,31,43</sup> (Figures 2 and 4A), we found that percep-  
651 tual history facilitates post-perceptual processes such as speed of response<sup>42</sup> (Figure 2G) and  
652 subjective confidence in humans (Figure 2I).

653 At the level of individual traits, increased biases toward preceding choices were associated  
654 with reduced sensitivity to external information (Supplemental Figure 1C-D) and lower  
655 metacognitive efficiency. When investigating how serial dependencies evolve over time, we

656 observed dynamic changes in strength of perceptual history (Figures 2 and 4B) that cre-  
657 ated wavering biases toward internally- and externally-biased modes of sensory processing.  
658 Between-mode fluctuations may thus provide a new explanation for ongoing changes in per-  
659 ceptual performance<sup>6-11</sup>.

660 In computational terms, serial dependencies may leverage the temporal autocorrelation of  
661 natural environments<sup>31,48</sup> to increase the efficiency of decision-making<sup>35,43</sup>. Such temporal  
662 smoothing<sup>48</sup> of sensory inputs may be achieved by updating dynamic predictions about the  
663 world based on the sequence of noisy perceptual experiences<sup>22,31</sup>, using algorithms such as  
664 Kalman filtering<sup>35</sup>, Hierarchical Gaussian filtering<sup>59</sup> or sequential Bayes<sup>25,42,54</sup>. At the level  
665 of neural mechanisms, the integration of internal with external information may be realized  
666 by combining feedback from higher levels in the cortical hierarchy with incoming sensory  
667 signals that are fed forward from lower levels<sup>60</sup>.

668 Yet relying too strongly on serial dependencies may come at a cost: When accumulating over  
669 time, internal predictions may eventually override external information, leading to circular  
670 and false inferences about the state of the environment. In this work, we used model simula-  
671 tions to show that, akin to the wake-sleep-algorithm in machine learning<sup>61</sup>, bimodal inference  
672 may help to determine whether errors result from external input or from internally-stored pre-  
673 dictions (Figure 7): During internal mode, sensory processing is more strongly constrained by  
674 predictive processes that auto-encode the agent’s environment. Conversely, during external  
675 mode, the network is driven predominantly by sensory inputs<sup>18</sup>. Between-mode fluctua-  
676 tions may thus generate an unambiguous error signal that aligns internal predictions with  
677 the current state of the environment in iterative test-update-cycles<sup>61</sup>. On a broader scale,  
678 between-mode fluctuations may thus regulate the balance between feedforward versus feed-  
679 back contributions to perception and thereby play a adaptive role in metacognition and  
680 reality monitoring<sup>62</sup>.

681 **6.2 Arousal, attentional lapses, general response biases, insuffi-**  
682 **cient training and metacognitive strategies as alternative ex-**  
683 **planations for between-mode fluctuations**

684 These functional explanations for external and internal modes share the idea that, in order  
685 to form stable internal predictions about the statistical properties of the world (e.g., tracking  
686 the hazard rate of the environment) or metacognitive beliefs about processes occurring within  
687 the agent (e.g., monitoring ongoing changes in the reliability of feedback and feedforward  
688 processing), perception needs to temporarily disengage from internal predictions. By the  
689 same token, they presuppose that fluctuations in mode occur at the level of perceptual  
690 processing<sup>26,30,48,49</sup>, and are not a passive phenomenon that is primarily driven by factors  
691 situated up- or downstream of sensory analysis.

692 First, it may be argued that agents stereotypically repeat preceding choices when less alert.  
693 Our analyses address this alternative driver of serial dependencies by building on the as-  
694 sociation between RTs and arousal<sup>45,47</sup>. We found that RTs do not map linearly onto the  
695 mode of sensory processing, but become shorter for stronger biases toward both externally-  
696 and internally-oriented mode (Figure 2G-H; Figure 4I). These observations argue against  
697 the view that biases toward internal mode can be explained solely on the ground of ongoing  
698 changes in tonic arousal or fatigue<sup>44</sup>.

699 However, internal modes of sensory processing may also be attributed to attentional lapses<sup>63</sup>,  
700 which are caused by mind-wandering or mind-blanking and show a more complex relation to  
701 RTs<sup>63</sup>: While episodes of mind-blanking are characterized by an absence of subjective mental  
702 activity, more frequent misses, a relative increase in slow waves over posterior EEG electrodes  
703 and increased RTs, episodes of mind-wandering come along which rich inner experiences,  
704 more frequent false alarms, a relative increase of slow-wave amplitudes over frontal electrodes  
705 and decreased RTs<sup>63</sup>.

706 Yet in contrast to gradual between-mode fluctuations, engaging in mind-wandering as  
707 opposed to on-task attention seems to be an all-or-nothing phenomenon<sup>63</sup>. In addition,  
708 internally-biased processing did not increase either false alarms or misses, but induced  
709 choice errors through an enhanced impact of perceptual history (Figure 2 and 4A) that  
710 unfolded in alternating *streaks*<sup>9,13</sup> of elevated stimulus- and history-congruence. Finally, the  
711 increase in lapse rates during internal mode was not general, but history-dependent (Figures  
712 3 and 5). While these observations clearly distinguishes between-mode fluctuations from  
713 unspecific effects of lapses on decision-making, it remains an intriguing question for future  
714 research how mind-wandering and -blanking can be differentiated from internally-oriented  
715 modes of sensory processing in terms of their phenomenology, behavioral characteristics,  
716 neural signatures and noise profiles<sup>10,63</sup>.

717 Second, it may be proposed that humans and mice apply a metacognitive response strategy  
718 that repeats preceding choices when less confident about their responses or when insufficiently  
719 trained on the task. In humans, however, confidence increased for stronger biases toward  
720 both external and internal mode (Figure 2I-J). For humans and mice, history-effects grew  
721 stronger with increasing exposure to (and expertise in) the task (Supplemental Figure S6). In  
722 addition, the existence of external and internal modes in murine perceptual decision-making  
723 (Figure 4) implies that between-mode fluctuations do not depend exclusively on the rich  
724 cognitive functions associated with human prefrontal cortex<sup>64</sup>.

725 Third, our computational modeling results provide further evidence against both of the above  
726 caveats: Simulations based on estimated model parameters closely matched the empirical  
727 data (Figure 6), reproduced aspects of behavior it was not fitted to (such as trial-wise con-  
728 fidence reports and RTs/TD for human and mice, respectively), and predicted that history-  
729 congruent choices occur more frequently after high-confidence trials<sup>30,31</sup>. These findings  
730 suggest that perceptual choices and post-perceptual processes such as response behavior or  
731 metacognition are jointly driven by a dynamic decision variable<sup>50</sup> that encodes uncertainty<sup>31</sup>

732 and is affected by ongoing changes in the integration of external versus internal information.

733 Of note, a recent computational study<sup>65</sup> has used a Hidden Markov Model (HMM) to in-  
734 vestigate perceptual decision-making in the IBL database<sup>21</sup>. In analogy to our findings, the  
735 authors observed that mice switch between temporally extended *strategies* that last for more  
736 than 100 trials: During *engaged* states, perception was highly sensitive to external sensory  
737 information. During *disengaged* states, in turn, choice behavior was prone to errors due  
738 to enhanced biases toward one of the two perceptual outcomes<sup>65</sup>. Despite the conceptual  
739 differences to our approach (discrete states in a HMM that correspond to switches between  
740 distinct decision-making strategies<sup>65</sup> vs. gradual changes in mode that emerge from sequen-  
741 tial Bayesian inference and ongoing fluctuations in the impact of external relative to internal  
742 information), it is tempting to speculate that engaged/disengaged states and between-mode  
743 fluctuations might tap into the same underlying phenomenon.

### 744 6.3 Fluctuations in mode as a driver of 1/f dynamics in perception

745 In light of the above, our results support the idea that, instead of unspecific effects of arousal,  
746 attention, training or metacognitive response strategies, perceptual choices are shaped by  
747 dynamic processes that occur at the level of sensory analysis<sup>26,30,49</sup>: (i), the integration  
748 of incoming signals over time and, (ii), ongoing fluctuations in the impact of external ver-  
749 sus internal sources of decision-related information. It is particularly interesting that these  
750 two model components reproduce the established 1/f characteristic<sup>36,37</sup> of fluctuating perfor-  
751 mance in perception (see Figure 2-4D and previous work<sup>9,10,13</sup>), since this feature has been  
752 attributed to both a memory process<sup>13</sup> (corresponding to model component (i): internal pre-  
753 dictions that are dynamically updated in response to new inputs) and wave-like variations in  
754 perceptual resources<sup>9</sup> (corresponding to model component (ii): ongoing fluctuations in the  
755 impact of internal and external information).

756 1/f noise is an ubiquitous attribute of dynamic complex systems that integrate sequences

757 of contingent sub-processes<sup>36</sup> and exhibit self-organized criticality<sup>37</sup>. As most real-world  
758 processes are *critical*, i.e. not completely uniform (or subcritical) nor completely random (or  
759 supercritical)<sup>37,66</sup>, the brain may have evolved to operate at a critical point as well<sup>38</sup>: Subcrit-  
760 ical brains would be impervious to new inputs, whereas supercritical brains would be driven  
761 by noise. The 1/f observed in this study thus provides an intriguing connection between  
762 the notion that the brain's self-organized criticality is crucial for balancing network stability  
763 with information transmission<sup>38</sup> and the adaptive functions of between-mode fluctuations<sup>18</sup>,  
764 which we propose to support the build-up of robust internal predictions despite an ongoing  
765 stream of noisy sensory inputs.

## 766 6.4 Dopamine-dependent changes in E-I-balance as a neural mech- 767 anism of between-mode fluctuations

768 The link to self-organized criticality suggests that balanced cortical excitation and  
769 inhibition<sup>67</sup> (E-I), which may enable efficient coding<sup>67</sup> by maintaining neural networks  
770 in critical states<sup>68</sup>, could provide a potential neural mechanism of between-mode fluctu-  
771 ations. Previous work has proposed that the balance between glutamatergic excitation  
772 and GABA-ergic inhibition is regulated by activity-dependent feedback through NMDA  
773 receptors<sup>69</sup>. Such NMDA-mediated feedback has been related to the integration of external  
774 inputs over time<sup>67</sup> (model component (i), Figure 1E), thereby generating serial dependen-  
775 cies in decision-making<sup>70–73</sup>. Intriguingly, slow neuromodulation by dopamine enhances  
776 NMDA-dependent signaling<sup>70,74,75</sup> and fluctuates at infra-slow frequencies<sup>76,77</sup> that match  
777 the temporal dynamics of between-mode fluctuations observed in humans (Figure 2) and  
778 mice (Figure 4). Ongoing fluctuations in the impact of external versus internal information  
779 (model component (ii)) may thus be caused by phasic changes in E-I-balance that are  
780 induced by dopaminergic neuromodulation.

<sup>781</sup> **6.5 Limitations and open questions**

<sup>782</sup> In this study, we show that perception is attracted toward preceding choices in mice<sup>21</sup> (Figure 4A) and humans (Figure 2A; see Supplemental Figure S1 for analyses within individual studies of the Confidence database<sup>20</sup>). Of note, previous work has shown that perceptual decision-making is concurrently affected by both attractive and repulsive serial biases that operate on distinct time-scales and serve complementary functions for sensory processing<sup>27,78,79</sup>:

<sup>787</sup> Short-term attraction may serve the decoding of noisy sensory inputs and increase the stability of perception, whereas long-term repulsion may enable efficient encoding and sensitivity to change<sup>27</sup>.

<sup>790</sup> Importantly, repulsive biases operate in parallel to attractive biases<sup>27</sup> and are therefore unlikely to account for the ongoing changes in mode that occur in alternating cycles of internally- and externally-oriented processing. To elucidate whether attraction and repulsion both fluctuate in their impact on perceptual decision-making will be an important task for future research, since this would help to understand whether attractive and repulsive biases are linked in terms of their computational function and neural implementation<sup>27</sup>.

<sup>796</sup> A second open question concerns the neurobiological underpinnings of ongoing changes in mode. Albeit purely behavioral, our results tentatively suggest dopaminergic neuromodulation of NMDA-mediated feedback as one potential mechanism of externally- and internally-biased modes. Since between-mode fluctuations were found in both humans and mice, future studies can apply both non-invasive and invasive neuro-imaging and electrophysiology to better understand the neural mechanisms that generate ongoing changes in mode in terms of neuro-anatomy, -chemistry and -circuitry.

<sup>803</sup> Finally, establishing the neural correlates of externally- and internally-biased modes will enable exciting opportunities to investigate their role for adaptive perception and decision-making. Causal interventions via pharmacological challenges, optogenetic manipulations or (non-)invasive brain stimulation will help to understand whether between-mode fluctuations

807 are implicated in resolving credit-assignment problems<sup>18,80</sup> or in calibrating metacognition  
808 and reality monitoring<sup>62</sup>. Addressing these questions may therefore provide new insight  
809 into the pathophysiology of hallucinations and delusions, which have been characterized by  
810 an imbalance in the impact of external versus internal information<sup>60,81,82</sup> and are typically  
811 associated with metacognitive failures and a departure from consensual reality<sup>82</sup>.

812 **7 Methods**

813 **7.1 Ressource availability**

814 **7.1.1 Lead contact**

815 Further information and requests for resources should be directed to and will be fulfilled by  
816 the lead contact, Veith Weilnhammer (veith.weilnhammer@gmail.com).

817 **7.1.2 Materials availability**

818 This study did not generate new unique reagents.

819 **7.1.3 Data and code availability**

820 All custom code and behavioral data are available on <https://github.com/veithweilnh>  
821 ammer/Modes. This manuscript was created using the *R Markdown* framework, which  
822 integrates all data-related computations and the formatted text within one document. With  
823 this, we wish to make our approach fully transparent and reproducible for reviewers and  
824 future readers.

825 **7.2 Experimental model and subject details**

826 **7.2.1 Confidence database**

827 We downloaded the human data from the Confidence database<sup>20</sup> on 21/10/2020, limiting our  
828 analyses to the database category *perception*. Within this category, we selected studies in  
829 which participants made binary perceptual decision between two alternative outcomes (see  
830 Supplemental Table 1). We excluded two studies in which the average perceptual accuracy  
831 fell below 50%. After excluding these studies, our sample consisted of 21.05 million trials  
832 obtained from 4317 human participants and 66 individual studies.

833 **7.2.2 IBL database**

834 We downloaded the murine data from the IBL database<sup>21</sup> on 28/04/2021. We limited our  
835 analyses to the *basic task*, during which mice responded to gratings that appeared with  
836 equal probability in the left or right hemifield. Within each mouse, we excluded sessions in  
837 which perceptual accuracy was below 80% for stimuli presented at a contrast  $\geq 50\%$ . After  
838 exclusion, our sample consisted of 1.46 million trials obtained from  $N = 165$  mice.

839 **7.3 Method details**

840 **7.3.1 Variables of interest**

841 **Primary variables of interest:** We extracted trial-wise data on the presented stimulus and  
842 the associated perceptual decision. Stimulus-congruent choices were defined by perceptual  
843 decisions that matched the presented stimuli. History-congruent choices were defined by  
844 perceptual choices that matched the perceptual choice at the immediately preceding trial.  
845 The dynamic probabilities of stimulus- and history-congruence were computed in sliding  
846 windows of  $\pm 5$  trials.

847 The *mode* of sensory processing was derived by subtracting the dynamic probability of history-  
848 congruence from the dynamic probability of stimulus-congruence, such that positive values  
849 indicate externally-oriented processing, whereas negative values indicate internally-oriented  
850 processing. When visualizing the relation of the mode of sensory processing to confidence,  
851 response times or trial duration (see below), we binned the mode variable in 10% intervals.  
852 We excluded bins than contained less than 0.5% of the total number of available data-points.

853 **Secondary variables of interest:** From the Confidence Database<sup>20</sup>, we furthermore ex-  
854 tracted trial-wise confidence reports and response times (RTs; if RTs were available for both  
855 the perceptual decision and the confidence report, we only extracted the RT associated with  
856 the perceptual decision). To enable comparability between studies, we normalized RTs and  
857 confidence reports within individual studies using the *scale* R function. If not available for

858 a particular study, RTs and confidence reports were treated as missing variables. From the  
859 IBL database<sup>21</sup>, we extracted trial durations (TDs) as defined by interval between stimulus  
860 onset and feedback, which represents a coarse measure of RT<sup>21</sup>.

861 **Exclusion criteria for individual data-points:** For non-normalized data (TDs from the  
862 IBL database<sup>21</sup>; d-prime, meta-dprime and M-ratio from the Confidence database<sup>20</sup> and  
863 simulated confidence reports), we excluded data-points that differed from the median by  
864 more than 3 x MAD (median absolute distance<sup>52</sup>). For normalized data (RTs and confidence  
865 reports from the Confidence database<sup>20</sup>), we excluded data-points that differed from the  
866 mean by more than 3 x SD (standard deviation).

### 867 7.3.2 Control variables

868 Next to the sequence of presented stimuli, we assessed the autocorrelation of task difficulty  
869 as an alternative explanation for any autocorrelation in stimulus- and history-congruence.  
870 For the Confidence Database<sup>20</sup>, task difficulty was indicated by one of the following labels:  
871 *Difficulty, Difference, Signal-to-Noise, Dot-Difference, Congruency, Coherence(-Level), Dot-*  
872 *Proportion, Contrast(-Difference), Validity, Setsize, Noise-Level(-Degree) or Temporal Dis-*  
873 *tance.* When none of the above was available for a given study, task difficulty was treated  
874 as a missing variable. In analogy to RTs and confidence, difficulty levels were normalized  
875 within individual studies. For the IBL Database<sup>21</sup>, task difficulty was defined by the contrast  
876 of the presented grating.

### 877 7.3.3 Autocorrelations

878 For each participant, trial-wise autocorrelation coefficients were estimated using the R-  
879 function *acf* with a maximum lag defined by the number of trials available per subject.  
880 Autocorrelation coefficients are displayed against the lag (in numbers of trials, ranging from  
881 1 to 20) relative to the index trial ( $t = 0$ , see Figure 2B-C, 4B-C and 6B-C). To account  
882 for spurious autocorrelations that occur due to imbalances in the analyzed variables, we

883 estimated autocorrelations for randomly permuted data (100 iterations). For group-level  
884 autocorrelations, we computed the differences between the true autocorrelation coefficients  
885 and the mean autocorrelation observed for randomly permuted data and averaged across  
886 participants.

887 At a given trial, group-level autocorrelation coefficients were considered significant when  
888 linear mixed effects modeling indicated that the difference between real and permuted au-  
889 tocorrelation coefficients was above zero at an alpha level of 0.05%. To test whether the  
890 autocorrelation of stimulus- and history-congruence remained significant when controlling  
891 for task difficulty and the sequence of presented stimuli, we added the respective autocorre-  
892 lation as an additional factor to the linear mixed effects model that computed the group-level  
893 statistics (see also *Mixed effects modeling*).

894 To assess autocorrelations at the level of individual participants, we counted the number of  
895 subsequent trials (starting at the first trial after the index trial) for which less than 50% of  
896 the permuted autocorrelation coefficients exceeded the true autocorrelation coefficient. For  
897 example, a count of zero indicates that the true autocorrelation coefficients exceeded *less*  
898 *than 50%* of the autocorrelation coefficients computed for randomly permuted data at the  
899 first trial following the index trial. A count of five indicates that, for the first five trials  
900 following the index trial, the true autocorrelation coefficients exceeded *more than 50%* of  
901 the respective autocorrelation coefficients for the randomly permuted data; at the 6th trial  
902 following the index trial, however, *less than 50%* of the autocorrelation coefficients exceeded  
903 the respective permuted autocorrelation coefficients.

#### 904 7.3.4 Spectral analysis

905 We used the R function *spectrum* to compute the spectral densities for the dynamic proba-  
906 bilities of stimulus- and history-congruence as well as the phase (i.e., frequency-specific shift  
907 between the two time-series ranging from 0 to  $2\pi$ ) and squared coherence (frequency-specific  
908 variable that denotes the degree to which the shift between the two time-series is constant,

909 ranging from 0 to 100%). Periodograms were smoothed using modified Daniell smoothers at  
910 a width of 50.

911 Since the dynamic probabilities of history- and stimulus-congruence were computed using  
912 a sliding windows of  $\pm 5$  trials (i.e., intervals containing a total of 11 trials), we report the  
913 spectral density, coherence and phase for frequencies below  $1/11 \text{ } 1/N_{trials}$ . Spectral densities  
914 have one value per subject and frequency (data shown in Figures 2D and 4D). To assess the  
915 relation between stimulus- and history-congruence in this frequency range, we report average  
916 phase and average squared coherence for all frequencies below  $1/11 \text{ } 1/N_{trials}$  (i.e., one value  
917 per subject; data shown in Figure 2E-F and 4E-F).

918 Since the data extracted from the Confidence Database<sup>20</sup> consist of a large set of individual  
919 studies that differ with respect to inter-trial intervals, we defined the variable *frequency* in the  
920 dimension of cycles per trial  $1/N_{trials}$  rather than cycles per second (Hz). For consistency,  
921 we chose  $1/N_{trials}$  as the unit of frequency for the IBL database<sup>21</sup> as well.

## 922 7.4 Quantification and statistical procedures

923 All aggregate data are reported and displayed with errorbars as mean  $\pm$  standard error of  
924 the mean.

### 925 7.4.1 Mixed effects modeling

926 Unless indicated otherwise, we performed group-level inference using the R-packages *lmer*  
927 and *afex* for linear mixed effects modeling and *glmer* with a binomial link-function for logistic  
928 regression. We compared models based on Akaike Information Criteria (AIC). To account for  
929 variability between the studies available from the Confidence Database<sup>20</sup>, mixed modeling  
930 was conducted using random intercepts defined for each study. To account for variability  
931 across experimental session within the IBL database<sup>21</sup>, mixed modeling was conducted using  
932 random intercepts defined for each individual session. When multiple within-participant

933 datapoints were analyzed, we estimated random intercepts for each participant that were  
934 *nested* within the respective study of the Confidence database<sup>20</sup>. By analogy, for the IBL  
935 database<sup>21</sup>, we estimated random intercepts for each session that were nested within the  
936 respective mouse. We report  $\beta$  values referring to the estimates provided by mixed effects  
937 modeling, followed by the respective T statistic (linear models) or z statistic (logistic models).

938 The effects of stimulus- and history-congruence on RTs and confidence reports (Figure 2,  
939 4 and 6, subpanels G-I) were assessed in linear mixed effects models that tested for main  
940 effects of both stimulus- and history-congruence as well as the between-factor interaction.  
941 Thus, the significance of any effect of history-congruence on RTs and confidence reports was  
942 assessed while controlling for the respective effect of stimulus-congruence (and vice versa).

943 **7.4.2 Psychometric function**

944 We obtained psychometric curves by fitting the following error function to the behavioral  
945 data:

$$y_p = \gamma + (1 - \gamma - \delta) * (\operatorname{erf}(\frac{s_w + \mu}{t}) + 1)/2 \quad (17)$$

946 We used a maximum likelihood procedure to predict individual choices  $y$  (outcome A:  $y = 0$ ;  
947 outcome B:  $y = 1$ ) from the choice probability  $y_p$ . In humans, we computed  $s_w$  multiplying  
948 the inputs  $s$  (stimulus A: 0; outcome B: 1) with the task difficulty  $D_b$  (binarized across 7  
949 levels):

$$s_w = (s - 0.5) * D_b \quad (18)$$

950 In mice,  $s_w$  was defined by the respective stimulus contrast in the two hemifields:

$$s_w = \operatorname{Contrast}_{Right} - \operatorname{Contrast}_{Left} \quad (19)$$

951 Parameters of the psychometric error function were fitted using the R-package *optimx*. The  
952 psychometric error function was defined via the parameters  $\gamma$  (lower lapse; lower bound =  
953 0, upper bound = 0.5),  $\delta$  (upper lapse; lower bound = 0, upper bound = 0.5),  $\mu$  (bias; lower  
954 bound humans = -5; upper bound humans = 5, lower bound mice = -0.5, upper bound mice  
955 = 0.5) and threshold  $t$  (lower bound humans = 0.5, upper bound humans = 25; lower bound  
956 mice = 0.01, upper bound mice = 1.5).

957 **7.4.3 Computational modeling**

958 **Model definition:** Our modeling analysis is an extension of a model proposed by Glaze  
959 et al.<sup>54</sup>, who defined a normative account of evidence accumulation for decision-making. In  
960 this model, trial-wise choices are explained by applying Bayes theorem to infer moment-  
961 by-moment changes in the state of environment from trial-wise noisy observations across  
962 trials.

963 Following Glaze et al.<sup>54</sup>, we applied Bayes rule to compute the posterior evidence for the  
964 two alternative choices (i.e., the log posterior ratio  $L$ ) from the sensory evidence available  
965 at time-point  $t$  (i.e., the log likelihood ratio  $LLR$ ) with the prior probability  $\psi$ :

$$L_t = LLR_t * \omega_{LLR} + \psi_t(L_{t-1}, H) * \omega_\psi \quad (20)$$

966 In the trial-wise design studied here, a transition between the two states of the environment  
967 (i.e., the sources generating the noisy observations available to the participant) can occur  
968 at any time. Despite the random nature of the psychophysical paradigms studied here<sup>20,21</sup>,  
969 humans and mice showed significant biases toward preceding choices (Figure 2A and 4A).  
970 We thus assumed that the prior probability of the two possible outcomes depends on the  
971 posterior choice probability at the preceding trial and the hazard rate  $H$  assumed by the  
972 participant. Following Glaze et al.<sup>54</sup>, the prior  $\psi$  is thus computed as follows:

$$\psi_t(L_{t-1}, H) = L_{t-1} + \log\left(\frac{1-H}{H} + \exp(-L_{t-1})\right) - \log\left(\frac{1-H}{H} + \exp(L_{t-1})\right) \quad (21)$$

973 In this model, humans, mice and simulated agents make perceptual choices based on noisy  
 974 observations  $u$ . These are computed by applying a sensitivity parameter  $\alpha$  to the content of  
 975 external sensory information  $s$ . For humans, we defined the input  $s$  by the two alternative  
 976 states of the environment (stimulus A:  $s = 0$ ; stimulus B:  $s = 1$ ), which generated the  
 977 observations  $u$  through a sigmoid function that applied a sensitivity parameter  $\alpha$ :

$$u_t = \frac{1}{1 + \exp(-\alpha * (s_t - 0.5))} \quad (22)$$

978 In mice, the inputs  $s$  were defined by the respective stimulus contrast in the two hemifields:

$$s_t = \text{Contrast}_{Right} - \text{Contrast}_{Left} \quad (23)$$

979 As in humans, we derived the input  $u$  by applying a sigmoid function with a sensitivity  
 980 parameter  $\alpha$  to input  $s$ :

$$u_t = \frac{1}{1 + \exp(-\alpha * s_t)} \quad (24)$$

981 For humans, mice and in simulations, the log likelihood ratio  $LLR$  was computed from  $u$  as  
 982 follows:

$$LLR_t = \log\left(\frac{u_t}{1 - u_t}\right) \quad (25)$$

983 To allow for long-range autocorrelation in stimulus- and history-congruence (Figure 2B and  
 984 4B), our modeling approach differed from Glaze et al.<sup>54</sup> in that it allowed for systematic  
 985 fluctuation in the impact of sensory information (i.e.,  $LLR$ ) and the prior probability of

986 choices  $\psi$  on the posterior probability  $L$ . This was achieved by multiplying the log likelihood  
 987 ratio and the log prior ratio with coherent anti-phase fluctuations according to  $\omega_{LLR} =$   
 988  $a_{LLR} * \sin(f * t + phase) + 1$  and  $\omega_\psi = a_\psi * \sin(f * t + phase + \pi) + 1$ .

989 **Model fitting:** In model fitting, we predicted the trial-wise choices  $y_t$  (option A: 0; option  
 990 B: 1) from inputs  $s$ . To this end, we minimized the log loss between  $y_t$  and the choice  
 991 probability  $y_{pt}$  in the unit interval.  $y_{pt}$  was derived from  $L_t$  using a sigmoid function defined  
 992 by the inverse decision temperature  $\zeta$ :

$$y_{pt} = \frac{1}{1 + \exp(-\zeta * L_t)} \quad (26)$$

993 This allowed us to infer the free parameters  $H$  (lower bound = 0, upper bound = 1; human  
 994 posterior =  $0.45 \pm 4.8 \times 10^{-5}$ ; murine posterior =  $0.46 \pm 2.97 \times 10^{-4}$ ),  $\alpha$  (lower bound  
 995 = 0, upper bound = 5; human posterior =  $0.5 \pm 1.12 \times 10^{-4}$ ; murine posterior =  $1.06 \pm$   
 996  $2.88 \times 10^{-3}$ ),  $a_\psi$  (lower bound = 0, upper bound = 10; human posterior =  $1.44 \pm 5.27 \times 10^{-4}$ ;  
 997 murine posterior =  $1.71 \pm 7.15 \times 10^{-3}$ ),  $amp_{LLR}$  (lower bound = 0, upper bound = 10;  
 998 human posterior =  $0.5 \pm 2.02 \times 10^{-4}$ ; murine posterior =  $0.39 \pm 1.08 \times 10^{-3}$ ), frequency  $f$   
 999 (lower bound = 1/40, upper bound = 1/5; human posterior =  $0.11 \pm 1.68 \times 10^{-5}$ ; murine  
 1000 posterior =  $0.11 \pm 1.63 \times 10^{-4}$ ),  $p$  (lower bound = 0, upper bound =  $2*\pi$ ; human posterior =  
 1001  $2.72 \pm 4.41 \times 10^{-4}$ ; murine posterior =  $2.83 \pm 3.95 \times 10^{-3}$ ) and inverse decision temperature  
 1002  $\zeta$  (lower bound = 1, upper bound = 10; human posterior =  $4.63 \pm 1.95 \times 10^{-4}$ ; murine  
 1003 posterior =  $4.82 \pm 3.03 \times 10^{-3}$ ) using the R-function *optimx*.

1004 To validate our model, we correlated individual posterior parameter estimates with the re-  
 1005 spective conventional variables. We assumed that, (i), the estimated hazard rate  $H$  should  
 1006 correlate negatively with the frequency of history-congruent choices and that, (ii), the es-  
 1007 timated  $\alpha$  should correlate positively with the frequency of stimulus-congruent choices. In  
 1008 addition, we tested whether the posterior decision certainty (i.e. the absolute of the pos-  
 1009 terior log ratio) correlated negatively with RTs and positively with subjective confidence.

1010 This allowed us to assess whether our model could explain aspects of the data it was not  
1011 fitted to (i.e., RTs and confidence). Finally, we used simulations (see below) to show that  
1012 all model components, including the anti-phase oscillations governed by  $a_\psi$ ,  $a_{LLR}$ ,  $f$  and  $p$ ,  
1013 were necessary for our model to reproduce the empirical data observed for the Confidence  
1014 database<sup>20</sup> and IBL database<sup>21</sup>.

1015 **Model simulation 1: Data recovery:** We used the posterior model parameters observed  
1016 for humans ( $H$ ,  $\alpha$ ,  $a_\psi$ ,  $a_{LLR}$  and  $f$ ) to define individual parameters for simulation in 4317  
1017 simulated participants (i.e., equivalent to the number of human participants). For each  
1018 participant, the number of simulated choices was drawn from a uniform distribution ranging  
1019 from 300 to 700 trials. Inputs  $s$  were drawn at random for each trial, such that the sequence  
1020 of inputs to the simulation did not contain any systematic seriality. Noisy observations  $u$   
1021 were generated by applying the posterior parameter  $\alpha$  to inputs  $s$ , thus generating stimulus-  
1022 congruent choices in  $71.36 \pm 2.6 \times 10^{-3}\%$  of trials. Choices were simulated based on the  
1023 trial-wise choice probabilities  $y_p$ . Simulated data were analyzed in analogy to the human  
1024 and murine data. As a substitute of subjective confidence, we computed the absolute of the  
1025 trial-wise posterior log ratio  $|L|$  (i.e., the posterior decision certainty).

1026 **Model simulation 2: Testing the adaptive benefits of bimodal inference:** In contrast  
1027 to the model applied to the behavioral data, our second set of simulations considered a  
1028 situation in which agents learn about the properties of the environment from experience.  
1029 We modeled dynamic updates in the trial-wise estimates  $H_t$  about the true hazard rate  
1030  $\hat{H} = P(s_t \neq s_{t-1})$  and trial-wise estimates  $M_t$  about the precision of sensory encoding  
1031  $\hat{M} = 1 - (|s_t - u_t|)$ .

1032 In the absence of feedback, leaning about  $\hat{H}$  was driven by the error-term  $\epsilon_H$ , which reflected  
1033 the difference between the currently assumed hazard rate  $H_t$  and the presence of a *perceived*  
1034 change in the environment  $|y_t - y_{t-1}|$ :

$$\epsilon_H = |y_t - y_{t-1}| - H_t \quad (27)$$

<sub>1035</sub> In the presence of feedback,  $\epsilon_H$  reflected the difference between the currently assumed hazard  
<sub>1036</sub> rate  $H_t$  and an presence of a *true* change in the environment  $|s_t - s_{t-1}|$ :

$$\epsilon_H = |s_t - s_{t-1}| - H_t \quad (28)$$

<sub>1037</sub> In the absence of feedback, learning about  $\hat{M}$  was driven by the error-term  $\epsilon_M$ , reflecting  
<sub>1038</sub> the difference between  $M_t$  and the posterior decision-certainty  $(1 - |y_t - P(y_t = 1)|)$ :

$$\epsilon_M = (1 - |y_t - P(y_t = 1)|) - M_t \quad (29)$$

<sub>1039</sub> In the presence of feedback,  $\epsilon_M$  reflected the difference between  $M_t$  and the stimulus-  
<sub>1040</sub> congruence of the current response  $(1 - (|y_t - s_t|))$ :

$$\epsilon_M = (1 - (|y_t - s_t|)) - M_t \quad (30)$$

<sub>1041</sub> Updates to  $H$  and  $M$  were computed in logit-space using a Rescorla-Wagner-rule with learn-  
<sub>1042</sub> ing rates defined by the product of  $\beta_{H/M}$  and  $\omega_{LLR}$ .  $H_t$  and  $M_t$  are computed by trans-  
<sub>1043</sub> forming  $H'_t$  and  $M'_t$  into the unit interval using a sigmoid function:

$$H'_t = H'_{t-1} + \beta_H * \omega_{LLR} * \epsilon_H \quad (31)$$

$$H_t = \frac{1}{1 + exp(-(H'_t))} \quad (32)$$

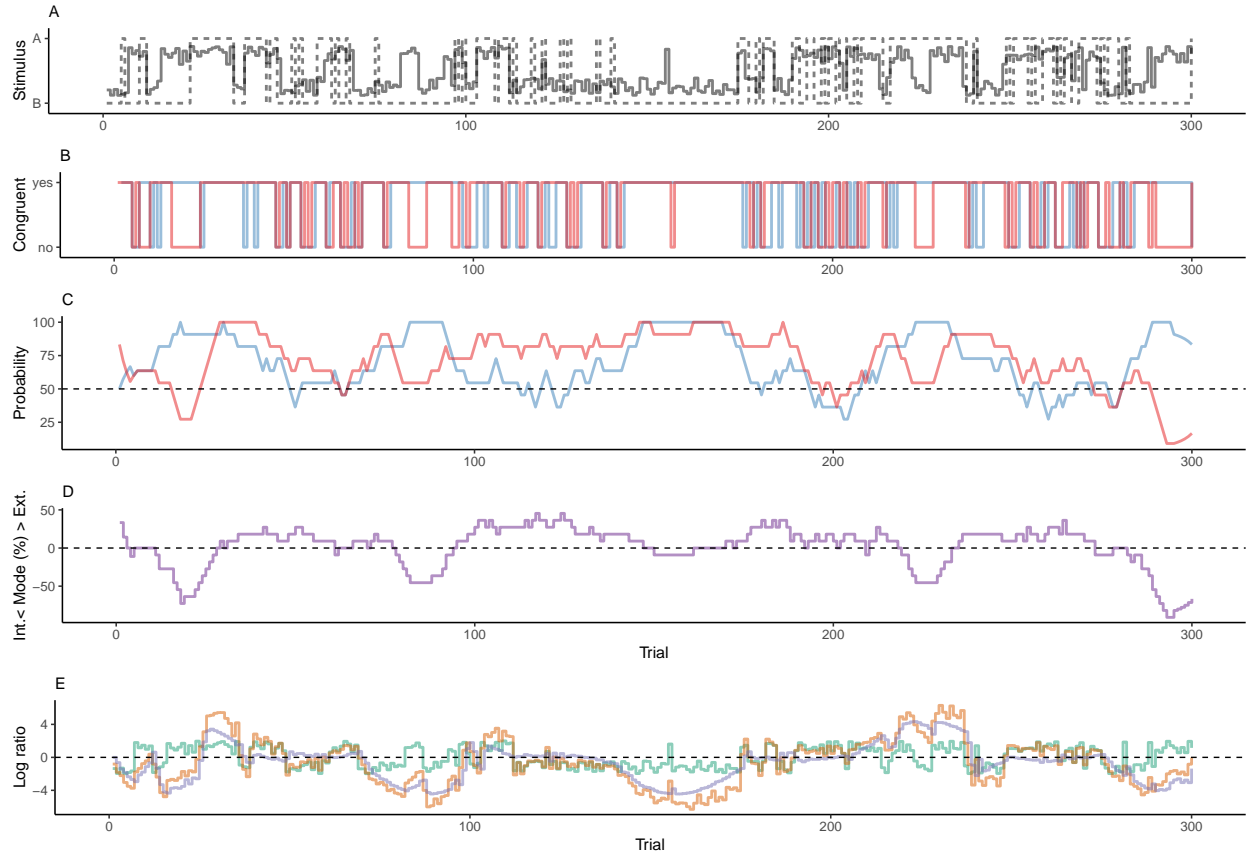
$$M'_t = M'_{t-1} + \beta_M * \omega_{LLR} * \epsilon_M \quad (33)$$

$$M_t = \frac{1}{1 + \exp(-(M'_t))} \quad (34)$$

1044 We simulated data for a total of 1000 participants for a total of 20 blocks of 100 trials each.  
 1045 Each block differed with respect to the true hazard rate  $\hat{H}$  (either 0.1, 0.3, 0.5, 0.7 or 0.9)  
 1046 and the sensitivity parameter  $\alpha$  (either 2, 3, 4, 5 or 6, corresponding to values of  $\hat{M}$  of 0.73,  
 1047 0.82, 0.88, 0.92 or 0.95). Across participants, model parameters were set as follows:  $H'_1$   
 1048 initialized at random in a unit interval between -0.25 to 0;  $P'_1$  initialized at random in a  
 1049 unit interval between 0.25 to 2;  $a = 1$ ;  $f$  between 0.05 and 0.15  $1/N_{trials}$ ;  $\zeta = 1$ ;  $\beta_H$  and  
 1050  $\beta_M$  between 0.05 and 0.25. For each participant, we ran separate simulations with external  
 1051 feedback provided in 0%, 10%, 20%, 30%, 40%, 50%, 60%, 70%, 80%, 90% and 100% of  
 1052 trials.

1053 **8 Figures**

1054 **8.1 Figure 1**



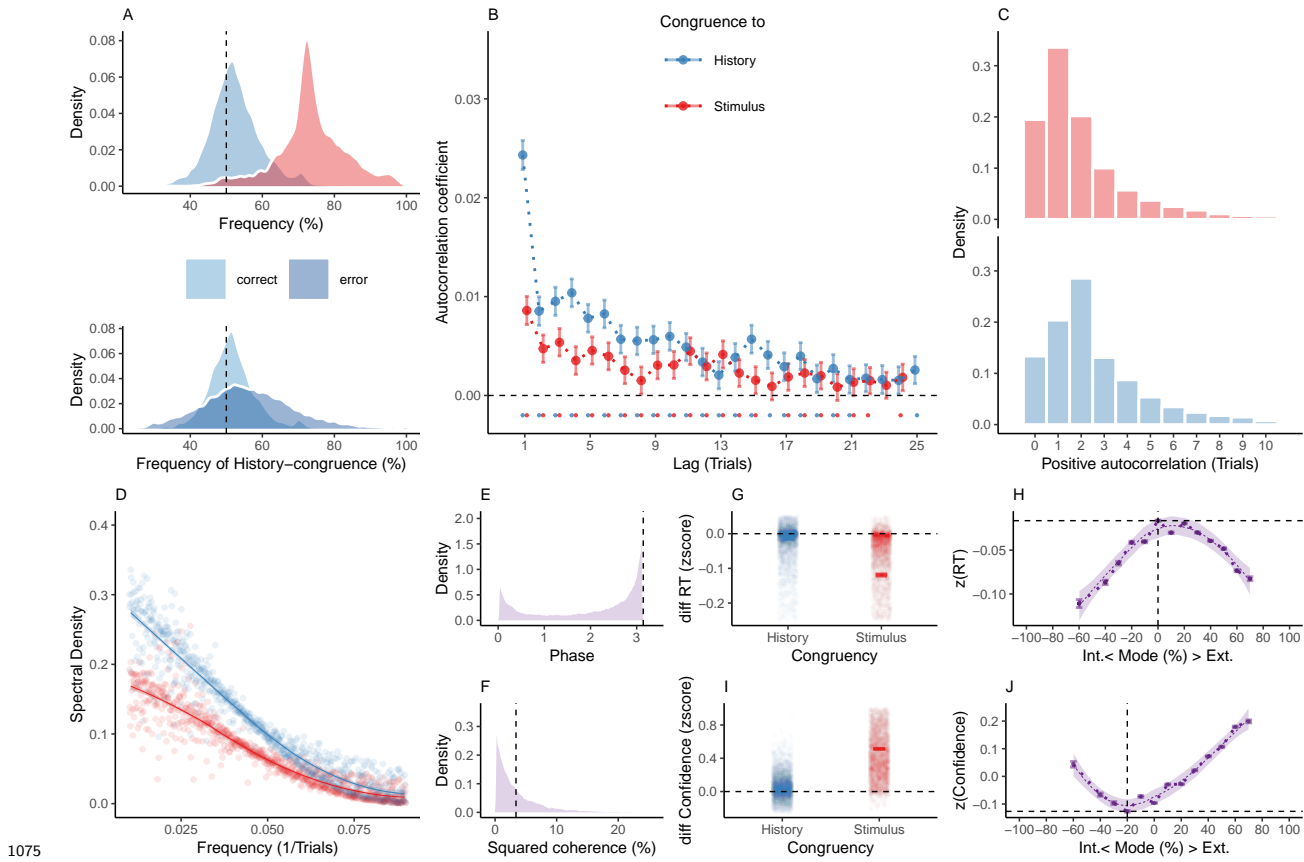
1055 **Figure 1. Concept.**

- 1056 A. In binary perceptual decision-making, a participant is presented with stimuli from two categories (A vs. B; dotted line) and reports consecutive perceptual choices via button presses (solid line). All panels below refer to this example data.
- 1057 B. When the response matched the external stimulus information (i.e., overlap between 1058 dotted and solid line in panel A), perceptual choices are *stimulus-congruent* (red line). When 1059 the response matches the response at the preceding trial, perceptual choices are *history- 1060 congruent* (blue line).
- 1061 C. The dynamic probabilities of stimulus- and history-congruence (i.e., computed in sliding 1062 windows of  $\pm 5$  trials) fluctuate over time.
- 1063
- 1064
- 1065

<sub>1066</sub> D. The *mode* of perceptual processing is derived by computing the difference between the  
<sub>1067</sub> dynamic probabilities of stimulus- and history-congruence. Values above 0% indicate a  
<sub>1068</sub> bias toward external information, whereas values below 0% indicate a bias toward internal  
<sub>1069</sub> information.

<sub>1070</sub> E. In computational modeling, internal mode is caused by an enhanced impact of perceptual  
<sub>1071</sub> history. This causes the posterior (black line) to be close to the prior (blue line). Conversely,  
<sub>1072</sub> during external mode, the posterior is close to the sensory information (log likelihood ratio,  
<sub>1073</sub> red line).

1074 **8.2 Figure 2**



1075 **Figure 2. Internal and external modes in human perceptual decision-making.**

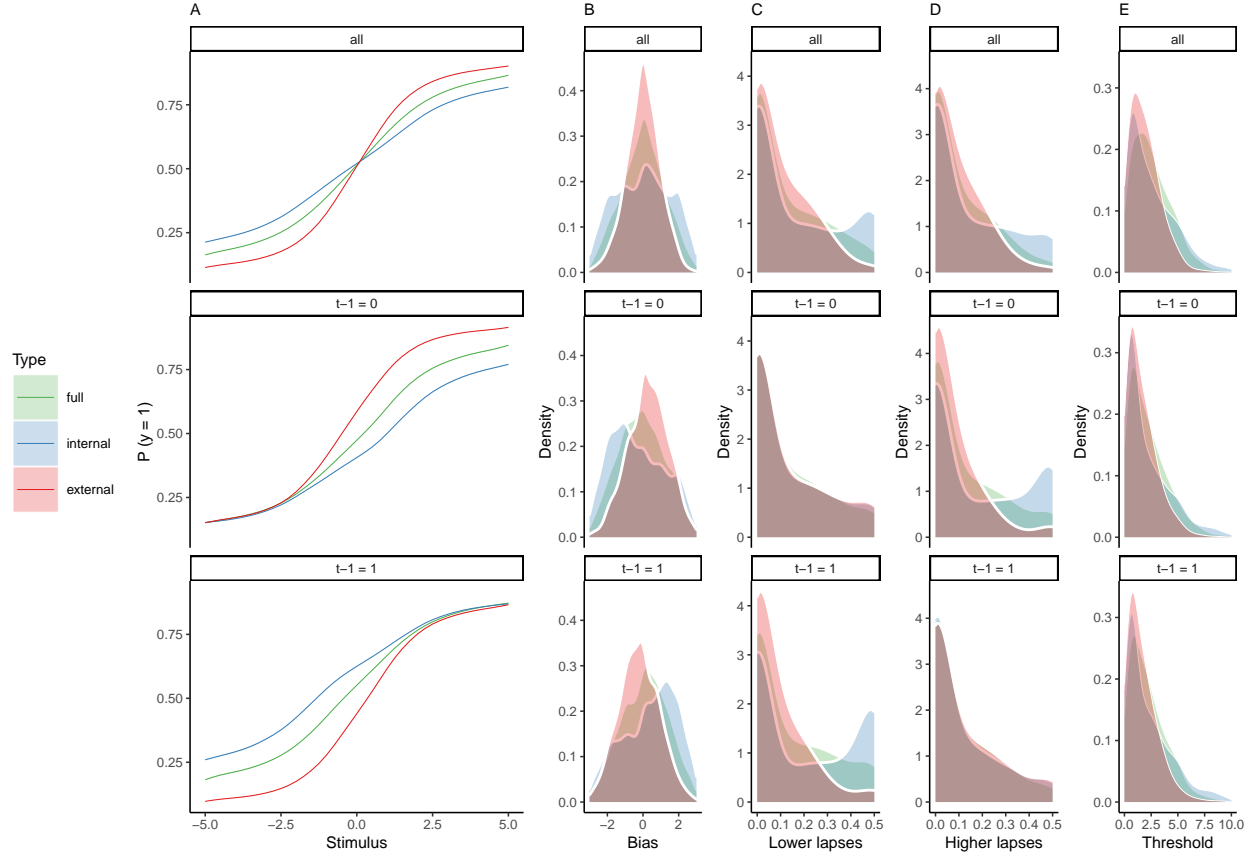
1076 A. In humans, perception was stimulus-congruent in  $73.46\% \pm 0.15\%$  (in red) and history-congruent in  $52.7\% \pm 0.12\%$  of trials (in blue; upper panel). History-congruent perceptual choices were more frequent when perception was stimulus-incongruent (i.e., on *error* trials; lower panel), indicating that history effects impair performance in randomized psychophysical designs.

1077 B. Relative to randomly permuted data, we found highly significant autocorrelations of  
1078 stimulus-congruence and history-congruence (dots indicate intercepts  $\neq 0$  in trial-wise linear  
1079 mixed effects modeling at  $p < 0.05$ ). Across trials, the autocorrelation coefficients were  
1080 best fit by an exponential function (adjusted  $R^2$  for stimulus-congruence: 0.53; history-  
1081 congruence: 0.71) as compared to a linear function (adjusted  $R^2$  for stimulus-congruence:  
1082 0.52; history-congruence: 0.49).

- 1088 C. Here, we depict the number of consecutive trials at which autocorrelation coefficients  
1089 exceeded the respective autocorrelation of randomly permuted data within individual partic-  
1090 ipants. For stimulus-congruence (upper panel), the lag of positive autocorrelation amounted  
1091 to  $3.24 \pm 2.39 \times 10^{-3}$  on average, showing a peak at trial t+1 after the index trial. For  
1092 history-congruence (lower panel), the lag of positive autocorrelation amounted to  $4.87 \pm$   
1093  $3.36 \times 10^{-3}$  on average, peaking at trial t+2 after the index trial.
- 1094 D. The smoothed probabilities of stimulus- and history-congruence (sliding windows of  $\pm 5$   
1095 trials) fluctuated as *1/f noise*, i.e., at power densities that were inversely proportional to the  
1096 frequency.
- 1097 E. The distribution of phase shift between fluctuations in stimulus- and history-congruence  
1098 peaked at half a cycle ( $\pi$  denoted by dotted line).
- 1099 F. The average squared coherence between fluctuations in stimulus- and history-congruence  
1100 (black dottet line) amounted to  $6.49 \pm 2.07 \times 10^{-3}\%$
- 1101 G. We observed faster response times (RTs) for both stimulus-congruence (as opposed to  
1102 stimulus-incongruence,  $\beta = -0.14 \pm 1.61 \times 10^{-3}$ ,  $T(1.99 \times 10^6) = -85.91$ ,  $p = 0$ ) and history-  
1103 congruence ( $\beta = -9.73 \times 10^{-3} \pm 1.38 \times 10^{-3}$ ,  $T(1.99 \times 10^6) = -7.06$ ,  $p = 1.66 \times 10^{-12}$ ).
- 1104 H. The mode of perceptual processing (i.e., the difference between the smoothed probability  
1105 of stimulus- vs. history-congruence) showed a quadratic relationship to RTs, with faster  
1106 response times for stronger biases toward both external sensory information and internal  
1107 predictions provided by perceptual history ( $\beta_2 = -19.86 \pm 0.52$ ,  $T(1.98 \times 10^6) = -38.43$ ,  
1108  $p = 5 \times 10^{-323}$ ). The horizontal and vertical dotted lines indicate maximum RT and the  
1109 associated mode, respectively.
- 1110 I. Confidence was enhanced for both stimulus-congruence (as opposed to stimulus-  
1111 incongruence,  $\beta = 0.48 \pm 1.38 \times 10^{-3}$ ,  $T(2.06 \times 10^6) = 351.89$ ,  $p = 0$ ) and history-congruence  
1112 ( $\beta = 0.04 \pm 1.18 \times 10^{-3}$ ,  $T(2.06 \times 10^6) = 36.86$ ,  $p = 2.93 \times 10^{-297}$ ).

<sub>1113</sub> J. In analogy to RTs, we found a quadratic relationship between the mode of perceptual pro-  
<sub>1114</sub> cessing and confidence, which increased when both externally- and internally-biased modes  
<sub>1115</sub> grew stronger ( $\beta_2 = 39.3 \pm 0.94$ ,  $T(2.06 \times 10^6) = 41.95$ ,  $p = 0$ ). The horizontal and vertical  
<sub>1116</sub> dotted lines indicate minimum confidence and the associated mode, respectively.

1117 **8.3 Figure 3**



1118 **Figure 3. Full and history-conditioned psychometric functions across modes in**  
1119 **humans.**

1120 A. Here, we show average psychometric functions for the full dataset (upper panel) and  
1121 conditioned on perceptual history ( $y_{t-1} = 1$  and  $y_{t-1} = 0$ ; middle and lower panel) across  
1122 modes (green line) and for internal mode (blue line) and external mode (red line) separately.  
1123

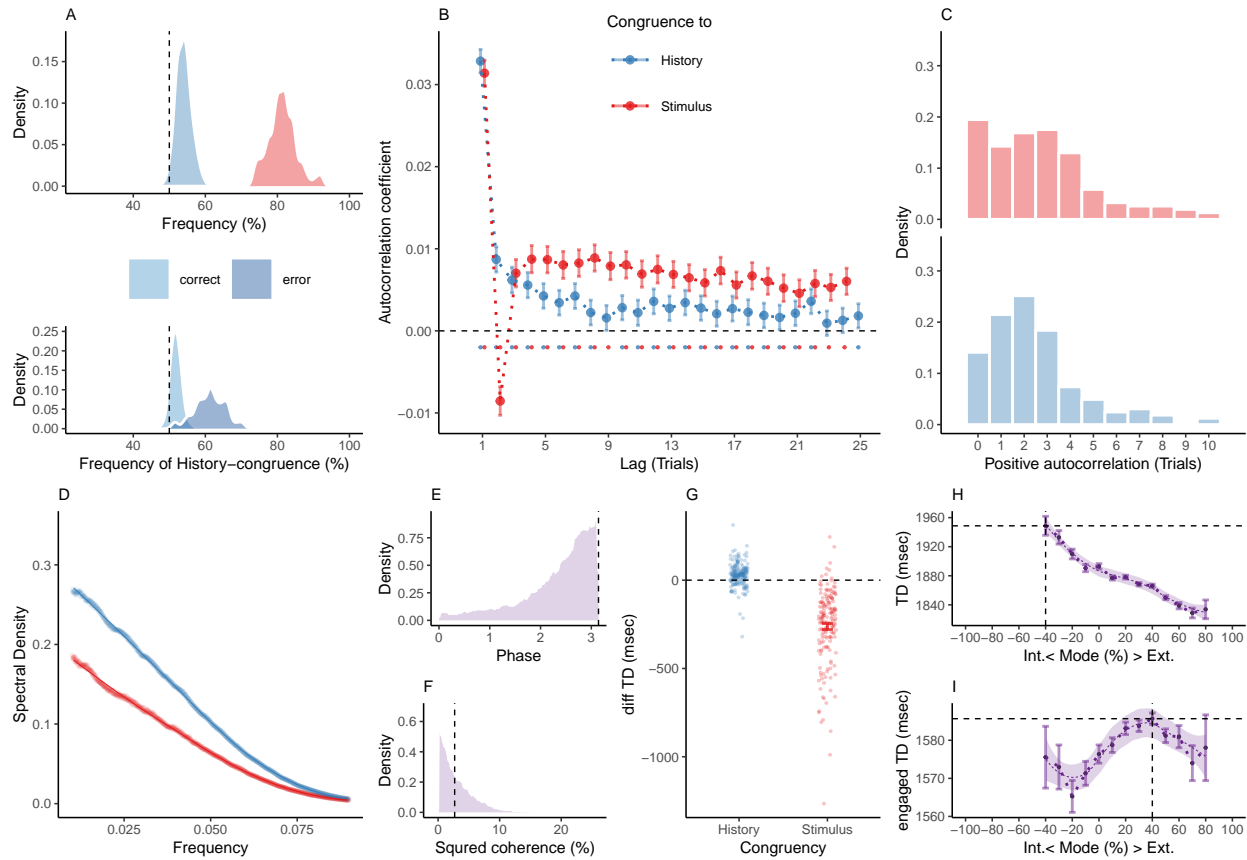
1124 B. Across the full dataset, biases  $\mu$  were distributed around zero ( $\beta_0 = 7.37 \times 10^{-3} \pm$   
1125 0.09,  $T(36.8) = 0.08$ ,  $p = 0.94$ ; upper panel), with larger absolute biases  $|\mu|$  for internal  
1126 as compared to external mode ( $\beta_0 = -0.62 \pm 0.07$ ,  $T(45.62) = -8.38$ ,  $p = 8.59 \times 10^{-11}$ ;  
1127 controlling for differences in lapses and thresholds). When conditioned on perceptual history,  
1128 we observed negative biases for  $y_{t-1} = 0$  ( $\beta_0 = 0.56 \pm 0.12$ ,  $T(43.39) = 4.6$ ,  $p = 3.64 \times 10^{-5}$ ;  
1129 middle panel) and positive biases for  $y_{t-1} = 1$  ( $\beta_0 = 0.56 \pm 0.12$ ,  $T(43.39) = 4.6$ ,  $p =$   
1130  $3.64 \times 10^{-5}$ ; lower panel).

<sub>1131</sub> C. Lapse rates were higher in internal mode as compared to external mode ( $\beta_0 = -0.05 \pm$   
<sub>1132</sub>  $5.73 \times 10^{-3}$ ,  $T(47.03) = -9.11$ ,  $p = 5.94 \times 10^{-12}$ ; controlling for differences in biases and  
<sub>1133</sub> thresholds; see upper panel and subplot D). Importantly, the between-mode difference in  
<sub>1134</sub> lapses depended on perceptual history: We found no significant difference in lower lapses  
<sub>1135</sub>  $\gamma$  for  $y_{t-1} = 0$  ( $\beta_0 = 0.01 \pm 7.77 \times 10^{-3}$ ,  $T(33.1) = 1.61$ ,  $p = 0.12$ ; middle panel), but a  
<sub>1136</sub> significant difference for  $y_{t-1} = 1$  ( $\beta_0 = -0.11 \pm 0.01$ ,  $T(40.11) = -9.59$ ,  $p = 6.14 \times 10^{-12}$ ;  
<sub>1137</sub> lower panel).

<sub>1138</sub> D. Conversely, higher lapses  $\delta$  were significantly increased for  $y_{t-1} = 0$  ( $\beta_0 = -0.1 \pm 9.58 \times$   
<sub>1139</sub>  $10^{-3}$ ,  $T(36.87) = -10.16$ ,  $p = 3.06 \times 10^{-12}$ ; middle panel), but not for  $y_{t-1} = 1$  ( $\beta_0 = 0.01$   
<sub>1140</sub>  $\pm 7.74 \times 10^{-3}$ ,  $T(33.66) = 1.58$ ,  $p = 0.12$ ; lower panel).

<sub>1141</sub> E. The thresholds  $t$  were larger in internal as compared to external mode ( $\beta_0 = -1.77 \pm$   
<sub>1142</sub>  $0.25$ ,  $T(50.45) = -7.14$ ,  $p = 3.48 \times 10^{-9}$ ; controlling for differences in biases and lapses)  
<sub>1143</sub> and were not modulated by perceptual history ( $\beta_0 = 0.04 \pm 0.06$ ,  $T(2.97 \times 10^3) = 0.73$ ,  $p$   
<sub>1144</sub>  $= 0.47$ ).

1145 **8.4 Figure 4**



1146

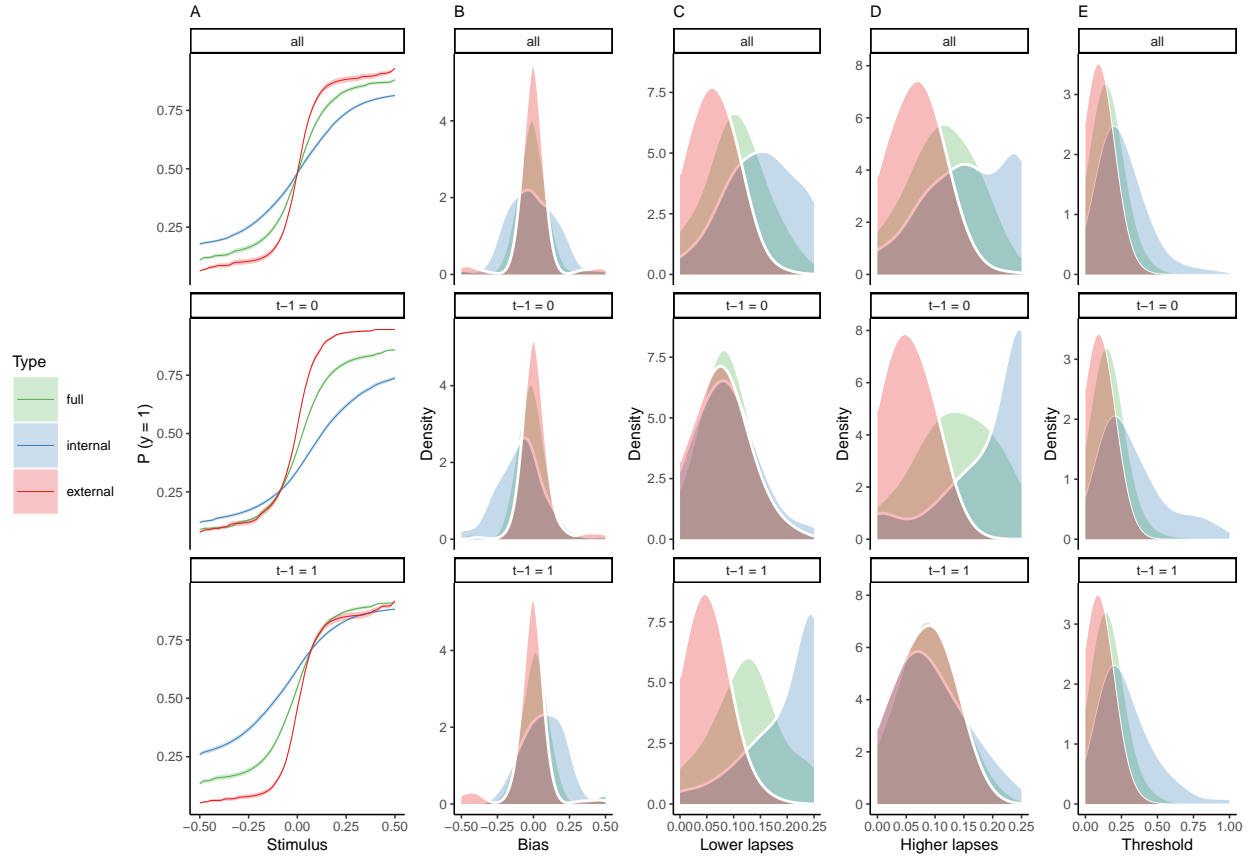
1147 **Figure 4. Internal and external modes in murine perceptual decision-making.**

1148 A. In mice,  $81.37\% \pm 0.3\%$  of trials were stimulus-congruent (in red) and  $54.03\% \pm 0.17\%$  of  
 1149 trials were history-congruent (in blue; upper panel). History-congruent perceptual choices  
 1150 were not a consequence of the experimental design, but a source of error, as they were more  
 1151 frequent on stimulus-incongruent trials (lower panel).

1152 B. Relative to randomly permuted data, we found highly significant autocorrelations of  
 1153 stimulus-congruence and history-congruence (dots indicate intercepts  $\neq 0$  in trial-wise lin-  
 1154 ear mixed effects modeling at  $p < 0.05$ ). Please note that the negative autocorrelation of  
 1155 stimulus-congruence at trial 2 was a consequence of the experimental design (see Supplemen-  
 1156 tal Figure 2D-F). As in humans, autocorrelation coefficients were best fit by an exponential  
 1157 function (adjusted  $R^2$  for stimulus-congruence: 0.44; history-congruence: 0.52) as compared  
 1158 to a linear function (adjusted  $R^2$  for stimulus-congruence:  $3.16 \times 10^{-3}$ ; history-congruence:

- <sub>1159</sub> 0.26).
- <sub>1160</sub> C. For stimulus-congruence (upper panel), the lag of positive autocorrelation was longer  
<sub>1161</sub> in comparison to humans ( $4.59 \pm 0.06$  on average). For history-congruence (lower panel),  
<sub>1162</sub> the lag of positive autocorrelation was slightly shorter relative to humans ( $2.58 \pm 0.01$  on  
<sub>1163</sub> average, peaking at trial  $t+2$  after the index trial).
- <sub>1164</sub> D. In mice, the dynamic probabilities of stimulus- and history-congruence (sliding windows  
<sub>1165</sub> of  $\pm 5$  trials) fluctuated as *1/f noise*.
- <sub>1166</sub> E. The distribution of phase shift between fluctuations in stimulus- and history-congruence  
<sub>1167</sub> peaked at half a cycle ( $\pi$  denoted by dotted line).
- <sub>1168</sub> F. The average squared coherence between fluctuations in stimulus- and history-congruence  
<sub>1169</sub> (black dotted line) amounted to  $3.45 \pm 0.01\%$
- <sub>1170</sub> G. We observed shorter trial durations (TDs) for stimulus-congruence (as opposed to  
<sub>1171</sub> stimulus-incongruence,  $\beta = -1.12 \pm 8.53 \times 10^{-3}$ ,  $T(1.34 \times 10^6) = -131.78$ ,  $p = 0$ ), but  
<sub>1172</sub> longer TDs for history-congruence ( $\beta = 0.06 \pm 6.76 \times 10^{-3}$ ,  $T(1.34 \times 10^6) = 8.52$ ,  $p =$   
<sub>1173</sub>  $1.58 \times 10^{-17}$ ).
- <sub>1174</sub> H. TDs decreased monotonically for stronger biases toward external mode ( $\beta_1 = -4.16 \times 10^4$   
<sub>1175</sub>  $\pm 1.29 \times 10^3$ ,  $T(1.35 \times 10^6) = -32.31$ ,  $p = 6.03 \times 10^{-229}$ ). The horizontal and vertical dotted  
<sub>1176</sub> lines indicate maximum TD and the associated mode, respectively.
- <sub>1177</sub> I. For TDs that differed from the median TD by no more than  $1.5 \times \text{MAD}$  (median absolute  
<sub>1178</sub> distance<sup>52</sup>), mice exhibited a quadratic component in the relationship between the mode  
<sub>1179</sub> of sensory processing and TDs ( $\beta_2 = -1.97 \times 10^3 \pm 843.74$ ,  $T(1.19 \times 10^6) = -2.34$ ,  $p =$   
<sub>1180</sub> 0.02, Figure 4I). This explorative post-hoc analysis focuses on trials at which mice engage  
<sub>1181</sub> more swiftly with the experimental task. The horizontal and vertical dotted lines indicate  
<sub>1182</sub> maximum TD and the associated mode, respectively.

1183 **8.5 Figure 5**



1184 **Figure 5. Full and history-conditioned psychometric functions across modes in**  
 1185 **mice.**

1186 A. Here, we show average psychometric functions for the full IBL dataset (upper panel) and  
 1187 conditioned on perceptual history ( $y_{t-1} = 1$  and  $y_{t-1} = 0$ ; middle and lower panel) across  
 1188 modes (green line) and for internal mode (blue line) and external mode (red line) separately.  
 1189

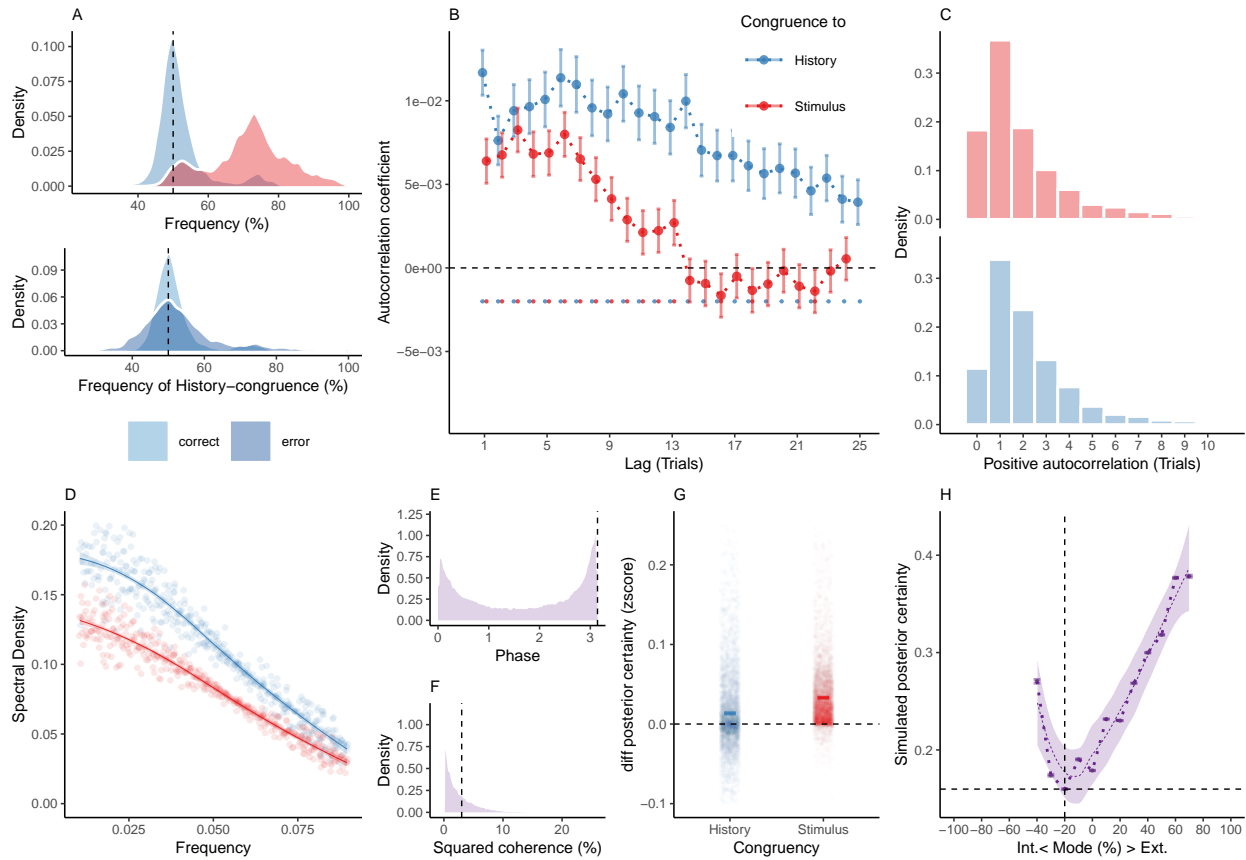
1190 B. Across the full dataset, biases  $\mu$  were distributed around zero ( $T(164) = 0.39$ ,  $p = 0.69$ ;  
 1191 upper panel), with larger absolute biases  $|\mu|$  for internal as compared to external mode ( $\beta_0 =$   
 1192  $-0.18 \pm 0.03$ ,  $T = -6.38$ ,  $p = 1.77 \times 10^{-9}$ ; controlling for differences in lapses and thresholds).  
 1193 When conditioned on perceptual history, we observed negative biases for  $y_{t-1} = 0$  ( $T(164)$   
 1194  $= -1.99$ ,  $p = 0.05$ ; middle panel) and positive biases for  $y_{t-1} = 1$  ( $T(164) = 1.91$ ,  $p = 0.06$ ;  
 1195 lower panel).

<sub>1196</sub> C. Lapse rates were higher in internal as compared to external mode ( $\beta_0 = -0.11 \pm 4.39 \times$   
<sub>1197</sub>  $10^{-3}$ ,  $T = -24.8$ ,  $p = 4.91 \times 10^{-57}$ ; controlling for differences in biases and thresholds; upper  
<sub>1198</sub> panel, see also subplot D). For  $y_{t-1} = 1$ , the difference between internal and external mode  
<sub>1199</sub> was more pronounced for lower lapses  $\gamma$  ( $T(164) = -18.24$ ,  $p = 2.68 \times 10^{-41}$ ) as compared  
<sub>1200</sub> to higher lapses  $\delta$  (see subplot D). In mice, lower lapses  $\gamma$  were significantly elevated during  
<sub>1201</sub> internal mode irrespective of the preceding perceptual choice (middle panel: lower lapses  $\gamma$   
<sub>1202</sub> for  $y_{t-1} = 0$ ;  $T(164) = -2.5$ ,  $p = 0.01$ , lower panel: lower lapses  $\gamma$  for  $y_{t-1} = 1$ ;  $T(164) =$   
<sub>1203</sub>  $-32.44$ ,  $p = 2.92 \times 10^{-73}$ ).

<sub>1204</sub> D. For  $y_{t-1} = 0$ , the difference between internal and external mode was more pronounced  
<sub>1205</sub> for higher lapses  $\delta$  ( $T(164) = 21.44$ ,  $p = 1.93 \times 10^{-49}$ , see subplot C). Higher lapses were  
<sub>1206</sub> significantly elevated during internal mode irrespective of the preceding perceptual choice  
<sub>1207</sub> (middle panel: higher lapses  $\delta$  for  $y_{t-1} = 0$ ;  $T(164) = -28.29$ ,  $p = 5.62 \times 10^{-65}$  lower panel:  
<sub>1208</sub> higher lapses  $\delta$  for  $y_{t-1} = 1$ ;  $T(164) = -2.65$ ,  $p = 8.91 \times 10^{-3}$ ; ).

<sub>1209</sub> E. Thresholds  $t$  were higher in internal as compared to external mode ( $\beta_0 = -0.28 \pm 0.04$ ,  
<sub>1210</sub>  $T = -7.26$ ,  $p = 1.53 \times 10^{-11}$ ; controlling for differences in biases and lapses) and were not  
<sub>1211</sub> modulated by perceptual history ( $T(164) = 0.94$ ,  $p = 0.35$ ).

1212 **8.6 Figure 6**



1214 **Figure 6. Internal and external modes in simulated perceptual decision-making.**

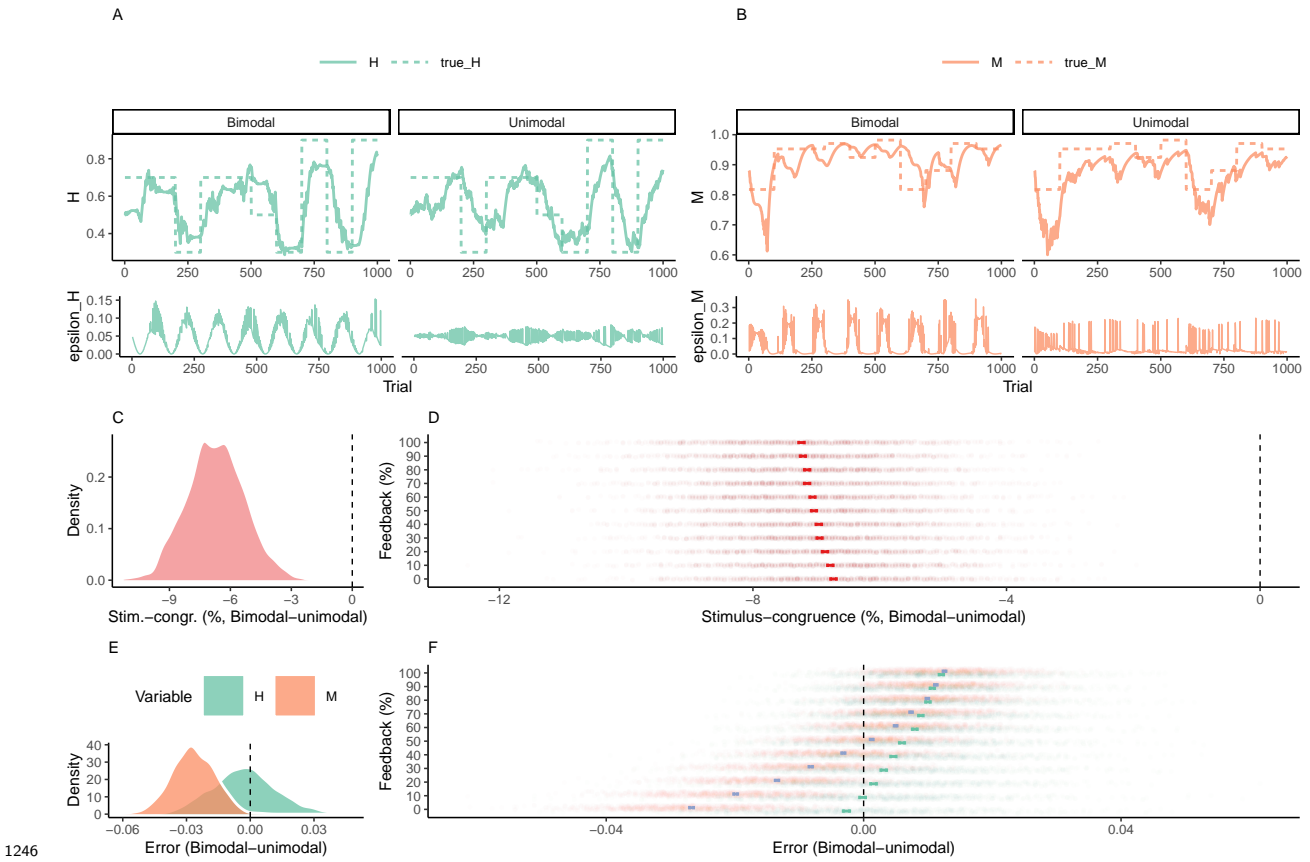
1215 A. Simulated perceptual choices were stimulus-congruent in  $71.36\% \pm 0.17\%$  (in red) and  
 1216 history-congruent in  $51.99\% \pm 0.11\%$  of trials (in blue;  $T(4.32 \times 10^3) = 17.42, p = 9.89 \times 10^{-66}$ ;  
 1217 upper panel). Due to the competition between stimulus- and history-congruence, history-  
 1218 congruent perceptual choices were more frequent when perception was stimulus-incongruent  
 1219 (i.e., on *error* trials;  $T(4.32 \times 10^3) = 11.19, p = 1.17 \times 10^{-28}$ ; lower panel) and thus impaired  
 1220 performance in the randomized psychophysical design simulated here.

1221 B. At the simulated group level, we found significant autocorrelations in both stimulus-  
 1222 congruence (13 consecutive trials) and history-congruence (30 consecutive trials).

1223 C. On the level of individual simulated participants, autocorrelation coefficients exceeded the  
 1224 autocorrelation coefficients of randomly permuted data within a lag of  $2.46 \pm 1.17 \times 10^{-3}$

- 1225 trials for stimulus-congruence and  $4.24 \pm 1.85 \times 10^{-3}$  trials for history-congruence.
- 1226 D. The smoothed probabilities of stimulus- and history-congruence (sliding windows of  $\pm 5$   
1227 trials) fluctuated as *1/f noise*, i.e., at power densities that were inversely proportional to the  
1228 frequency (power  $\sim 1/f^\beta$ ; stimulus-congruence:  $\beta = -0.81 \pm 1.18 \times 10^{-3}$ ,  $T(1.92 \times 10^5) =$   
1229  $-687.58$ ,  $p = 0$ ; history-congruence:  $\beta = -0.83 \pm 1.27 \times 10^{-3}$ ,  $T(1.92 \times 10^5) = -652.11$ ,  $p$   
1230  $= 0$ ).
- 1231 E. The distribution of phase shift between fluctuations in simulated stimulus- and history-  
1232 congruence peaked at half a cycle ( $\pi$  denoted by dotted line). The dynamic probabilities of  
1233 simulated stimulus- and history-congruence were therefore were strongly anti-correlated ( $\beta$   
1234  $= -0.03 \pm 8.22 \times 10^{-4}$ ,  $T(2.12 \times 10^6) = -40.52$ ,  $p = 0$ ).
- 1235 F. The average squared coherence between fluctuations in simulated stimulus- and history-  
1236 congruence (black dotted line) amounted to  $6.49 \pm 2.07 \times 10^{-3}\%$ .
- 1237 G. Simulated confidence was enhanced for stimulus-congruence ( $\beta = 0.03 \pm 1.71 \times 10^{-4}$ ,  
1238  $T(2.03 \times 10^6) = 178.39$ ,  $p = 0$ ) and history-congruence ( $\beta = 0.01 \pm 1.5 \times 10^{-4}$ ,  $T(2.03 \times 10^6)$   
1239  $= 74.18$ ,  $p = 0$ ).
- 1240 H. In analogy to humans, the simulated data showed a quadratic relationship between the  
1241 mode of perceptual processing and posterior certainty, which increased for stronger external  
1242 and internal biases ( $\beta_2 = 31.03 \pm 0.15$ ,  $T(2.04 \times 10^6) = 205.95$ ,  $p = 0$ ). The horizontal  
1243 and vertical dotted lines indicate minimum posterior certainty and the associated mode,  
1244 respectively.

1245 **8.7 Figure 7**



1246 **Figure 7. Adaptive benefits of bimodal inference.**

1247 A. When the sensory environment changes unpredictably over time, agents have to update  
 1248 estimates  $H_t$  (solid green line, upper panel) about the true hazard rate  $\hat{H}_t$  from experience  
 1249 (dotted green line, upper panel). Updates to  $H_t$  are driven by an error term  $\epsilon_H$  (solid  
 1250 green line, lower panel) that is defined by the difference between  $H_t$  and the presence of a  
 1251 perceived change in the environment. In contrast to the unimodal model (right panels),  $\epsilon_H$   
 1252 of the bimodal model (left panels) is modulated by a phasic component reflecting ongoing  
 1253 fluctuations between internal and external mode.

1254  
 1255 B. When the precision of sensory encoding changes unpredictably over time, agents have  
 1256 to update estimates  $M_t$  (solid orange line, upper panel) about the true precision of sensory  
 1257 encoding  $\hat{M}_t$  from experience (dotted orange line, upper panel). Updates to  $M_t$  are driven  
 1258 by an error term  $\epsilon_M$  (red line, lower panel) that is defined by the difference between  $M_t$

<sub>1259</sub> and the posterior decision-certainty. In contrast to the unimodal model (right panels),  $\epsilon_M$   
<sub>1260</sub> of the bimodal model (left panels) is modulated by a phasic component reflecting ongoing  
<sub>1261</sub> fluctuations between internal and external mode.

<sub>1262</sub> C. In the absence of feedback, the bimodal inference model achieved lower stimulus-  
<sub>1263</sub> congruence as compared the unimodal control model ( $\beta_1 = -6.71 \pm 0.03$ ,  $T(8.42 \times 10^3) =$   
<sub>1264</sub>  $-234.31$ ,  $p = 0$ ).

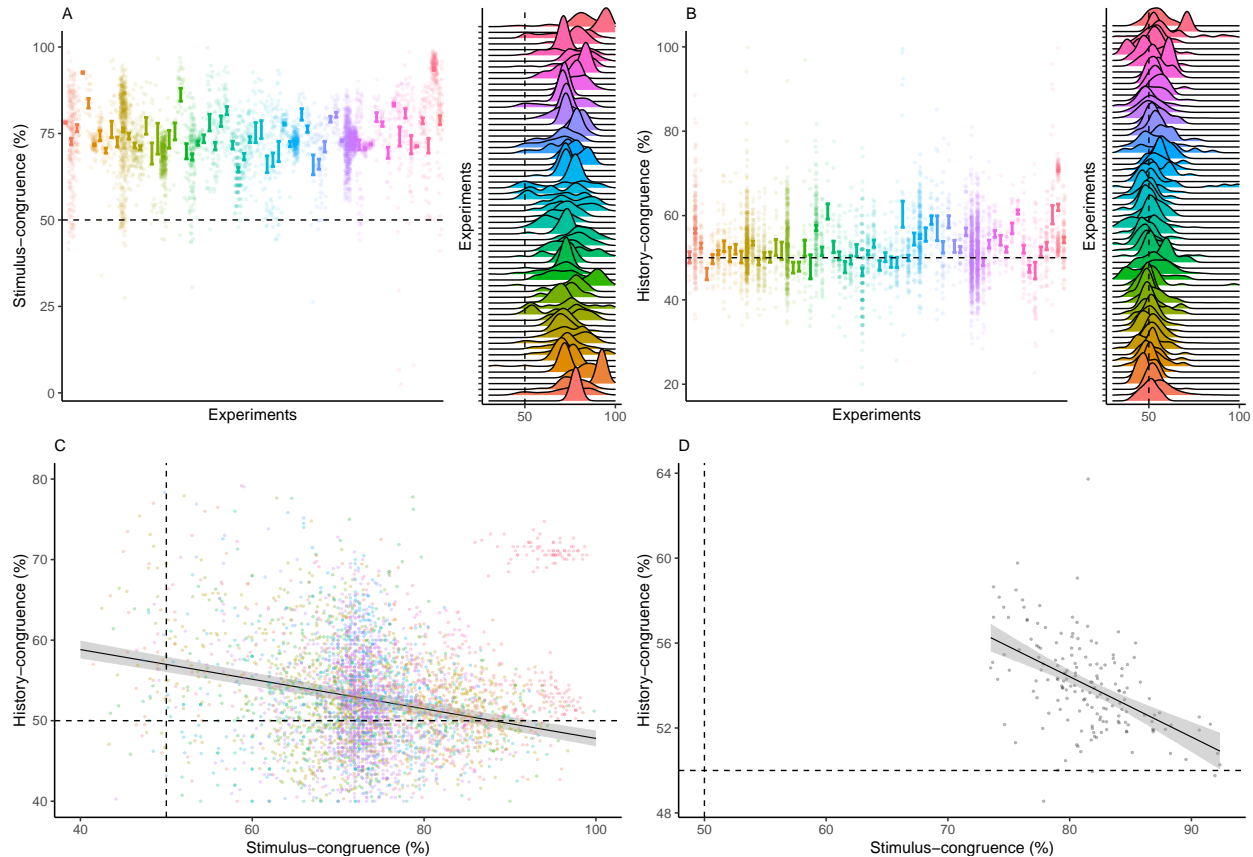
<sub>1265</sub> D. The unimodal control model benefited more strongly from the presence of external feed-  
<sub>1266</sub> back, leading to a relative decrease in stimulus-congruence for the bimodal inference model at  
<sub>1267</sub> higher feedback levels ( $\beta_2 = -0.05 \pm 4.13 \times 10^{-3}$ ,  $T(10 \times 10^3) = -12.32$ ,  $p = 1.25 \times 10^{-34}$ ).

<sub>1268</sub> E. In the absence of feedback, the bimodal inference model achieved lower errors in the  
<sub>1269</sub> estimated hazard rate  $H$  ( $\beta_1 = -2.94 \times 10^{-3} \pm 2.89 \times 10^{-4}$ ,  $T(4.96 \times 10^3) = -10.18$ ,  $p$   
<sub>1270</sub>  $= 4.11 \times 10^{-24}$ ) as well as lower errors in the estimated probability of stimulus-congruent  
<sub>1271</sub> choices  $M$  ( $\beta_1 = -0.03 \pm 1.86 \times 10^{-4}$ ,  $T(6.07 \times 10^3) = -137.75$ ,  $p = 0$ ).

<sub>1272</sub> F. With an increasing availability of feedback, the advantage of the bimodal inference model  
<sub>1273</sub> was lost with respect to  $H$  ( $\beta_2 = 1.43 \times 10^{-3} \pm 3.71 \times 10^{-5}$ ,  $T(10 \times 10^3) = 38.58$ ,  $p =$   
<sub>1274</sub>  $9.44 \times 10^{-304}$ ) and  $M$  ( $\beta_2 = 3.91 \times 10^{-3} \pm 2.51 \times 10^{-5}$ ,  $T(10 \times 10^3) = 156.18$ ,  $p = 0$ ).

1275 **9 Supplemental Items**

1276 **9.1 Supplemental Figure S1**



1277 **Supplemental Figure S1. Stimulus- and history-congruence.**

1279 A. Stimulus-congruent choices in humans amounted to  $73.46\% \pm 0.15\%$  of trials and were  
1280 highly consistent across the experiments selected from the Confidence Database.

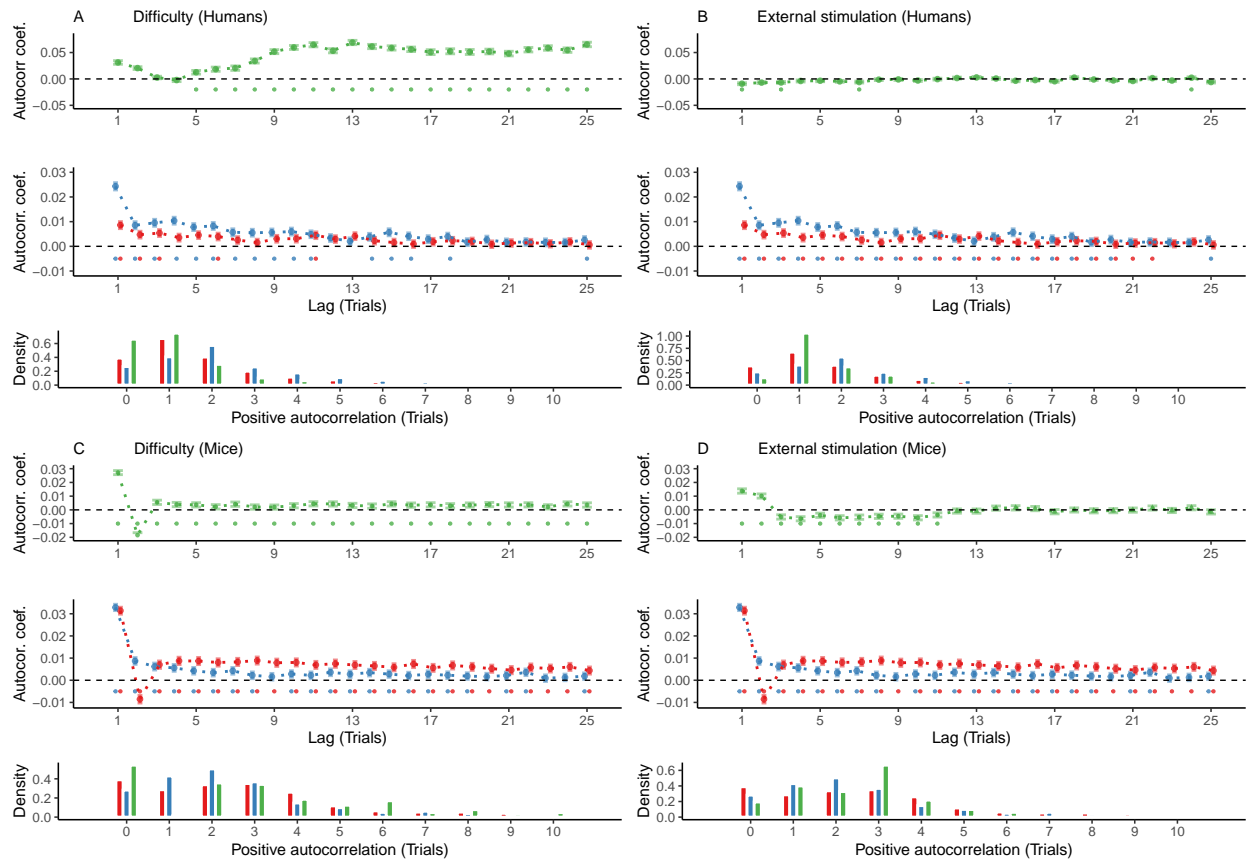
1281 B. History-congruent choices in humans amounted to  $52.7\% \pm 0.12\%$  of trials. In analogy to  
1282 stimulus-congruence, the prevalence of history-congruence was highly consistent across the  
1283 experiments selected from the Confidence Database. 48.48% of experiments showed signif-  
1284 icant ( $p < 0.05$ ) attractive biases toward preceding choices, whereas 3.03% of experiments  
1285 showed significant repulsive biases.

1286 C. In humans, we found an enhanced impact of perceptual history in participants who were

<sub>1287</sub> less sensitive to external sensory information ( $T(4.3 \times 10^3) = -14.27$ ,  $p = 3.78 \times 10^{-45}$ ),  
<sub>1288</sub> suggesting that perception results from the competition of external with internal information.

<sub>1289</sub> D. In analogy to humans, mice that were less sensitive to external sensory information  
<sub>1290</sub> showed stronger biases toward perceptual history ( $T(163) = -7.52$ ,  $p = 3.44 \times 10^{-12}$ , Pearson  
<sub>1291</sub> correlation).

1292 **9.2 Supplemental Figure S2**



1293

1294 **Supplemental Figure S2. Controlling for task difficulty and external stimulation.**

1295 In this study, we found highly significant autocorrelations of stimulus- and history-  
 1296 congruence in humans as well as in mice. Here, we show that these autocorrelations are not  
 1297 a trivial consequence of task difficulty or the sequence external stimulation. In addition, we  
 1298 computed trial-wise logistic regression coefficients as an alternative approach to assessing  
 1299 serial dependencies in stimulus- and history-congruence.

1300 A. In humans, task difficulty (in green) showed a significant autocorrelated starting at the  
 1301 5th trial (upper panel, dots at the bottom indicate intercepts  $\neq 0$  in trial-wise linear mixed  
 1302 effects modeling at  $p < 0.05$ ). When controlling for task difficulty, linear mixed effects  
 1303 modeling indicated a significant auto-correlation of stimulus-congruence (in red) for the first  
 1304 3 consecutive trials (middle panel). 20% of trials within the displayed time window remained  
 1305 significantly autocorrelated. The autocorrelation of history-congruence (in blue) remained

1306 significant for the first 11 consecutive trials (64% significantly autocorrelated trials within  
1307 the displayed time window). At the level of individual participants, the autocorrelation of  
1308 task difficulty exceeded the respective autocorrelation of randomly permuted within a lag of  
1309  $21.66 \pm 8.37 \times 10^{-3}$  trials (lower panel).

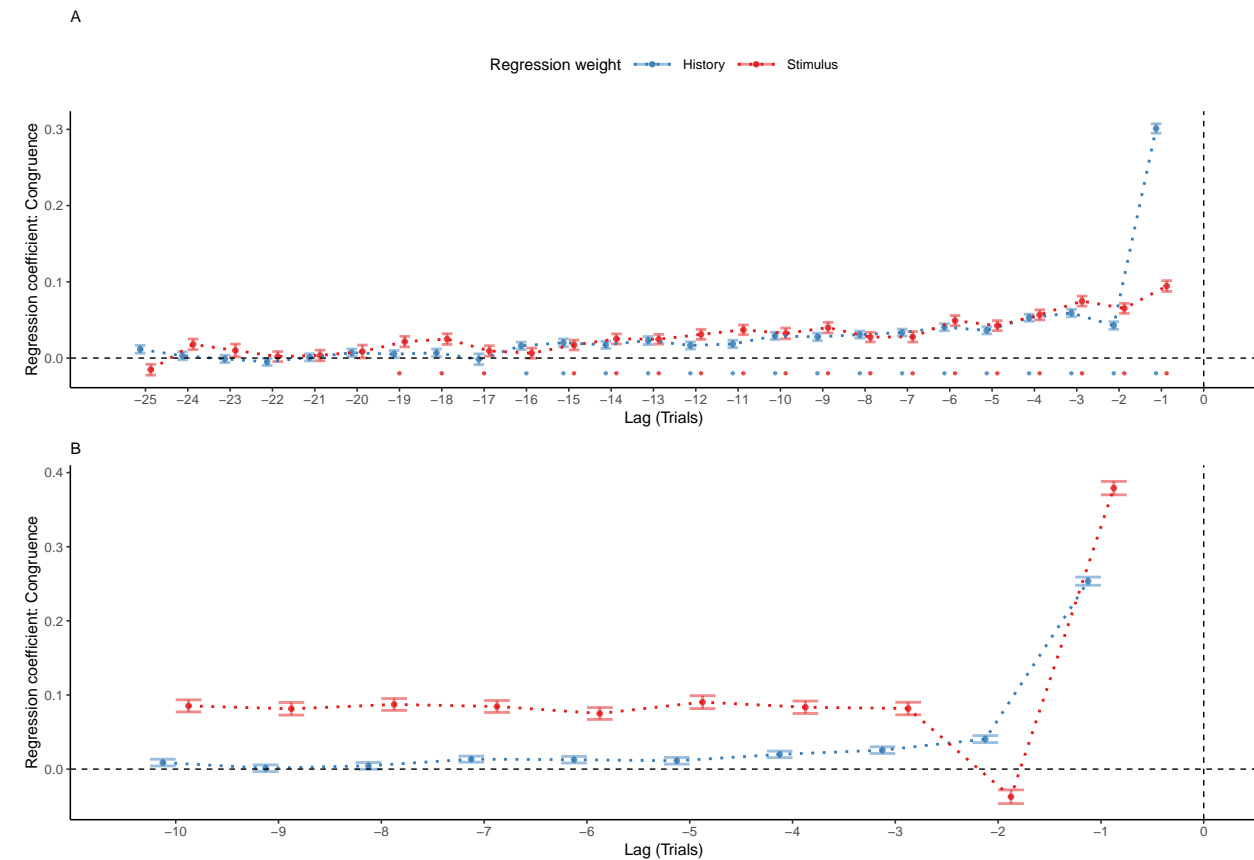
1310 B. The sequence of external stimulation (i.e., which of the two binary outcomes was sup-  
1311 ported by the presented stimuli; depicted in green) was negatively autocorrelated for 1 trial.  
1312 When controlling for the autocorrelation of external stimulation, stimulus-congruence re-  
1313 mained significantly autocorrelated for 22 consecutive trials (88% of trials within the dis-  
1314 played time window; lower panel) and history-congruence remained significantly autocor-  
1315 related for 20 consecutive trials (84% of trials within the displayed time window). At the level  
1316 of individual participants, the autocorrelation of external stimulation exceeded the respective  
1317 autocorrelation of randomly permuted within a lag of  $2.94 \pm 4.4 \times 10^{-3}$  consecutive trials  
1318 (lower panel).

1319 C. In mice, task difficulty showed an significant autocorrelated for the first 25 consecutive  
1320 trials (upper panel). When controlling for task difficulty, linear mixed effects modeling indi-  
1321 cated a significant auto-correlation of stimulus-congruence for the first 36 consecutive trials  
1322 (middle panel). In total, 100% of trials within the displayed time window remained signif-  
1323 icantly autocorrelated. The autocorrelation of history-congruence remained significant for  
1324 the first 8 consecutive trials, with 84% significantly autocorrelated trials within the displayed  
1325 time window. At the level of individual mice, autocorrelation coefficients for difficulty were  
1326 elevated above randomly permuted data within a lag of  $15.13 \pm 0.19$  consecutive trials (lower  
1327 panel).

1328 D. In mice, the sequence of external stimulation (i.e., which of the two binary outcomes was  
1329 supported by the presented stimuli) was negatively autocorrelated for 11 consecutive trials  
1330 (upper panel). When controlling for the autocorrelation of external stimulation, stimulus-  
1331 congruence remained significantly autocorrelated for 86 consecutive trials (100% of trials

<sub>1332</sub> within the displayed time window; middle) and history-congruence remained significantly  
<sub>1333</sub> autocorrelated for 8 consecutive trials (84% of trials within the displayed time window). At  
<sub>1334</sub> the level of individual mice, autocorrelation coefficients for external stimulation were elevated  
<sub>1335</sub> above randomly permuted data within a lag of  $2.53 \pm 9.8 \times 10^{-3}$  consecutive trials (lower  
<sub>1336</sub> panel).

1337 **9.3 Supplemental Figure S3**



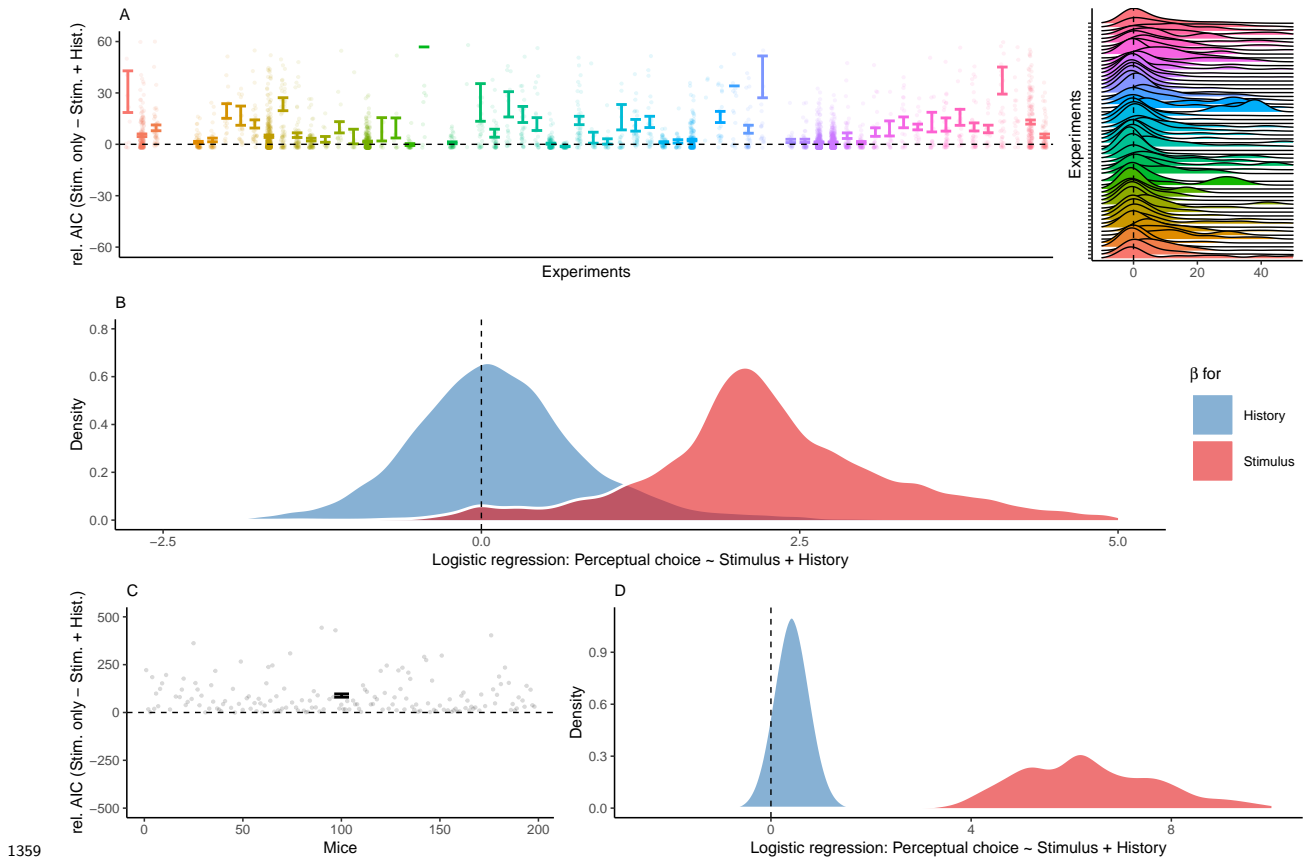
1339 **Supplemental Figure S3. Reproducing group-level autocorrelations using logistic  
1340 regression.**

1341 A. As an alternative to group-level autocorrelation coefficients, we used trial-wise logistic  
1342 regression to quantify serial dependencies in stimulus- and history-congruence. This analysis  
1343 predicted stimulus- and history-congruence at the index trial (trial  $t = 0$ , vertical line)  
1344 based on stimulus- and history-congruence at the 25 preceding trials. Mirroring the shape of  
1345 the group-level autocorrelations, trial-wise regression coefficients (depicted as mean  $\pm$  SEM,  
1346 dots mark trials with regression weights significantly greater than zero at  $p < 0.05$ ) increased  
1347 toward the index trial  $t = 0$  for the human data.

1348 B. Following our results in human data, regression coefficients that predicted history-  
1349 congruence at the index trial (trial  $t = 0$ , vertical line) increased exponentially for trials  
1350 closer to the index trial in mice. In contrast to history-congruence, stimulus-congruence

1351 showed a negative regression weight (or autocorrelation coefficient, see Figure 4B) at trial  
1352 -2. This was due to the experimental design (see also the autocorrelations of difficulty and  
1353 external stimulation in Supplemental Figure S2C and D): When mice made errors at easy  
1354 trials (contrast  $\geq 50\%$ ), the upcoming stimulus was shown at the same spatial location and  
1355 at high contrast. This increased the probability of stimulus-congruent perceptual choices  
1356 after stimulus-incongruent perceptual choices at easy trials, thereby creating a negative  
1357 regression weight (or autocorrelation coefficient) of stimulus-congruence at trial -2.

1358 **9.4 Supplemental Figure S4**



1359 **1360 Supplemental Figure S4. History-congruence in logistic regression.**

1361 A. To ensure that perceptual history played a significant role in perception despite the ongo-  
 1362 ing stream of external information, we tested whether human perceptual decision-making was  
 1363 better explained by the combination of external and internal information or, alternatively, by  
 1364 external information alone. To this end, we compared Aikake information criteria between lo-  
 1365 gistic regression models that predicted trial-wise perceptual responses either by both current  
 1366 external sensory information and the preceding percept, or by external sensory information  
 1367 alone (values above zero indicate a superiority of the full model). With high consistency  
 1368 across the experiments selected from the Confidence Database, this model-comparison con-  
 1369 firmed that perceptual history contributed significantly to perception (difference in AIC =  
 1370  $8.07 \pm 0.53$ ,  $T(57.22) = 4.1$ ,  $p = 1.31 \times 10^{-4}$ ).

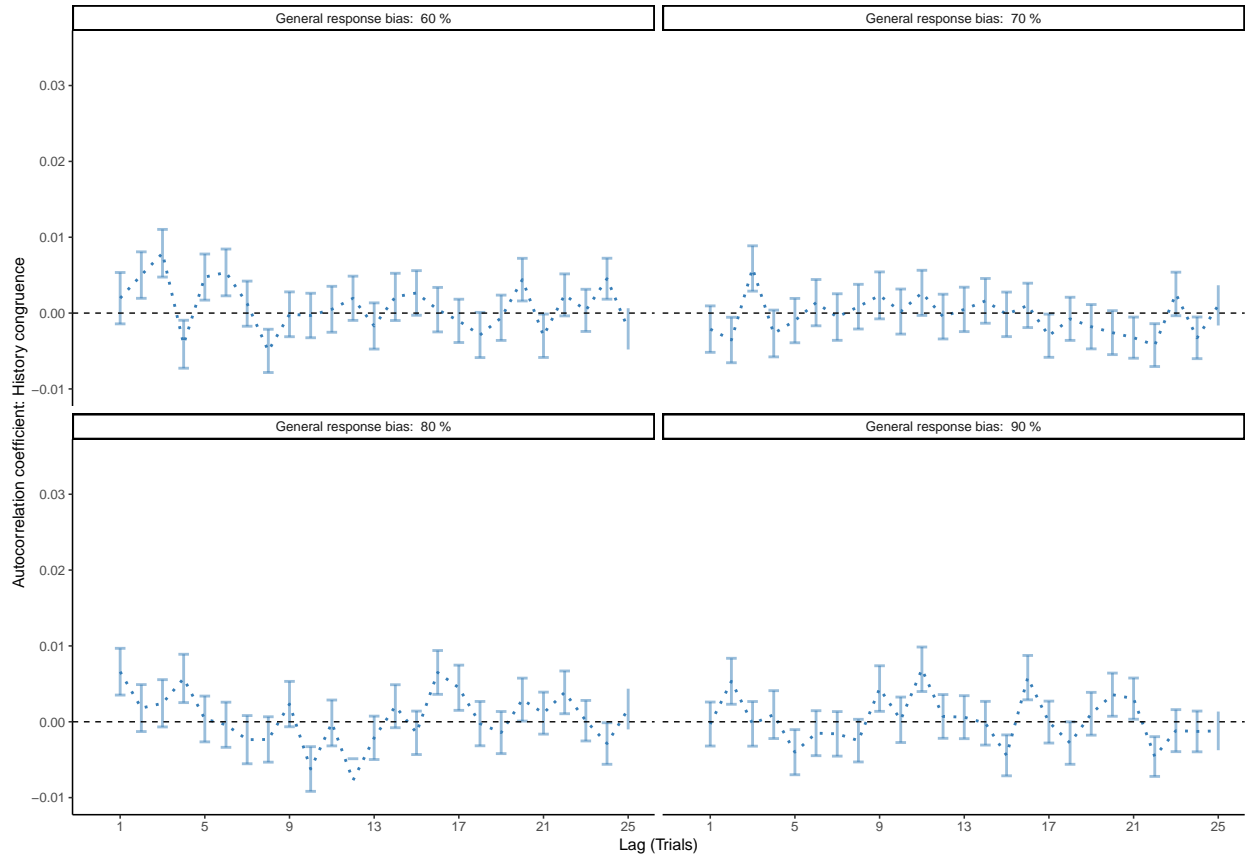
1371 B. Participant-wise regression coefficients amount to  $0.18 \pm 0.02$  for the effect of perceptual

<sub>1372</sub> history and  $2.51 \pm 0.03$  for external sensory stimulation.

<sub>1373</sub> C. In mice, an AIC-based model comparison indicated that perception was better explained  
<sub>1374</sub> by logistic regression models that predicted trial-wise perceptual responses based on both  
<sub>1375</sub> current external sensory information and the preceding percept (difference in AIC = 88.62  
<sub>1376</sub>  $\pm 8.57$ ,  $T(164) = -10.34$ ,  $p = 1.29 \times 10^{-19}$ ).

<sub>1377</sub> D. In mice, individual regression coefficients amounted to  $0.42 \pm 0.02$  for the effect of per-  
<sub>1378</sub> ceptual history and  $6.91 \pm 0.21$  for external sensory stimulation.

1379 **9.5 Supplemental Figure S5**

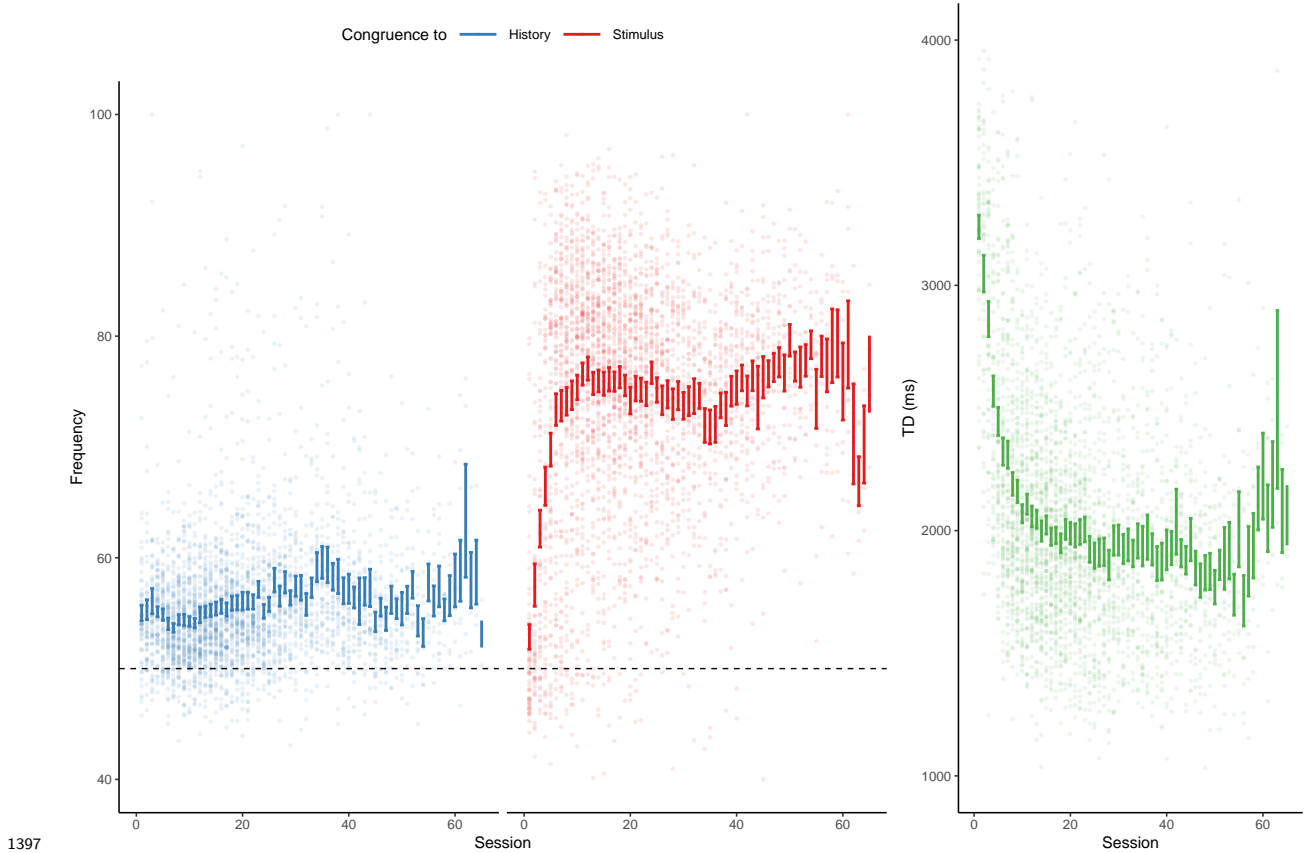


1380 **1381 Supplemental Figure S5. Correcting for general response biases.**

1382 Here, we ask whether the autocorrelation of history-congruence (as shown in Figure 2-3C)  
1383 may be driven by general response biases (i.e., a general propensity to choose one of the  
1384 two possible outcomes more frequently than the alternative). To this end, we generated  
1385 sequences of 100 perceptual choices with general response biases ranging from 60 to 90%  
1386 for 1000 simulated participants each. We then computed the autocorrelation of history-  
1387 congruence for these simulated data. Crucially, we used the correction procedure that is  
1388 applied to all autocorrelation curves shown in this manuscript: All reported autocorrelation  
1389 coefficients are computed relative to the average autocorrelation coefficients obtained for  
1390 100 iterations of randomly permuted trial sequences. The above simulation show that this  
1391 correction procedure removes any potential contribution of general response biases to the  
1392 auto-correlation of history-congruence. This indicates that the autocorrelation of history-

<sub>1393</sub> congruence (as shown in Figure 2-3C) is not driven by general response biases that were  
<sub>1394</sub> present in the empirical data at a level of  $58.71\% \pm 0.22\%$  in humans and  $54.6\% \pm 0.3\%$  in  
<sub>1395</sub> mice.

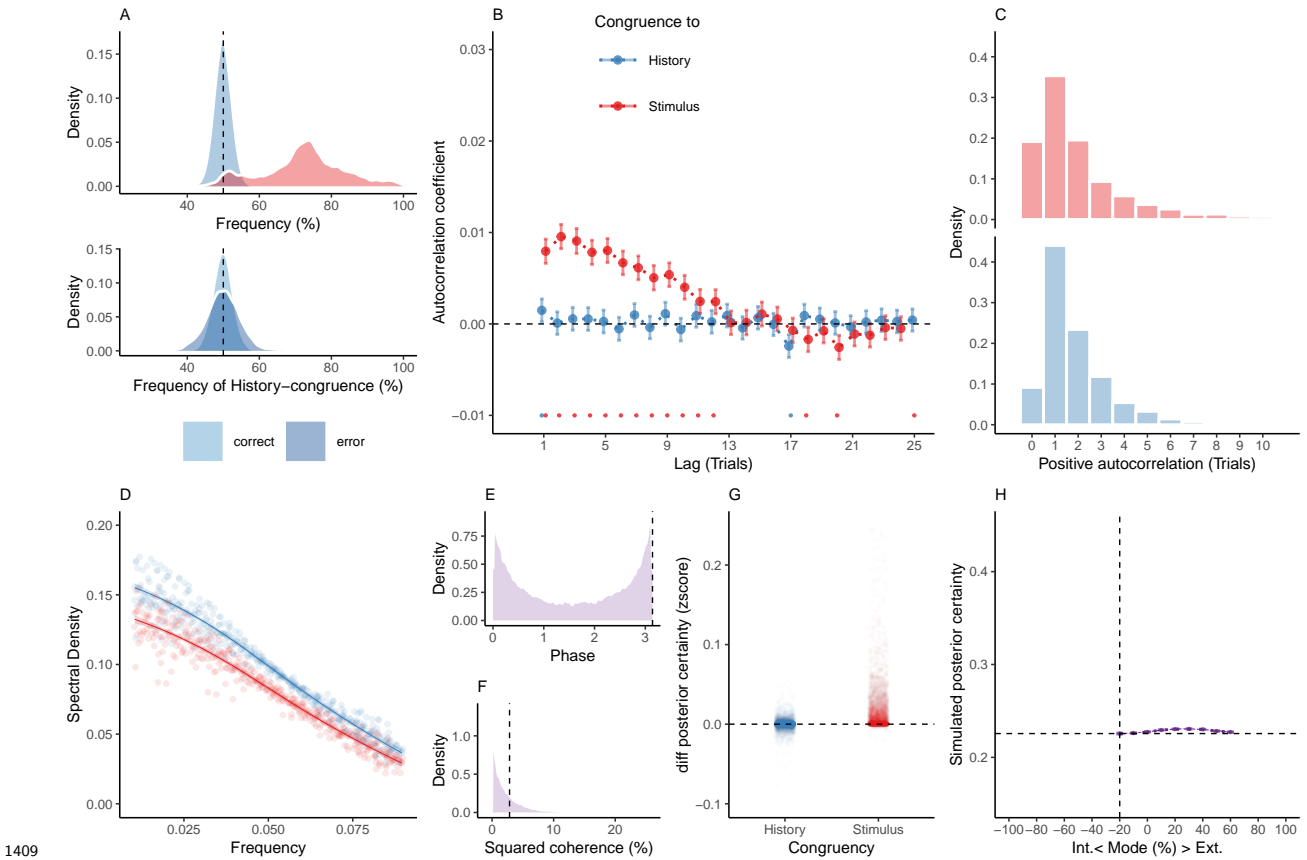
1396 **9.6 Supplemental Figure S6**



1398 **Supplemental Figure S6. History-/stimulus-congruence and TDs during training  
1399 of the basic task.**

1400 Here, we depict the progression of history- and stimulus-congruence (depicted in blue and  
1401 red, respectively; left panel) as well as TDs (in green; right panel) across training sessions in  
1402 mice that achieved proficiency (i.e., stimulus-congruence  $\geq 80\%$ ) in the *basic* task of the IBL  
1403 dataset. We found that both history-congruent perceptual choices ( $\beta = 0.13 \pm 4.67 \times 10^{-3}$ ,  
1404  $T(8.4 \times 10^3) = 27.04$ ,  $p = 1.96 \times 10^{-154}$ ) and stimulus-congruent perceptual choices ( $\beta =$   
1405  $0.34 \pm 7.13 \times 10^{-3}$ ,  $T(8.51 \times 10^3) = 47.66$ ,  $p = 0$ ) became more frequent with training.  
1406 As in humans, mice showed shorter TDs with increase exposure to the task ( $\beta = -22.14 \pm$   
1407  $17.06$ ,  $T(1.14 \times 10^3) = -1.3$ ,  $p = 0$ ).

1408 **9.7 Supplemental Figure S7**



1410 **Supplemental Figure S7. Reduced Control Model 1: No accumulation of infor-**  
 1411 **mation across trials.** When simulating data for the *no-accumulation model*, we removed  
 1412 the accumulation of information across trials by setting the Hazard rate  $H$  to 0.5. Simu-  
 1413 lated data thus depended only on the participant-wise estimates for the amplitudes  $a_{LLR/\psi}$ ,  
 1414 frequency  $f$ , phase  $p$  and inverse decision temperature  $\zeta$ .

1415 A. Similar to the full model (Figure 6), simulated perceptual choices were stimulus-congruent  
 1416 in  $72.14\% \pm 0.17\%$  of trials (in red). History-congruent amounted to  $49.89\% \pm 0.03\%$  of  
 1417 trials (in blue). In contrast to the full model, the no-accumulation model showed a significant  
 1418 bias against perceptual history  $T(4.32 \times 10^3) = -3.28$ ,  $p = 1.06 \times 10^{-3}$ ; upper panel). In  
 1419 contrast to the full model, there was no difference in the frequency of history-congruent  
 1420 choices between correct and error trials ( $T(4.31 \times 10^3) = 0.76$ ,  $p = 0.44$ ; lower panel).

1421 B. In the no-accumulation model, we found no significant autocorrelation of history-

<sup>1422</sup> congruence beyond the first trial, whereas the autocorrelation of stimulus-congruence was  
<sup>1423</sup> preserved.

<sup>1424</sup> C. In the no-accumulation model, the number of consecutive trials at which true autocor-  
<sup>1425</sup> relation coefficients exceeded the autocorrelation coefficients for randomly permuted data  
<sup>1426</sup> increased with respect to stimulus-congruence ( $2.83 \pm 1.49 \times 10^{-3}$  trials;  $T(4.31 \times 10^3) =$   
<sup>1427</sup>  $3.45$ ,  $p = 5.73 \times 10^{-4}$ ) and decreased with respect to history-congruence ( $1.85 \pm 3.49 \times 10^{-4}$   
<sup>1428</sup> trials;  $T(4.32 \times 10^3) = -19.37$ ,  $p = 3.49 \times 10^{-80}$ ) relative to the full model.

<sup>1429</sup> D. In the no-accumulation model, the smoothed probabilities of stimulus- and history-  
<sup>1430</sup> congruence (sliding windows of  $\pm 5$  trials) fluctuated as *1/f noise*, i.e., at power densities  
<sup>1431</sup> that were inversely proportional to the frequency (power  $\sim 1/f^\beta$ ; stimulus-congruence:  $\beta =$   
<sup>1432</sup>  $-0.82 \pm 1.2 \times 10^{-3}$ ,  $T(1.92 \times 10^5) = -681.98$ ,  $p = 0$ ; history-congruence:  $\beta = -0.78 \pm$   
<sup>1433</sup>  $1.11 \times 10^{-3}$ ,  $T(1.92 \times 10^5) = -706.57$ ,  $p = 0$ ).

<sup>1434</sup> E. In the no-accumulation model, the distribution of phase shift between fluctuations in  
<sup>1435</sup> simulated stimulus- and history-congruence peaked at half a cycle ( $\pi$  denoted by dotted  
<sup>1436</sup> line). In contrast to the full model, the dynamic probabilities of simulated stimulus- and  
<sup>1437</sup> history-congruence were not significantly anti-correlated ( $\beta = 6.39 \times 10^{-4} \pm 7.22 \times 10^{-4}$ ,  
<sup>1438</sup>  $T(8.89 \times 10^5) = 0.89$ ,  $p = 0.38$ ).

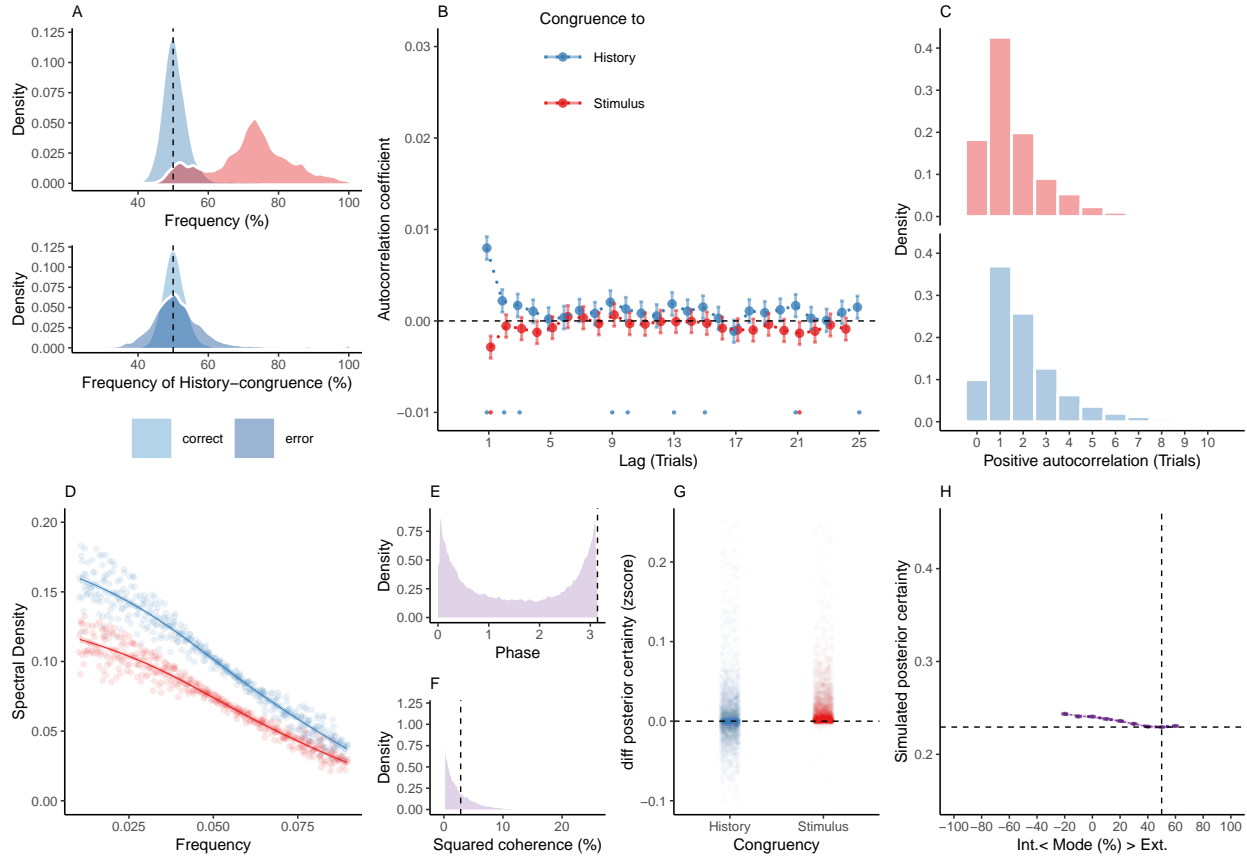
<sup>1439</sup> F. In the no-accumulation model, the average squared coherence between fluctuations in  
<sup>1440</sup> simulated stimulus- and history-congruence (black dotted line) was reduced in comparison to  
<sup>1441</sup> the full model ( $T(3.56 \times 10^3) = -9.96$ ,  $p = 4.63 \times 10^{-23}$ ) and amounted to  $2.8 \pm 7.29 \times 10^{-4}\%$ .

<sup>1442</sup> G. Similar to the full model, confidence simulated from the no-accumulation model was  
<sup>1443</sup> enhanced for stimulus-congruent choices ( $\beta = 0.01 \pm 9.4 \times 10^{-5}$ ,  $T(2.11 \times 10^6) = 158.1$ ,  $p =$   
<sup>1444</sup> 0). In contrast to the full model (Figure 6), history-congruent choices were not characterized  
<sup>1445</sup> by enhanced confidence ( $\beta = 8.78 \times 10^{-5} \pm 8.21 \times 10^{-5}$ ,  $T(2.11 \times 10^6) = 1.07$ ,  $p = 0.29$ ).

<sup>1446</sup> H. In the no-accumulation model, the positive quadratic relationship between the mode of  
<sup>1447</sup> perceptual processing and confidence was markedly reduced in comparison to the full model

<sub>1448</sub>  $(\beta_2 = 0.19 \pm 0.06, T(2.11 \times 10^6) = 3, p = 2.69 \times 10^{-3})$ . The horizontal and vertical dotted  
<sub>1449</sub> lines indicate minimum posterior certainty and the associated mode, respectively.

1450 **9.8 Supplemental Figure S8**



1451 **Supplemental Figure S8. Reduced Control Model 2: No oscillations.** When  
 1452 simulating data for the *no-oscillation model*, we removed the oscillation from the likelihood  
 1453 and prior terms by setting the amplitudes  $a_{LLR}$  and  $a_\psi$  to zero. Simulated data thus  
 1454 depended only on the participant-wise estimates for hazard rate  $H$  and inverse decision  
 1455 temperature  $\zeta$ .

1456 A. Similar to the full model (Figure 6), simulated perceptual choices were stimulus-congruent  
 1457 in  $71.97\% \pm 0.17\%$  of trials (in red). History-congruent amounted to  $50.73\% \pm 0.07\%$  of  
 1458 trials (in blue). As in the full model, the no-oscillation model showed a significant bias  
 1459 toward perceptual history  $T(4.32 \times 10^3) = 9.94$ ,  $p = 4.88 \times 10^{-23}$ ; upper panel). Similarly,  
 1460 history-congruent choices were more frequent at error trials ( $T(4.31 \times 10^3) = 10.59$ ,  $p =$   
 1461  $7.02 \times 10^{-26}$ ; lower panel).

1462 B. In the no-oscillation model, we did not find significant autocorrelations for stimulus-

<sup>1464</sup> congruence. Likewise, we did not observe any autocorrelation of history-congruence beyond  
<sup>1465</sup> the first three consecutive trials.

<sup>1466</sup> C. In the no-oscillation model, the number of consecutive trials at which true autocorrelation  
<sup>1467</sup> coefficients exceeded the autocorrelation coefficients for randomly permuted data decreased  
<sup>1468</sup> with respect to both stimulus-congruence ( $1.8 \pm 1.59 \times 10^{-3}$  trials;  $T(4.31 \times 10^3) = -5.21$ ,  
<sup>1469</sup>  $p = 2 \times 10^{-7}$ ) and history-congruence ( $2.18 \pm 5.48 \times 10^{-4}$  trials;  $T(4.32 \times 10^3) = -17.1$ ,  $p$   
<sup>1470</sup>  $= 1.75 \times 10^{-63}$ ) relative to the full model.

<sup>1471</sup> D. In the no-oscillation model, the smoothed probabilities of stimulus- and history-  
<sup>1472</sup> congruence (sliding windows of  $\pm 5$  trials) fluctuated as *1/f noise*, i.e., at power densities  
<sup>1473</sup> that were inversely proportional to the frequency (power  $\sim 1/f^\beta$ ; stimulus-congruence:  $\beta =$   
<sup>1474</sup>  $-0.78 \pm 1.1 \times 10^{-3}$ ,  $T(1.92 \times 10^5) = -706.93$ ,  $p = 0$ ; history-congruence:  $\beta = -0.79 \pm$   
<sup>1475</sup>  $1.12 \times 10^{-3}$ ,  $T(1.92 \times 10^5) = -702.46$ ,  $p = 0$ ).

<sup>1476</sup> E. In the no-oscillation model, the distribution of phase shift between fluctuations in sim-  
<sup>1477</sup> uated stimulus- and history-congruence peaked at half a cycle ( $\pi$  denoted by dotted line).  
<sup>1478</sup> In contrast to the full model, the dynamic probabilities of simulated stimulus- and history-  
<sup>1479</sup> congruence were positively correlated ( $\beta = 4.3 \times 10^{-3} \pm 7.97 \times 10^{-4}$ ,  $T(1.98 \times 10^6) = 5.4$ ,  
<sup>1480</sup>  $p = 6.59 \times 10^{-8}$ ).

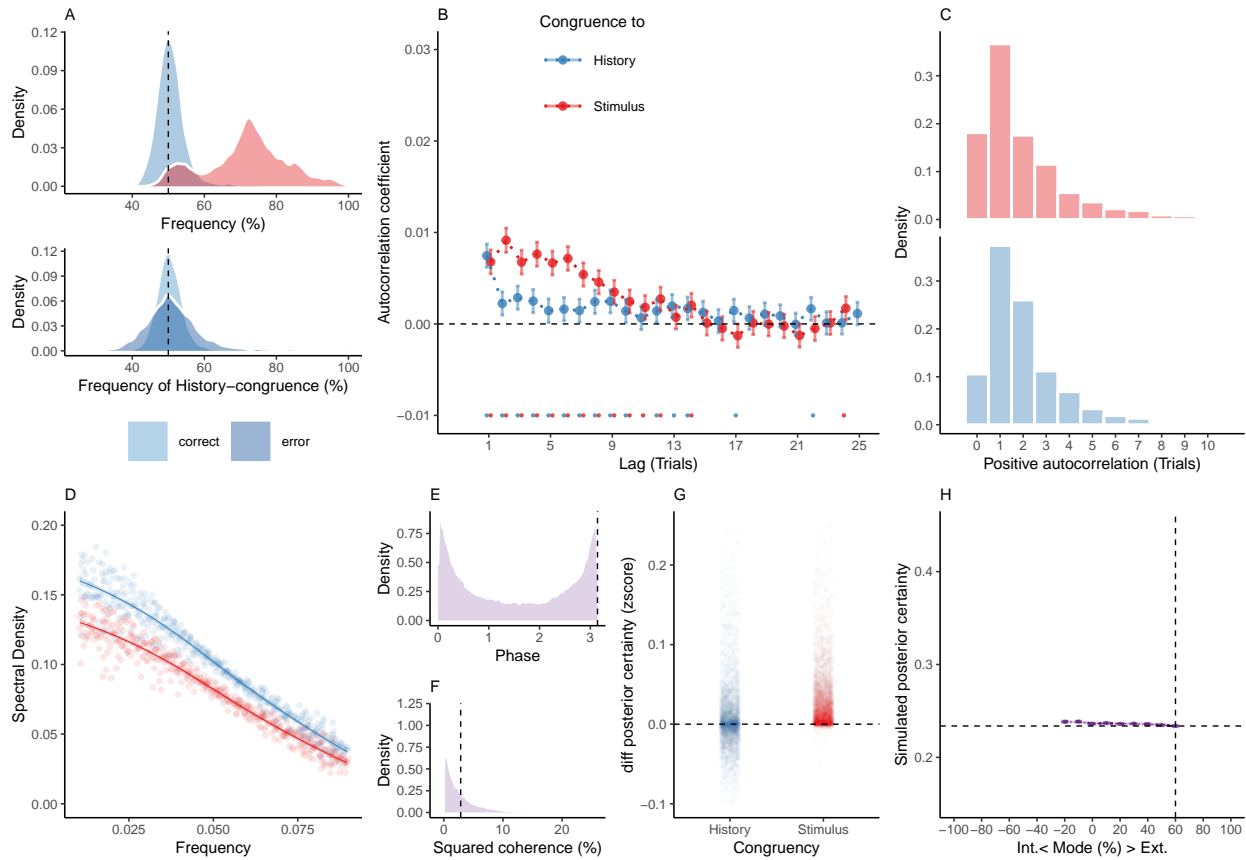
<sup>1481</sup> F. In the no-oscillation model, the average squared coherence between fluctuations in simu-  
<sup>1482</sup> lated stimulus- and history-congruence (black dottet line) was reduced in comparison to the  
<sup>1483</sup> full model ( $T(3.52 \times 10^3) = -6.27$ ,  $p = 3.97 \times 10^{-10}$ ) and amounted to  $3.26 \pm 8.88 \times 10^{-4}\%$ .

<sup>1484</sup> G. Similar to the full model, confidence simulated from the no-oscillation model was enhanced  
<sup>1485</sup> for stimulus-congruent choices ( $\beta = 0.01 \pm 1.05 \times 10^{-4}$ ,  $T(2.1 \times 10^6) = 139.17$ ,  $p = 0$ ) and  
<sup>1486</sup> history-congruent choices ( $\beta = 8.05 \times 10^{-3} \pm 9.2 \times 10^{-5}$ ,  $T(2.1 \times 10^6) = 87.54$ ,  $p = 0$ ).

<sup>1487</sup> H. In the no-oscillation model, the positive quadratic relationship between the mode of  
<sup>1488</sup> perceptual processing and confidence was markedly reduced in comparison to the full model  
<sup>1489</sup> ( $\beta_2 = 0.14 \pm 0.07$ ,  $T(2.1 \times 10^6) = 1.95$ ,  $p = 0.05$ ). The horizontal and vertical dotted lines

<sup>1490</sup> indicate minimum posterior certainty and the associated mode, respectively.

1491 **9.9 Supplemental Figure S9**



1493 **Supplemental Figure S9. Reduced Control Model 3: Only oscillation of the**  
 1494 **likelihood.** When simulating data for the *likelihood-oscillation-only model*, we removed  
 1495 the oscillation from the prior term by setting the amplitude  $a_\psi$  to zero. Simulated data  
 1496 thus depended only on the participant-wise estimates for hazard rate  $H$ , amplitude  $a_{LLR}$ ,  
 1497 frequency  $f$ , phase  $p$  and inverse decision temperature  $\zeta$ .

1498 A. Similar to the full model (Figure 6), simulated perceptual choices were stimulus-congruent  
 1499 in  $71.97\% \pm 0.17\%$  of trials (in red). History-congruent amounted to  $50.76\% \pm 0.07\%$  of trials  
 1500 (in blue). As in the full model, the likelihood-oscillation-only model showed a significant bias  
 1501 toward perceptual history  $T(4.32 \times 10^3) = 10.29$ ,  $p = 1.54 \times 10^{-24}$ ; upper panel). Similarly,  
 1502 history-congruent choices were more frequent at error trials ( $T(4.32 \times 10^3) = 9.71$ ,  $p =$   
 1503  $4.6 \times 10^{-22}$ ; lower panel).

1504 B. In the likelihood-oscillation-only model, we observed that the autocorrelation coeffi-

1505 cients for history-congruence were reduced below the autocorrelation coefficients of stimulus-  
1506 congruence. This is an approximately five-fold reduction relative to the empirical results  
1507 observed in humans (Figure 2B), where the autocorrelation of history-congruence was above  
1508 the autocorrelation of stimulus-congruence. Moreover, in the reduced model shown here, the  
1509 number of consecutive trials that showed significant autocorrelation of history-congruence  
1510 was reduced to 11.

1511 C. In the likelihood-oscillation-only model, the number of consecutive trials at which true  
1512 autocorrelation coefficients exceeded the autocorrelation coefficients for randomly permuted  
1513 data did not differ with respect to stimulus-congruence ( $2.62 \pm 1.39 \times 10^{-3}$  trials;  $T(4.32 \times$   
1514  $10^3) = 1.85$ ,  $p = 0.06$ ), but decreased with respect to history-congruence ( $2.4 \pm 8.45 \times 10^{-4}$   
1515 trials;  $T(4.32 \times 10^3) = -15.26$ ,  $p = 3.11 \times 10^{-51}$ ) relative to the full model.

1516 D. In the likelihood-oscillation-only model, the smoothed probabilities of stimulus- and  
1517 history-congruence (sliding windows of  $\pm 5$  trials) fluctuated as *1/f noise*, i.e., at power den-  
1518 sities that were inversely proportional to the frequency (power  $\sim 1/f^\beta$ ; stimulus-congruence:  
1519  $\beta = -0.81 \pm 1.17 \times 10^{-3}$ ,  $T(1.92 \times 10^5) = -688.65$ ,  $p = 0$ ; history-congruence:  $\beta = -0.79$   
1520  $\pm 1.14 \times 10^{-3}$ ,  $T(1.92 \times 10^5) = -698.13$ ,  $p = 0$ ).

1521 E. In the likelihood-oscillation-only model, the distribution of phase shift between fluctua-  
1522 tions in simulated stimulus- and history-congruence peaked at half a cycle ( $\pi$  denoted by  
1523 dotted line). In contrast to the full model, the dynamic probabilities of simulated stimulus-  
1524 and history-congruence were positively correlated ( $\beta = 2.7 \times 10^{-3} \pm 7.6 \times 10^{-4}$ ,  $T(2.02 \times 10^6)$   
1525  $= 3.55$ ,  $p = 3.8 \times 10^{-4}$ ).

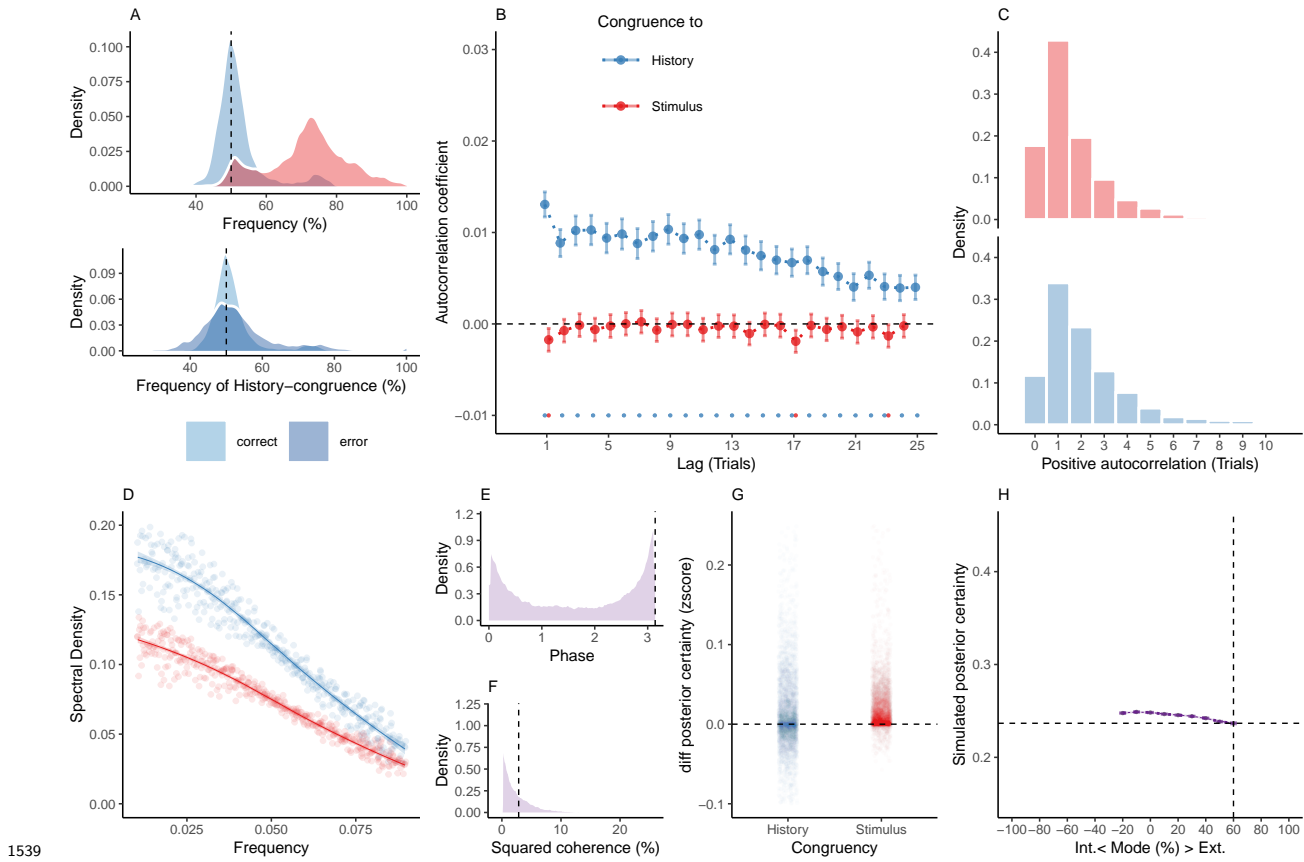
1526 F. In the likelihood-oscillation-only model, the average squared coherence between fluctu-  
1527 ations in simulated stimulus- and history-congruence (black dottet line) was reduced in  
1528 comparison to the full model ( $T(3.51 \times 10^3) = -4.56$ ,  $p = 5.27 \times 10^{-6}$ ) and amounted to  $3.43$   
1529  $\pm 1.02 \times 10^{-3}\%$ .

1530 G. Similar to the full model, confidence simulated from the likelihood-oscillation-only model

<sub>1531</sub> was enhanced for stimulus-congruent choices ( $\beta = 0.03 \pm 1.42 \times 10^{-4}$ ,  $T(2.1 \times 10^6) = 191.78$ ,  
<sub>1532</sub>  $p = 0$ ) and history-congruent choices ( $\beta = 9.1 \times 10^{-3} \pm 1.25 \times 10^{-4}$ ,  $T(2.1 \times 10^6) = 72.51$ ,  
<sub>1533</sub>  $p = 0$ ).

<sub>1534</sub> H. In the likelihood-oscillation-only model, the positive quadratic relationship between the  
<sub>1535</sub> mode of perceptual processing and confidence was markedly reduced in comparison to the full  
<sub>1536</sub> model ( $\beta_2 = 0.34 \pm 0.1$ ,  $T(2.1 \times 10^6) = 3.49$ ,  $p = 4.78 \times 10^{-4}$ ). The horizontal and vertical  
<sub>1537</sub> dotted lines indicate minimum posterior certainty and the associated mode, respectively.

1538 **9.10 Supplemental Figure S10**



1539 **Supplemental Figure S10. Reduced Control Model 4: Only oscillation of the prior.** When simulating data for the *prior-oscillation-only model*, we removed the oscillation from the prior term by setting the amplitude  $a_{LLR}$  to zero. Simulated data thus depended only on the participant-wise estimates for hazard rate  $H$ , amplitude  $a_\psi$ , frequency  $f$ , phase  $p$  and inverse decision temperature  $\zeta$ .

1545 A. Similar to the full model (Figure 6), simulated perceptual choices were stimulus-congruent  
 1546 in  $71.97\% \pm 0.17\%$  of trials (in red). History-congruent amounted to  $52.1\% \pm 0.11\%$  of trials  
 1547 (in blue). As in the full model, the prior-oscillation-only showed a significant bias toward  
 1548 perceptual history  $T(4.32 \times 10^3) = 18.34, p = 1.98 \times 10^{-72}$ ; upper panel). Similarly, history-  
 1549 congruent choices were more frequent at error trials ( $T(4.31 \times 10^3) = 12.35, p = 1.88 \times 10^{-34}$ ;  
 1550 lower panel).

1551 B. In the prior-oscillation-only model, we did not observe any significant positive autocor-

1552 relation of stimulus-congruence , whereas the autocorrelation of history-congruence was pre-  
1553 served.

1554 C. In the prior-oscillation-only model, the number of consecutive trials at which true au-  
1555 tocorrelation coefficients exceeded the autocorrelation coefficients for randomly permuted  
1556 data did was decreased with respect to stimulus-congruence relative to the full model ( $1.8 \pm$   
1557  $1.01 \times 10^{-3}$  trials;  $T(4.31 \times 10^3) = -6.48$ ,  $p = 1.03 \times 10^{-10}$ ), but did not differ from the full  
1558 model with respect to history-congruence ( $4.25 \pm 1.84 \times 10^{-3}$  trials;  $T(4.32 \times 10^3) = 0.07$ ,  
1559  $p = 0.95$ ).

1560 D. In the prior-oscillation-only model, the smoothed probabilities of stimulus- and history-  
1561 congruence (sliding windows of  $\pm 5$  trials) fluctuated as *1/f noise*, i.e., at power densities  
1562 that were inversely proportional to the frequency (power  $\sim 1/f^\beta$ ; stimulus-congruence:  $\beta =$   
1563  $-0.78 \pm 1.11 \times 10^{-3}$ ,  $T(1.92 \times 10^5) = -706.62$ ,  $p = 0$ ; history-congruence:  $\beta = -0.83 \pm$   
1564  $1.27 \times 10^{-3}$ ,  $T(1.92 \times 10^5) = -651.6$ ,  $p = 0$ ).

1565 E. In the prior-oscillation-only model, the distribution of phase shift between fluctuations  
1566 in simulated stimulus- and history-congruence peaked at half a cycle ( $\pi$  denoted by dotted  
1567 line). Similar to the full model, the dynamic probabilities of simulated stimulus- and history-  
1568 congruence were anti-correlated ( $\beta = -0.03 \pm 8.61 \times 10^{-4}$ ,  $T(2.12 \times 10^6) = -34.03$ ,  $p =$   
1569  $8.17 \times 10^{-254}$ ).

1570 F. In the prior-oscillation-only model, the average squared coherence between fluctuations in  
1571 simulated stimulus- and history-congruence (black dottet line) was reduced in comparison to  
1572 the full model ( $T(3.54 \times 10^3) = -3.22$ ,  $p = 1.28 \times 10^{-3}$ ) and amounted to  $3.52 \pm 1.04 \times 10^{-3}\%$ .

1573 G. Similar to the full model, confidence simulated from the prior-oscillation-only model was  
1574 enhanced for stimulus-congruent choices ( $\beta = 0.02 \pm 1.44 \times 10^{-4}$ ,  $T(2.03 \times 10^6) = 128.53$ ,  
1575  $p = 0$ ) and history-congruent choices ( $\beta = 0.01 \pm 1.26 \times 10^{-4}$ ,  $T(2.03 \times 10^6) = 88.24$ ,  $p =$   
1576  $0$ ).

1577 H. In contrast to the full model, the prior-oscillation-only model did not yield a positive

<sub>1578</sub> quadratic relationship between the mode of perceptual processing and confidence ( $\beta_2 =$   
<sub>1579</sub>  $-0.17 \pm 0.1$ ,  $T(2.04 \times 10^6) = -1.66$ ,  $p = 0.1$ ). The horizontal and vertical dotted lines  
<sub>1580</sub> indicate minimum posterior certainty and the associated mode, respectively.

1581 9.11 Supplemental Table T1

Authors	Journal	Year
Bang, Shekhar, Rahnev	JEP:General	2019
Bang, Shekhar, Rahnev	JEP:General	2019
Calder-Travis, Charles, Bogacz, Yeung	Unpublished	NA
Clark & Merfeld	Journal of Neurophysiology	2018
Clark	Unpublished	NA
Faivre, Filevich, Solovey, Kuhn, Blanke	Journal of Neuroscience	2018
Faivre, Vuillaume, Blanke, Cleeremans	bioRxiv	2018
Filevich & Fandakova	Unplublished	NA
Gajdos, Fleming, Saez Garcia, Weindel, Davranche	Neuroscience of Consciousness	2019
Gherman & Philiastides	eLife	2018
Haddara & Rahnev	PsyArXiv	2020
Haddara & Rahnev	PsyArXiv	2020
Hainguierlot, Vergnaud, & de Gardelle	Scientific Reports	2018
Hainguierlot, Gajdos, Vergnaud, & de Gardelle	Unpublished	NA
Jachs, Blanco, Grantham-Hill, Soto	JEP:HPP	2015
Jachs, Blanco, Grantham-Hill, Soto	JEP:HPP	2015
Jachs, Blanco, Grantham-Hill, Soto	JEP:HPP	2015
Jaquiere, Yeung	Unpublished	NA
Kvam, Pleskac, Yu, Busemeyer	PNAS	2015
Kvam, Pleskac, Yu, Busemeyer	PNAS	2015
Kvam and Pleskac	Cognition	2016
Law, Lee	Unpublished	NA
Lebreton, et al.	Sci. Advances	2018
Lempert, Chen, & Fleming	PlosOne	2015
Locke*, Gaffin-Cahn*, Hosseiniavah, Mamassian, & Landy	Attention, Perception, & Psychophysics	2020
Maniscalco, McCurdy,Odegaard, & Lau	J Neurosci	2017
Maniscalco, McCurdy,Odegaard, & Lau	J Neurosci	2017
Maniscalco, McCurdy,Odegaard, & Lau	J Neurosci	2017
Maniscalco, McCurdy,Odegaard, & Lau	J Neurosci	2017
Martin, Hsu	Unpublished	NA
Massoni & Roux	Journal of Mathematical Psychology	2017
Massoni	Unpublished	NA
Mazor, Friston & Fleming	eLife	2020
Mei, Rankine,Olafsson, Soto	bioRxiv	2019
Mei, Rankine,Olafsson, Soto	bioRxiv	2019
O'Hora, Zgonnikov, Kenny, Wong-Lin	Fechner Day proceedings	2017
O'Hora, Zgonnikov, CiChocki	Unpublished	NA

(continued)

Authors	Journal	Year
O'Hora, Zgonnikov, Neverauskaite	Unpublished	NA
Palser et al	Consciousness & Cognition	2018
Pereira, Faivre, Iturrate et al.	bioRxiv	2018
Prieto et al.	Submitted	NA
Rahnev et al	J Neurophysiol	2013
Rausch & Zehetleitner	Front Psychol	2016
Rausch et al	Attention, Perception, & Psychophysics	2018
Rausch et al	Attention, Perception, & Psychophysics	2018
Rausch, Zehetleitner, Steinhauser, & Maier	NeuroImage	2020
Recht, de Gardelle & Mamassian	Unpublished	NA
Reyes et al.	PlosOne	2015
Reyes et al.	Submitted	NA
Rouault, Seow, Gillan, Fleming	Biol. Psychiatry	2018
Rouault, Seow, Gillan, Fleming	Biol. Psychiatry	2018
Rouault, Dayan, Fleming	Nat Commun	2019
Sadeghi et al	Scientific Reports	2017
Schmidt et al.	Consc Cog	2019
Shekhar & Rahnev	J Neuroscience	2018
Shekhar & Rahnev	PsyArXiv	2020
Sherman et al	Journal of Neuroscience	2016
Sherman et al	Journal of Cognitive Neuroscience	2016
Sherman et al	Unpublished	NA
Sherman et al	Unpublished	NA
Siedlecka, Wereszczyski, Paulewicz, Wierzchon	bioRxiv	2019
Song et al	Consciousness & Cognition	2011
van Boxtel, Orchard, Tsuchiya	bioRxiv	2019
van Boxtel, Orchard, Tsuchiya	bioRxiv	2019
Wierzchon, Paulewicz, Asanowicz, Timmermans & Cleeremans	Consciousness and Cognition	2014
Wierzchon, Anzulewicz, Hobot, Paulewicz & Sackur	Consciousness and Cognition	2019

## 1582 10 Response to Reviewers

### 1583 10.1 Reviewer 1:

1584 This was an interesting and thought-provoking submission. I note that it is  
1585 a revision: I am therefore supposing that the authors have already responded  
1586 to one round of reviewer comments and that you are potentially interested in  
1587 publishing this work. In brief, I think there are many elements of this report that  
1588 warrant publication; however, there are some parts that are less compelling and  
1589 could be deferred to a subsequent paper. The paper is far too long and would  
1590 benefit greatly from being streamlined. Furthermore, some of the modelling is  
1591 overengineered and is difficult to follow. I have tried to suggest how the authors  
1592 might improve the presentation of their work in my comments to authors.

1593 I enjoyed reading this long but thought-provoking report of fluctuations in the  
1594 sensitivity to sensory evidence in perceptual decision-making tasks. There were  
1595 some parts of this report that were compelling and interesting. Other parts were  
1596 less convincing and difficult to understand. Overall, this paper is far too long.  
1597 An analogy that might help here is that a dinner guest is very entertaining for the  
1598 first hour or so - and then overstays their welcome; until you start wishing they  
1599 would leave. Another analogy, which came to mind, was that the modelling—  
1600 and its interpretation—was a bit autistic (i.e., lots of fascinating if questionable  
1601 detail with a lack of central coherence).

1602 I think that both issues could be resolved by shortening the paper and removing  
1603 (or, at least, greatly simplifying) the final simulation studies of metacognition.  
1604 I try to unpack this suggestion in the following.

1605 We would like to thank Prof. Friston for the very insightful and helpful comments on our  
1606 manuscript. We fully agree that our ideas about the computational function of between-

1607 mode fluctuations and the associated simulation may be presented in a more accessible form  
1608 in a standalone paper. As we outline below in more detail, we have followed the suggestion  
1609 of streamlining our findings and rewrote the paper to reduce it's length by shortening the  
1610 sections on computational modeling.

1611 **Major points:**

1612 **As I understand it, you have used publicly available data on perceptual decision-**  
1613 **making to demonstrate slow fluctuations in the tendency to predicate perceptual**  
1614 **decisions on the stimuli and on the history of recent decisions. You find scale-free**  
1615 **fluctuations in this tendency — that are anti-correlated — and interpret this as**  
1616 **fluctuations in the precision afforded sensory evidence, relative to prior beliefs.**  
1617 **This interpretation is based upon a model of serial dependencies (parameterised**  
1618 **with a hazard function).**

1619 **The stimulus and history (i.e., likelihood and prior) sensitivities are anti-**  
1620 **correlated and both show scale free behaviour. This is reproduced in men and**  
1621 **mice. You then proceed to model this with periodic fluctuations in the precisions**  
1622 **or weights applied to the likelihood and prior that are in anti-phase - and then**  
1623 **estimate the parameters of the ensuing model. Finally, you then simulate the**  
1624 **learning of the hazard parameter — and something called metacognition - to**  
1625 **show that periodic fluctuations improve estimates of metacognition (based upon**  
1626 **a Rescorla-Wagner model of learning). You motivate this by suggesting that**  
1627 **the fluctuations in sensitivity are somehow necessary to elude circular inference**  
1628 **and provide better estimates of precision.**

1629 **Note that I am reading the parameters omega\_LL and omega\_ as the preci-**  
1630 **sion of the likelihood and prior, where the precision of the likelihood is called**  
1631 **sensory precision. This contrasts with your use of sensory precision, which seems**  
1632 **to be attributed to a metacognitive construct M.**

<sub>1633</sub> As noted above, all of this is fascinating but there are too many moving parts  
<sub>1634</sub> that do not fit together comfortably. I will list a few examples:

<sub>1635</sub> **10.1.1 Comment 1**

<sub>1636</sub> If, empirically, the fluctuations in sensitivity are scale-free with a 1/f power law,  
<sub>1637</sub> why did you elect to model fluctuations in precision as a periodic function with  
<sub>1638</sub> one unique timescale (i.e., f).?

<sub>1639</sub> The reason for choosing a unique timescale  $f$  was to enable our model to depict the the  
<sub>1640</sub> dominant timescale at which prior and likelihood precision are temporarily suspended, giving  
<sub>1641</sub> rise to what we believe constitutes between-mode fluctuations. Simulating from our model  
<sub>1642</sub> (Figure 6) replicates the 1/f feature of the empirical data. Please note that the individual  
<sub>1643</sub> trial is the smallest unit of *measurement* for these fluctuations, such that our analysis only  
<sub>1644</sub> deals with frequencies below 1 ( $1/N_{trials}$ ).

<sub>1645</sub> **10.1.2 Comment 2**

<sub>1646</sub> At present, the estimates of meta-cognition (M) play the role of accumulated  
<sub>1647</sub> estimates of (sensory or prior) precision. Why are these not used in your model  
<sub>1648</sub> of perceptual decisions in Equation 2.

<sub>1649</sub> We would like to thank Prof. Friston for this comment. In our model, the parameter  $\alpha$   
<sub>1650</sub> controls the encoding precision by governing the transformation from sensory stimuli to the  
<sub>1651</sub> log likelihood ratio (LLR) via the following equations, which is closer to zero for lower values  
<sub>1652</sub> of  $\alpha$ .

$$u_t = \frac{1}{1 + \exp(-\alpha * s_t)} \quad (35)$$

$$LLR_t = \log\left(\frac{u_t}{1-u_t}\right) \quad (36)$$

1653 Our model simulations on the adaptive benefits of bimodal inference rest on the assumption  
 1654 that  $\alpha$  may change unpredictably. The construct  $M$  is a belief about  $\alpha$  that may be useful  
 1655 for, e.g., communicating the precision of sensory encoding to other cognitive domains or  
 1656 agents. To our mind,  $\alpha$  is a feature of low-level sensory encoding that cannot be modulated  
 1657 by top-down beliefs such as  $M$ . This is why we did not include  $M$  in equation (2).

1658 **10.1.3 Comment 3**

1659 **Why do you assume that non-specific increases in attention and arousal will**  
 1660 **increase reaction times? If one has very precise prior beliefs (and is not attending**  
 1661 **to stimuli), would you not expect a decrease in reaction time?**

1662 Thanks a lot for pointing this out (see also the comment below and comment X.X.X by  
 1663 Reviewer 3). As we understand, both high prior and high likelihood precision lead to higher  
 1664 absolute values of the posterior log ratio (reflecting decision certainty), and thus faster re-  
 1665 sponse times (RTs). This is reflected empirically by RTs in humans (Figure 2) and to a  
 1666 lesser degree in mice (Figure 4) and to a lesser degree in mice): RTs tended to be shorter for  
 1667 stronger biases toward both external and internal mode. Our full model, which incorporates  
 1668 (i), the accumulation of information across trials, and (ii), antiphase fluctuations, recapitu-  
 1669 lates this feature of the data, which is lost or greatly attenuated when eliminating (i) and/or  
 1670 (ii). Our data thus confirm the hypothesis that both high prior and likelihood precision lead  
 1671 to faster RTs.

1672 At the same time, we included the relation between mode and RTs and confidence as a  
 1673 defensive analysis. One might argue that fluctuations in perceptual performance are not  
 1674 influenced at all by periods of enhanced prior precision (which decrease performance in fully  
 1675 randomized designs), but by periods where participants may not attend to the task at all,

<sup>1676</sup> i.e., neither to sensory information nor to prior precision. We think that analysis of response  
<sup>1677</sup> times and confidence can give some insight into whether such alternative mechanisms may  
<sup>1678</sup> be at play, as we would assume longer response times and lower confidence if participants  
<sup>1679</sup> failed to attend to the task at all (e.g., due to low arousal).

<sup>1680</sup> We realize that, due to the potential non-linearity in their relation to arousal (see also  
<sup>1681</sup> comment X.X.X by Reviewer 3), RTs and confidence cannot provide a definitive map of  
<sup>1682</sup> where fluctuations in mode are situated in relation to arousal/attention. This can potentially  
<sup>1683</sup> be provided by eye-tracking, motor behavior or neural data, which is not available for the  
<sup>1684</sup> studies in the Confidence Database, but was recently published for the IBL database. We  
<sup>1685</sup> will assess the relation of pupil diameter, motor behavior (turning of the response wheel)  
<sup>1686</sup> and LFPs to between-mode fluctuations in a future publication.

<sup>1687</sup> In light of the above, we have adapted the manuscript in the following ways:

- <sup>1688</sup> • explanation of how fluctuations in prior and likelihood precision may impact RTs and  
<sup>1689</sup> confidence
- <sup>1690</sup> • reference to the potential non-linearity
- <sup>1691</sup> • reference to future work that will use pupillometry, video tracking and neural signals  
<sup>1692</sup> to discern between-mode fluctuations from global and?or unspecific flucations in perfor-  
<sup>1693</sup> mance.

#### <sup>1694</sup> 10.1.4 Comment 4

<sup>1695</sup> In the predictive processing literature, attention is thought to correspond to  
<sup>1696</sup> fluctuations in sensory and prior precision. Why did you then consider attention  
<sup>1697</sup> as some additional or unrelated confound?

<sup>1698</sup> We feel that this point is closely related to the comment above. We realize that, in the  
<sup>1699</sup> predictive coding field, attention is equated the precision of factors that contribute to the

<sup>1700</sup> perceptual decision, such that an observer can attend strongly to sensory information (high  
<sup>1701</sup> likelihood precision) or to internal predictions derived from the sequence of preceding per-  
<sup>1702</sup> cepts (high prior precision). Therefore, when following the above predictive coding definition,  
<sup>1703</sup> fluctuations in attention can be equated with fluctuations in mode.

<sup>1704</sup> However, we feel that outside of the predictive coding field, attention is not always conceived  
<sup>1705</sup> in that way, such that low attention may reflect low engagement with the task, relating to  
<sup>1706</sup> low likelihood and low prior precision. Is it against this notion that we have included the  
<sup>1707</sup> analysis of attention as a separate control analysis (with the caveats outlined in our response  
<sup>1708</sup> to the comment above).

<sup>1709</sup> We now provide a more nuanced interpretation of our findings of RTs and confidence in  
<sup>1710</sup> relation to attention, with a specific focus on predictive coding and precision:

- <sup>1711</sup> • attention and precision in PC

#### <sup>1712</sup> 10.1.5 Comment 5

<sup>1713</sup> **What licences the assumption that “agents depend upon internal confidence**  
<sup>1714</sup> **signals” in the absence of feedback?**

<sup>1715</sup> In the absence of feedback, observers can only rely on internal estimates of performance to  
<sup>1716</sup> guide updates to their model of the reliability of their sensory apparatus (inferences about  
<sup>1717</sup>  $M$ ). Previous work (e.g. Guggenmos et al., Elife 2106, <https://doi.org/10.7554/eLife.13388>)  
<sup>1718</sup> has shown that confidence signals can provide signals that drive perceptual learning in the  
<sup>1719</sup> absence of feedback. This has motivated our model simulation on the adaptive benefits of  
<sup>1720</sup> bimodal inference for metacognition, where the learning signal  $\epsilon_M$  drives inferences about  
<sup>1721</sup>  $M$ :

$$\epsilon_M = (1 - |y_t - P(y_t = 1)|) - M_t \quad (37)$$

1722 10.1.6 Comment 6

1723 And what licences the assumption that internal confidence feedback corresponds  
1724 to “the absolute of the posterior log ratio” (did you mean the log of the posterior  
1725 ratio)?

1726 We mean the log of the posterior ratio. Following first order models (see e.g., Fleming &  
1727 Daw, Self-evaluation of decision-making: A general Bayesian framework for metacognitive  
1728 computation, Psychol. Rev. 2017, <https://doi.org/10.1037/rev0000045>), the perceptual  
1729 decision and the confidence report rely on the posterior. The distance of the log of the  
1730 posterior ratio  $L_t$  from zero becomes a measure of decision-certainty or confidence.

1731 10.1.7 Comment 7

1732 I got a bit lost here when you say that “the precision of sensory coding M a  
1733 function of  $u_t$ . This is largely because I couldn’t find a definition of  $u_t$ .

1734 We apologize for this lack of clarity. In the model simulations on the adaptive benefits of  
1735 bimodal inference, we generated stimuli  $s_t$  from a Bernoulli-distribution with  $p + q + 0.5$ .  
1736 The value of  $u_t$  was then defined via equation (22), following our modeling of the human  
1737 data:

$$u_t = \frac{1}{1 + \exp(-\alpha * (s_t - 0.5))} \quad (38)$$

1738 10.1.8 Comment 8

1739 What licences an application of Rescorla-Wagner to learning the parameters (as  
1740 in Equation 11) and, learning sensory precision as described by M\_T (Equation  
1741 13). Are you moving from a Bayesian framework to a reinforcement learning  
1742 framework?

1743 We would like to thank the reviewer for pointing out this inconsistency. We chose the a

<sub>1744</sub> Rescorla-Wagner learning rule for simplicity: In our model, the speed of learning about  $H$   
<sub>1745</sub> and  $M$  varies according to the current mode of perceptual processing and a constant learning  
<sub>1746</sub> rate:

$$H'_t = H'_{t-1} + \beta_H * \omega_{LLR} * \epsilon_H \quad (39)$$

$$M'_t = M'_{t-1} + \beta_M * \omega_{LLR} * \epsilon_M \quad (40)$$

<sub>1747</sub> Allowing the learning rate itself to vary as a function of preceding experiences would add  
<sub>1748</sub> an additional level of complexity that we sought to omit in this analysis. However, we fully  
<sub>1749</sub> agree that choosing a Bayesian framework (e.g., a three-level HGF) would indeed be more  
<sub>1750</sub> consistent.

### <sub>1751</sub> 10.1.9 Comment 9

<sub>1752</sub> I am sure you have answers to these questions - but with each new question the reader is left  
<sub>1753</sub> more and more skeptical that there is a coherent story behind your analyses. It would have  
<sub>1754</sub> been more convincing had you just committed to a Bayesian filter and made your points  
<sub>1755</sub> using one update scheme, under ideal Bayesian observer assumptions.

<sub>1756</sub> Unlike your piecemeal scheme, things like the hierarchical Gaussian filter estimates the sen-  
<sub>1757</sub> sory and prior decisions explicitly and these estimates underwrite posterior inference. In  
<sub>1758</sub> your scheme, the sensory precision  $M$  appears to have no influence on perceptual inference  
<sub>1759</sub> (which is why, presumably you call it metacognition). The problem with this is that your  
<sub>1760</sub> motivation for systematic fluctuations in precision is weakened. This is because improved  
<sub>1761</sub> metacognition does not improve perception — it only improves the perception of perception.

<sub>1762</sub> In light of the above, can I suggest that you remove Section 5.8 and use your model in the  
<sub>1763</sub> preceding section to endorse your hypothesis along the following lines:

1764 “In summary, we hypothesized that subjects have certain hyperpriors that are apt for ac-  
1765 commodating fluctuations in the predictability of their environment; i.e., people believe that  
1766 their world is inherently volatile. This means that to be Bayes optimal it is necessary to  
1767 periodically re-evaluate posterior beliefs about model parameters. One way to do this is to pe-  
1768 riodically suspend the precision of prior beliefs and increase the precision afforded to sensory  
1769 evidence that updates (Bayesian) beliefs about model parameters. The empirical evidence  
1770 above suggests that the timescale of this periodic scheduling of evidence accumulation is  
1771 scale invariant. This means there exists a timescale of periodic fluctuations in precision over  
1772 every window or length of perceptual decision-making. In what follows, we model perceptual  
1773 decisions under a generative model (based upon a hazard function to model historical or se-  
1774 rial dependencies) with, a periodic fluctuation in the precision of sensory evidence relative to  
1775 prior beliefs at a particular timescale. Remarkably—using Bayesian model comparison—we  
1776 find that a model with fluctuating precisions has much greater evidence, relative to a model  
1777 in the absence of fluctuating precisions. Furthermore, we were able to quantify the dominant  
1778 timescale of periodic fluctuations; appropriate for these kinds of paradigm.”

1779 Note, again, I am reading your  $\omega_{LLR}$  and  $\omega_{\text{prior}}$  as precisions and that the periodic  
1780 modulation is the hyperprior that you are characterizing—and have discovered.

1781 This begs the question as to whether you want to pursue the  $1/f$  story. You refer to this  
1782 as “noise”. However, there is no noise in this setup. I think what you meant was that the  
1783 fluctuations are scale free, because they evinced a power law. I am sure that there are scale  
1784 free aspects of these kinds of hyperpriors; however, in the context of your paradigm I wonder  
1785 whether you should just ignore the scale free aspect and focus on your estimated temporal  
1786 scale implicit in  $f$ . This means you don’t have to hand wave about self-organized criticality  
1787 in the discussion and focus upon your hypothesis.

1788 A final move—to make the paper more focused and digestible—would be to put a lot of your  
1789 defensive analyses (e.g. about general arousal et cetera) in supplementary material. You

<sub>1790</sub> have to be careful not to exhaust the reader by putting up a lot of auxiliary material before  
<sub>1791</sub> the important messages in your report.

<sub>1792</sub> Minor points

<sub>1793</sub> I cannot resist suggesting that you change your title to “Bimodal Inference in Mice and Men”

<sub>1794</sub> Please replace “infra-slow fluctuations” with “slow fluctuations”. Infra-slow has some collo-  
<sub>1795</sub> quial meaning in fMRI studies but not in any scale free context.

<sub>1796</sub> Please replace “simulated data” with “simulations” in the abstract. Finally, please replace  
<sub>1797</sub> “robust learning and metacognition in volatile environments” with “enable optimal inference  
<sub>1798</sub> and learning in volatile environments.”

<sub>1799</sub> Line 50, please replace “about the degree of noise inherent in encoding of sensory information”  
<sub>1800</sub> with “the precision of sensory information relative to prior (Bayesian) beliefs.”

<sub>1801</sub> Line 125: please replace “a source of error” with “a source of bias”

<sub>1802</sub> Line 141: please replace “one 1/f noise” with a scale invariant process with a 1/f power law”  
<sub>1803</sub> (here and throughout) this is not “noise” it is a particular kind of fluctuation.

<sub>1804</sub> Line 178, when you say that the fluctuations may arise due to “changes in level of tonic  
<sub>1805</sub> arousal or on-task attention”, I think you need to qualify this. In predictive processing, on-  
<sub>1806</sub> task attention is exactly the modulation of sensory precision, relative to prior precision that  
<sub>1807</sub> you are characterising here. Tonic arousal may be another thing may or may not confound  
<sub>1808</sub> your current results.

<sub>1809</sub> When introducing Equation 2, please make it clear that the omega terms stand in for the  
<sub>1810</sub> precisions afforded to the likelihood ( $\text{omega\_LLR}$ ) and prior ( $\text{omega\_}$ ) that constitute the  
<sub>1811</sub> log posterior. You can then motivate Equation 6 and 7 as implementing the hyperprior in  
<sub>1812</sub> which the sensory and prior precisions fluctuate at a particular time scale.

<sub>1813</sub> You can also point out that the implicit anti-phase fluctuations are mandated by Bayes  
<sub>1814</sub> optimal formulations in which it is only the relative values of the prior and sensory precision

1815 that matter. Bayesian filters these precisions constitute the Kalman gain. You can find a  
1816 derivation of why this in treatments of the hierarchical Gaussian filter is by Mathys et al.

1817 In your first model simulations, I would make it clear in the main text which parameters you  
1818 are optimizing's; namely (H, alpha, a\_likelihood, a\_prior f). Perhaps a little table with a  
1819 brief description of the meaning of these hyper parameters would be useful?

1820 Please remove Section 5.8. If you do not, you need to explain why — on line 586 - setting a  
1821 = 0 is appropriate when a = 0, the log posterior in Equation 2 is zero because the precisions  
1822 (omegas) are zero (by Equations 6 and 7).

1823 I hope that these suggestions help, should any revision be required.

1824 Reviewer #2: Bimodal inference in humans and mice

1825 Veith Weilnhammer, Heiner Stuke, Kai Standvoss, Philipp Sterzer

1826 The authors elucidate whether periodicities in the sensitivity to external information repre-  
1827 sent an epiphenomenon of limited processing capacity or, alternatively, result from a struc-  
1828 tured and adaptive mechanism of perceptual inference. Analyzing large datasets of percep-  
1829 tual decision-making in humans and mice, they investigated whether the accuracy of visual  
1830 perception is constant over time or whether it fluctuates. The authors found significant au-  
1831 tocorrelations on the group level and on the level of individual participants, indicating that a  
1832 stimulus-congruent response in a given trial increased the probability of stimulus-congruent  
1833 responses in the future. Furthermore, the authors addressed whether observers cycle through  
1834 periods of enhanced and reduced sensitivity to external information or whether observers rely  
1835 on internal information in certain phases. This was quantified by whether a response at a  
1836 given trial was correlated with responses in previous trials. The authors used computational  
1837 modeling to infer the origin of the different modes (internal vs. external).

1838 Evaluation This is a very interesting and well-written manuscript, dealing with an important  
1839 question. The findings are novel and provide an innovative account of interpreting visual

1840 perception. I am not an expert in modeling, so I will restrict my comments to the theoretical  
1841 framework and the experimental approach. I have a few minor questions that I would like  
1842 the authors to answer or clarify.

1843 Minor questions 1. History congruent perception was defined on the basis of response repe-  
1844 titions. Are we really sure that responses are repeated due to some variant of a perceptual  
1845 decision process (internal or external) or may arise on the motor-level - independent of a per-  
1846 ceptual source? For instance, a response primed by residual activation in the motor system  
1847 may represent a local effect independent from a general response bias. 2. If indeed, a re-  
1848 sponse repetition is initiated by whatever reasons (non-perceptual), wouldn't this imply that  
1849 the repeated response is per se more related to previous than to current visual information  
1850 and would hence signal a reduced sensitivity to current external information? The authors  
1851 are discussing the option of stereotypically repeated responses in the context of alertness.  
1852 However, a tendency to repeat responses may arise due to other reasons. For instance, may  
1853 the motor priming effects mentioned possibly explain faster RTs along with a stronger bias  
1854 when in internal-mode.

1855 Reviewer #3: In this paper the authors propose that during perceptual decisions, humans  
1856 and mice exhibit regular oscillatory fluctuations between an “external” (that places more  
1857 weight on the perceptual evidence) and an “internal” (that places more weight on historical  
1858 experiences) mode. In particular, the authors propose a computational scheme in which  
1859 the influences of history and current stimulus on choice oscillate in anti phase, effectively  
1860 implementing “bimodal inference”. The computational advantages of these scheme as well  
1861 as its relation to the underlying neurophysiology are discussed.

1862 Overall, the authors make a very interesting proposal about what drives slow fluctuations  
1863 in perceptual performance during randomised two-alternative choice tasks. This proposal  
1864 relates changes in accuracy with changes in serial choice biases, which is a timely and syn-  
1865 thesising contribution. Furthermore, this proposal is backed by analyses over several human

<sub>1866</sub> datasets and a large dataset in mice.  
<sub>1867</sub> Despite its strong empirical contribution, the paper seems limited by the fact that alterna-  
<sub>1868</sub> tive computational hypotheses are not adequately considered (or at least considered in a  
<sub>1869</sub> systematic way). At the same time, and although the paper is well written, some parts are  
<sub>1870</sub> overly technical.

<sub>1871</sub> Major comments:

<sub>1872</sub> 1) The authors collapse across various datasets in which different tasks were employed.  
<sub>1873</sub> However, some details on the nature of these different tasks and a discussion on the  
<sub>1874</sub> rationale of collapsing behavioural metrics across them is missing. The authors mention  
<sub>1875</sub> that all tasks involved binary perceptual decisions. In some parts of the manuscript  
<sub>1876</sub> the term “false alarms” is mentioned, indicating a detection protocol. Other terms  
<sub>1877</sub> in the methods section (e.g., “set size”) might need further clarification. Importantly,  
<sub>1878</sub> it is not clear how reaction times were calculated in the various tasks and whether  
<sub>1879</sub> some experiments involved free response paradigms while others interrogation/ cued  
<sub>1880</sub> paradigms (in which case RTs can be defined as the latency between the response cue  
<sub>1881</sub> and the response).

<sub>1882</sub> 2) The key premise that when participants do not rely on the external stimulus they rely  
<sub>1883</sub> more on the previous trial needs to be more clearly (and statistically) contrasted against  
<sub>1884</sub> a null hypothesis. For instance, an null hypothesis could be that when participants place  
<sub>1885</sub> a lower weight on the stimulus they simply choose randomly. It is important to specify  
<sub>1886</sub> a null hypothesis such that the key premise does not appear self-evident or circular.

<sub>1887</sub> 3) From a mechanistic (sequential sampling) perspective, several previous papers have  
<sub>1888</sub> examined whether choice history biases influence the starting point or the drift rate  
<sub>1889</sub> of the evidence accumulation process. Under the former formulation, reliance on the  
<sub>1890</sub> evidence vs. reliance on the previous choice will be naturally anti-correlated (the less

1891 weight you place on the evidence the more impactful the choice history will be, assuming  
1892 that the last choice is represented as a starting point bias). This seems to be mapping  
1893 onto the computational model the authors describe, in which there is a weight on the  
1894 prior, a weight on the likelihood and the assumption that these weights fluctuate in anti-  
1895 phase. It is not obvious that this anti-phase relationship needs to be imposed ad-hoc.  
1896 Or whether it would emerge naturally (using a mechanistic or Bayesian framework).  
1897 More generally, the authors assert that without an external mechanism prior biases  
1898 would be impossible to overcome, and this would misfit the data. However, it would  
1899 be important to a) actually show that the results cannot be explained by a single  
1900 mechanism in which the anti-phase relationship is emergent rather than ad-hoc, b)  
1901 relate the current framework with previous mechanistic considerations of serial choice  
1902 biases.

- 1903 4) The authors need to unpack their definition of history biases since in previous work  
1904 biases due to the response or the identity of the stimulus at the previous trial are  
1905 treated differently. Here, the authors focus on response biases but it is not clear whether  
1906 they could examine also stimulus-driven history biases (in paradigms where stimulus-  
1907 response is remapped on each trial).
- 1908 5) Previous work, which the authors acknowledges in their Discussion (6.5), distinguishes  
1909 repetitive history biases from alternating biases. For instance, in Braun, Urai & Donner  
1910 (2018, JoN) participants are split into repetitive or alternating. Shouldn't the authors  
1911 define the history bias in a similar fashion? The authors point out that attracting and  
1912 repelling biases operate simultaneously across different timescales. However, this is not  
1913 warranted given Braun et. al and other similar papers. It is not clear how this more  
1914 nuanced definition of history bias would alter the conclusions.
- 1915 6) The arousal hypothesis seems to be ruled out too easily, merely in the presence of a  
1916 non-monotonic “state” vs. RT pattern. Arousal can have an inverted U-shaped effect

on behavioural performance and recent paper has demonstrated a non-monotonic effect of tonic arousal (baseline pupil) on RTs and accuracy (<https://www.biorxiv.org/content/10.1101/2023.07.28.550956.abstract>). More generally, the RT and confidence analyses need to be complemented, perhaps by computational modelling using sequential sampling models, as these behavioural metrics have multiple mechanistic mappings (e.g., a fast RT might correspond to high SNR or an impulsive decisions driven by a starting point bias).

7) In several analysis the authors present an effect and then show that this effects persists when key variables/ design aspects are also taken into account (see an example at around line 70). It makes more sense to present only one single analysis in which these key variables are controlled for. Results cannot be interpreted if they are spurious factors driving them so it is not clear why some of the results are presented in two versions (“uncontrolled” and “controlled” analyses).

8) The central empirical finding is potentially important but is currently shadowed by more speculative sections/ discussions. For instance, the section on the adaptive merits of the computational model is relatively weaker compared to the empirical results. In particular, the model is simulated without feedback (whereas most experiments employ trial by trial feedback) and does not outperform the baseline model in accuracy but in other secondary metrics.

Minor comments:

– The amount of statistical analysis and results is often overwhelming. The authors could streamline the presentation better such that the main result is brought to the foreground.

Currently the manuscript resembles a technical report.

– Some typos or omissions may alter the meaning in various places. Indicatively, in lines 273, 439, 649.

## 1942 References

- 1943 1. Schrödinger, E. *What is Life? The Physical Aspect of the Living Cell.* (Cambridge University Press, 1944).
- 1944 2. Ashby, W. R. Principles of the self-organizing dynamic system. *Journal of General Psychology* **37**, 125–128 (1947).
- 1945 3. Friston, K. Life as we know it. *Journal of The Royal Society Interface* **10**, 20130475 (2013).
- 1946 4. Palva, J. M. *et al.* Roles of multiscale brain activity fluctuations in shaping the variability and dynamics of psychophysical performance. in *Progress in brain research* vol. 193 335–350 (Elsevier B.V., 2011).
- 1947 5. VanRullen, R. Perceptual Cycles. *Trends in Cognitive Sciences* **20**, 723–735 (2016).
- 1948 6. Verplanck, W. S. *et al.* Nonindependence of successive responses in measurements of the visual threshold. *Journal of Experimental Psychology* **44**, 273–282 (1952).
- 1949 7. Atkinson, R. C. A variable sensitivity theory of signal detection. *Psychological Review* **70**, 91–106 (1963).
- 1950 8. Dehaene, S. Temporal Oscillations in Human Perception. *Psychological Science* **4**, 264–270 (1993).
- 1951 9. Gilden, D. L. *et al.* On the Nature of Streaks in Signal Detection. *Cognitive Psychology* **28**, 17–64 (1995).
- 1952 10. Gilden, D. L. *et al.* 1/f noise in human cognition. *Science* **67**, 1837–1839 (1995).
- 1953 11. Monto, S. *et al.* Very slow EEG fluctuations predict the dynamics of stimulus detection and oscillation amplitudes in humans. *Journal of Neuroscience* **28**, 8268–8272 (2008).

- 1965 12. Ashwood, Z. C. *et al.* Mice alternate between discrete strategies during perceptual  
1966 decision-making. *Nature Neuroscience* **25**, 201–212 (2022).
- 1967 13. Gilden, D. L. Cognitive emissions of 1/f noise. *Psychological Review* **108**, 33–56 (2001).
- 1968
- 1969 14. Duncan, K. *et al.* Memory’s Penumbra: Episodic memory decisions induce lingering  
1970 mnemonic biases. *Science* **337**, 485–487 (2012).
- 1971 15. Clare Kelly, A. M. *et al.* Competition between functional brain networks mediates  
1972 behavioral variability. *NeuroImage* **39**, 527–537 (2008).
- 1973 16. Hesselmann, G. *et al.* Spontaneous local variations in ongoing neural activity bias  
1974 perceptual decisions. *Proceedings of the National Academy of Sciences of the United  
States of America* **105**, 10984–10989 (2008).
- 1975 17. Schroeder, C. E. *et al.* Dynamics of Active Sensing and perceptual selection. *Current  
1976 Opinion in Neurobiology* **20**, 172–176 (2010).
- 1977 18. Honey, C. J. *et al.* Switching between internal and external modes: A multiscale  
1978 learning principle. *Network Neuroscience* **1**, 339–356 (2017).
- 1979 19. Weilnhammer, V. *et al.* Bistable perception alternates between internal and external  
1980 modes of sensory processing. *iScience* **24**, (2021).
- 1981 20. Rahnev, D. *et al.* The Confidence Database. *Nature Human Behaviour* **4**, 317–325  
1982 (2020).
- 1983 21. The International Brain Laboratory. Standardized and reproducible mea-  
1984 surement of decision-making in mice. *bioRxiv* 2020.01.17.909838 (2020)  
doi:10.1101/2020.01.17.909838.
- 1985 22. Fischer, J. *et al.* Serial dependence in visual perception. *Nat. Neurosci.* **17**, 738–743  
1986 (2014).

- 1987 23. Liberman, A. *et al.* Serial dependence in the perception of faces. *Current Biology* **24**,  
1988 2569–2574 (2014).
- 1989 24. Abrahamyan, A. *et al.* Adaptable history biases in human perceptual decisions. *Proceedings of the National Academy of Sciences of the United States of America* **113**,  
1990 E3548–E3557 (2016).
- 1991 25. Cicchini, G. M. *et al.* Compressive mapping of number to space reflects dynamic  
1992 encoding mechanisms, not static logarithmic transform. *Proceedings of the National  
Academy of Sciences of the United States of America* **111**, 7867–7872 (2014).
- 1993 26. Cicchini, G. M. *et al.* Serial dependencies act directly on perception. *Journal of Vision*  
1994 **17**, (2017).
- 1995 27. Fritzsche, M. *et al.* A bayesian and efficient observer model explains concurrent attrac-  
1996 tive and repulsive history biases in visual perception. *eLife* **9**, 1–32 (2020).
- 1997 28. Urai, A. E. *et al.* Pupil-linked arousal is driven by decision uncertainty and alters  
1998 serial choice bias. *Nature Communications* **8**, (2017).
- 1999 29. Akrami, A. *et al.* Posterior parietal cortex represents sensory history and mediates its  
2000 effects on behaviour. *Nature* **554**, 368–372 (2018).
- 2001 30. Braun, A. *et al.* Adaptive history biases result from confidence-weighted accumulation  
2002 of past choices. *Journal of Neuroscience* **38**, 2418–2429 (2018).
- 2003 31. Bergen, R. S. V. *et al.* Probabilistic representation in human visual cortex reflects  
2004 uncertainty in serial decisions. *Journal of Neuroscience* **39**, 8164–8176 (2019).
- 2005 32. Urai, A. E. *et al.* Choice history biases subsequent evidence accumulation. *eLife* **8**,  
2006 (2019).
- 2007 33. Hsu, S. M. *et al.* The roles of preceding stimuli and preceding responses on assimilative  
2008 and contrastive sequential effects during facial expression perception. *Cognition and  
Emotion* **34**, 890–905 (2020).

- 2009 34. Dong, D. W. *et al.* Statistics of natural time-varying images. *Network: Computation  
in Neural Systems* **6**, 345–358 (1995).
- 2010
- 2011 35. Burr, D. *et al.* Vision: Efficient adaptive coding. *Current Biology* **24**, R1096–R1098  
(2014).
- 2012
- 2013 36. Montroll, E. W. *et al.* On 1/f noise and other distributions with long tails. *Proceedings  
of the National Academy of Sciences* **79**, 3380–3383 (1982).
- 2014
- 2015 37. Bak, P. *et al.* Self-organized criticality: An explanation of the 1/f noise. *Physical  
Review Letters* **59**, 381–384 (1987).
- 2016
- 2017 38. Chialvo, D. R. Emergent complex neural dynamics. *Nature Physics* **6**, 744–750 (2010).
- 2018
- 2019 39. Wagenmakers, E. J. *et al.* Estimation and interpretation of 1/f $\alpha$  noise in human  
cognition. *Psychonomic Bulletin and Review* **11**, 579–615 (2004).
- 2020
- 2021 40. Van Orden, G. C. *et al.* Human cognition and 1/f scaling. *Journal of Experimental  
Psychology: General* **134**, 117–123 (2005).
- 2022
- 2023 41. Chopin, A. *et al.* Predictive properties of visual adaptation. *Current Biology* **22**,  
622–626 (2012).
- 2024
- 2025 42. Cicchini, G. M. *et al.* The functional role of serial dependence. *Proceedings of the  
Royal Society B: Biological Sciences* **285**, (2018).
- 2026
- 2027 43. Kiyonaga, A. *et al.* Serial Dependence across Perception, Attention, and Memory.  
*Trends in Cognitive Sciences* **21**, 493–497 (2017).
- 2028
- 2029 44. McGinley, M. J. *et al.* Waking State: Rapid Variations Modulate Neural and Behav-  
ioral Responses. *Neuron* **87**, 1143–1161 (2015).
- 2030
- 2031 45. Rosenberg, M. *et al.* Sustaining visual attention in the face of distraction: A novel  
gradual-onset continuous performance task. *Attention, Perception, and Psychophysics*  
**75**, 426–439 (2013).
- 2032

- 2033 46. Zalta, A. *et al.* Natural rhythms of periodic temporal attention. *Nature Communications* **11**, 1–12 (2020).
- 2034
- 2035 47. Prado, J. *et al.* Variations of response time in a selective attention task are linked to variations of functional connectivity in the attentional network. *NeuroImage* **54**, 541–549 (2011).
- 2036
- 2037 48. St. John-Saaltink, E. *et al.* Serial Dependence in Perceptual Decisions Is Reflected in Activity Patterns in Primary Visual Cortex. *Journal of Neuroscience* **36**, 6186–6192 (2016).
- 2038
- 2039 49. Cicchini, G. M. *et al.* Perceptual history propagates down to early levels of sensory analysis. *Current Biology* **31**, 1245–1250.e2 (2021).
- 2040
- 2041 50. Kepcs, A. *et al.* Neural correlates, computation and behavioural impact of decision confidence. *Nature* **455**, 227–231 (2008).
- 2042
- 2043 51. Fleming, S. M. *et al.* How to measure metacognition. *Frontiers in Human Neuroscience* **8**, 443 (2014).
- 2044
- 2045 52. Leys, C. *et al.* Detecting outliers: Do not use standard deviation around the mean, use absolute deviation around the median. *Journal of Experimental Social Psychology* **49**, 764–766 (2013).
- 2046
- 2047 53. Maloney, L. T. *et al.* Past trials influence perception of ambiguous motion quartets through pattern completion. *Proceedings of the National Academy of Sciences of the United States of America* **102**, 3164–3169 (2005).
- 2048
- 2049 54. Glaze, C. M. *et al.* Normative evidence accumulation in unpredictable environments. *eLife* **4**, (2015).
- 2050
- 2051 55. Wexler, M. *et al.* Persistent states in vision break universality and time invariance. *Proceedings of the National Academy of Sciences of the United States of America* **112**, 14990–14995 (2015).
- 2052

- 2053 56. Rao, R. P. *et al.* Predictive coding in the visual cortex: a functional interpretation of  
2054 some extra-classical receptive-field effects. *Nature neuroscience* **2**, 79–87 (1999).
- 2055 57. Jardri, R. *et al.* Experimental evidence for circular inference in schizophrenia. *Nature  
2056 Communications* **8**, 14218 (2017).
- 2057 58. Guggenmos, M. *et al.* Mesolimbic confidence signals guide perceptual learning in the  
2058 absence of external feedback. *eLife* **5**, (2016).
- 2059 59. Mathys, C. D. *et al.* Uncertainty in perception and the Hierarchical Gaussian Filter.  
2060 *Frontiers in human neuroscience* **8**, 825 (2014).
- 2061 60. Sterzer, P. *et al.* The Predictive Coding Account of Psychosis. *Biological Psychiatry*  
2062 **84**, 634–643 (2018).
- 2063 61. Bengio, Y. *et al.* Towards Biologically Plausible Deep Learning. *bioRxiv* (2015).
- 2064
- 2065 62. Dijkstra, N. *et al.* Perceptual reality monitoring: Neural mechanisms dissociating  
2066 imagination from reality. *PsyArXiv* (2021) doi:10.31234/OSF.IO/ZNGEQ.
- 2067 63. Andrillon, T. *et al.* Predicting lapses of attention with sleep-like slow waves. *Nature  
2068 Communications* **12**, 3657 (2021).
- 2069 64. Passingham, R. E. *Understanding the prefrontal cortex : selective advantage, connec-*  
2070 *tivity, and neural operations.* (Oxford University Press).
- 2071 65. Ashwood, Z. C. *et al.* Mice alternate between discrete strategies during perceptual  
2072 decision-making. *bioRxiv* 2020.10.19.346353 (2021) doi:10.1101/2020.10.19.346353.
- 2073 66. Bak, P. Complexity and Criticality. in *How nature works* 1–32 (Springer New York,  
2074 1996). doi:10.1007/978-1-4757-5426-1\_1.
- 2075 67. Denève, S. *et al.* Efficient codes and balanced networks. *Nature Neuroscience* **19**,  
2076 375–382 (2016).

- 2077 68. Beggs, J. M. *et al.* Neuronal Avalanches in Neocortical Circuits. *Journal of Neuro-*  
2078 *science* **23**, 11167–11177 (2003).
- 2079 69. Wang, X. J. Synaptic basis of cortical persistent activity: The importance of NMDA  
2080 receptors to working memory. *Journal of Neuroscience* **19**, 9587–9603 (1999).
- 2081 70. Wang, X. J. Synaptic reverberation underlying mnemonic persistent activity. *Trends*  
2082 *in Neurosciences* **24**, 455–463 (2001).
- 2083 71. Wang, M. *et al.* NMDA Receptors Subserve Persistent Neuronal Firing during Working  
2084 Memory in Dorsolateral Prefrontal Cortex. *Neuron* **77**, 736–749 (2013).
- 2085 72. Bliss, D. P. *et al.* Synaptic augmentation in a cortical circuit model reproduces serial  
2086 dependence in visual working memory. *PLOS ONE* **12**, e0188927 (2017).
- 2087 73. Stein, H. *et al.* Reduced serial dependence suggests deficits in synaptic potentiation  
2088 in anti-NMDAR encephalitis and schizophrenia. *Nature Communications* **11**, 1–11  
(2020).
- 2089 74. Durstewitz, D. *et al.* Neurocomputational Models of Working Memory. *Nature Neu-*  
2090 *roscience* **3**, 1184–1191 (2000).
- 2091 75. Seamans, J. K. *et al.* Dopamine D1/D5 receptor modulation of excitatory synaptic  
2092 inputs to layer V prefrontal cortex neurons. *Proceedings of the National Academy of*  
*Sciences of the United States of America* **98**, 301–306 (2001).
- 2093 76. Kobayashi, T. *et al.* Reproducing Infra-Slow Oscillations with Dopaminergic Modula-  
2094 tion. *Scientific Reports* **7**, 1–9 (2017).
- 2095 77. Chew, B. *et al.* Endogenous fluctuations in the dopaminergic midbrain drive behavioral  
2096 choice variability. *Proceedings of the National Academy of Sciences of the United States*  
*of America* **116**, 18732–18737 (2019).
- 2097 78. Fritzsche, M. *et al.* Opposite Effects of Recent History on Perception and Decision.  
2098 *Current Biology* **27**, 590–595 (2017).

- 2099 79. Gekas, N. *et al.* Disambiguating serial effects of multiple timescales. *Journal of Vision*  
2100 **19**, 1–14 (2019).
- 2101 80. Weilnhammer, V. *et al.* Psychotic Experiences in Schizophrenia and Sensitivity to  
2102 Sensory Evidence. *Schizophrenia bulletin* **46**, 927–936 (2020).
- 2103 81. Fletcher, P. C. *et al.* Perceiving is believing: a Bayesian approach to explaining the  
2104 positive symptoms of schizophrenia. *Nature reviews. Neuroscience* **10**, 48–58 (2009).
- 2105 82. Corlett, P. R. *et al.* Hallucinations and Strong Priors. *Tics* **23**, 114–127 (2019).

2106